Experimental and Theoretical Investigation of the Hydraulics of Storm water Drill Drop Manholes and Vertical Drains with Radial Inflow

by

Sahar Banisoltan

A thesis submitted in partial fulfillment of the requirements for the degree of

Doctor of Philosophy

in

Water Resources Engineering

Department of Civil and Environmental Engineering
University of Alberta

Abstract

Vertical drains have been always an important topic in hydraulic engineering because of their application in draining from large reservoirs such as in shaft spillways of dams. In these structures, a radial water flow is supplied to the vertical shaft. Nowadays, vertical drains have been mostly used in stormwater and sanitary manholes. In these structures, flow is affected by the momentum of inlet jet.

While in flow from large reservoirs, traditional flow regimes of weir and orifice flow are expected, some unsteadiness of water depth has been also observed by researchers. In some cases, unsteadiness caused a rapid rise of water depth. This was because the outlet could not pass the design discharge at that certain head and resulted in the serious risk of overflowing of the dam. In case of stormwater manholes, there is also a risk of overflowing into the streets and therefore it is essential to reevaluate the design, if rehabilitation is required, to ensure safe operation.

For example, a component of the stormwater management in urban systems; e.g. in the City of Edmonton, is the Drill Drop Manhole (DDM). DDM's consist of two concentric manholes attached in a vertical orientation. The diameter of the upper manhole is only twice or three times larger than the lower manhole and there can be different numbers of inlets with different sizes and configurations that convey water into the upper manhole. Recognizing this fact that most of previous studies and guidelines are related to large tanks discharging into smaller outlets, this experimental study was defined. As the first stage of the study, variation of the water depth h with the discharge Q was studied and new flow regimes were determined. Hydraulic design guidelines were developed so that based on the discharge, outlet size and inlet configurations and sizes, the water depth in the upper manhole could be calculated to prevent overflowing.

Among new flow regimes, a filling and emptying regime was observed that had similarities to the unsteady flow in shaft spillways. It was believed that the incoming momentum and small ratio between the tank and outlet were responsible for the unstable flow behavior. Therefore, in the second stage of this study, the effect of the incoming momentum was eliminated by providing radial flow and the diameter ratio was progressively reduced. It was observed that while the flow was at the weir flow regime, gulping occurred frequently. This initiated the formation of the orifice flow regime or an oscillatory variation of water depths. Water depths in each of these oscillatory stages were recorded and it was found that the formation of each stage was related to the different location of the control section; i.e., the top end or the bottom end of the vertical outlet. The principle of maximum discharge and vortex theories (free vortex and Rankine vortex) were used for this purpose. It has been shown that for the unsteadiness related to the maximum head, the control section is at the end of outlet and there is a critical air core to outlet diameter ratio which can explain the observed unsteadiness. Field water depth variation with discharge in one dam has been used for validation purposes. This criterion can be used to ensure a safe operation.

It was found that there is a tendency for the flow to form a free vortex in which the control section is located at the throat; i.e., just below the entrance to the lower pipe. In DDM, effect of the outlet size and throat length were discussed and the condition under which the discharge was controlled by the top of the vertical pipe was analyzed. Moreover, the continuity equation was used to calculate the outlet discharge and the results were examined.

Effect of tank size on discharge coefficient in weir flow regime has been discussed and compared with the recommended design values for shaft spillways. It has been shown that the aeration of nappe can affect the coefficient of discharge in these cases. Another part of this research

was related to the clarification of the effect of tank size on the coefficient of discharge and determination of the required freeboard in dropshaft structures.

Preface

The information required for the fabrication of the physical hydraulic model of the Drill Drop Manholes of the city of Edmonton in the first stage of this study, has been obtained from the City of Edmonton Drainage Services. Wayne Pelz and Darwin Smith cooperated in providing the necessary information.

Chapters 2, 3, 4, and 6 include the experimental data collected by myself in the T. Blench Hydraulic Laboratory at the University of Alberta under the supervision of, Professor D. Z. Zhu and Professor N. Rajaratnam. Chapter 5 includes the analysis of the experimental data found in the referenced literature. In all chapters of this thesis, modelling and data analysis are my original work and my collaborators are Professor D. Z. Zhu and Professor N. Rajaratnam .

Chapter 2 of this thesis has been published as Banisoltan, S., Rajaratnam, N., and Zhu, D. (2015). ”Experimental Study of Hydraulics of Drill-Drop Manholes.” ASCE *J. Hydraul. Eng.*, 141(10), 04015021. A report based on the finding of this chapter has also been submitted to the City of Edmonton. I was responsible for conducting the experiments, analysis and manuscript compositions. Professor N. Rajaratnam collaborated with the manuscript and concepts. The supervisory author was Professor D. Z. Zhu who was involved with concept establishments and manuscript work.

Chapter 3 of this thesis has been submitted as Banisoltan, S., Rajaratnam, N., and Zhu, D. (2016). “Experimental and Theoretical Investigation of Vertical Drains with Radial Inflow”to the ASCE *J. Hydraul. Eng.* It is currently under review with a manuscript number HYENG-9961. I was responsible for conducting the experiments, analysis and manuscript composition. Manuscript review and concept formations were collaborated with Professor N. Rajaratnam. Professor D. Z.

Zhu as the supervisory author, was involved in the manuscript and concept developments and formations.

Dedicated to

My Lovely Alireza

Acknowledgement

Words cannot describe how I am grateful to my supervisor Dr. David Zhu for his support and kindness during this study. I am also honored that I had the supervision of Dr. Nallamuthu Rajaratnam. His knowledge and inspiration showed me how to see the obstacles as challenges. I am also grateful to Dr. Peter Steffler for his encouragement and help in this study.

On the first day of school at the University of Alberta, I met the love of my life, Alireza Habibzadeh. His wisdom, patience and love were my great enthusiasms to finish this study. He made every day of my grad school a joyful one. I also would like to thank my mother, Nahid Mirzataheri for her unlimited love and my father Ali Banisoltan and my sister Sima Banisoltan for their belief in me. This thesis is also in loving memories of my uncles Ali Mirzataheri and Mohammad Mirzataheri who always encouraged education.

I am also thankful to the City of Edmonton Drainage Services for sponsoring the first stage of this study, and Perry Fedun for building of the experimental arrangements and helping with the experiments.

Table of Contents

List of Tables

List of Figures

Chapter 1) Introduction

1.1 Motivation and Background

Urban water systems have been developed over time as civilization has grown. In ancient Greece, there were indications of sustainable urban water management practices (Koutsoyiannis et al, 2008). In ancient Iran (Persia), the history goes back to more than 3000 years of using ground water by 170,000 miles of underground conduits called Qanat (Wulff 1968). Later, industrialization changed the technologies in urban water systems and even the perspective to water issues. For example, in case of stormwater, at first stormwater was approached as a problem in cities (Heaney et al, 2000). However, with increase in demand for water, it is now viewed as a "valuable resource" (Heaney et al, 2000). The similar attitude towards sanitary is also valid. To achieve the goal of reusing stormwater, an efficient way of receiving the runoff flow from urban watersheds is required. This requires manholes to convey water safely from street level to deep sewers in order to deliver it to storage or treatment facilities. In case of sanitary, again, manholes are required and it is recommended that the sanitary and stormwater be completely separated.

Operational conditions of stormwater or sanitary systems change with time. For example, city developments may force addition of new inlets to the storm water or sanitary manholes. Operational discharge may also exceed the design discharge due to climate change. In all of these sanitary and stormwater manholes, except vertical drain from large reservoirs, incoming flow from inlet affect the flow regime.

One type of stormwater and sanitary control in City of Edmonton is called the Drill Drop Manholes (DDM). They consist of two connected vertical manholes with the diameter of the upper manhole twice larger than that of the lower manhole. There could be a number of inlets with different sizes, quantities and configurations that convey flow to the upper manhole. Due to the

erosion and corrosion, the city is going to install new PVC pipes inside the lower manhole so that the diameter of the upper manhole becomes three times larger than the diameter of the lower manhole. The incoming flow from the inlets prevents traditional flow regimes such as weir flow or orifice flow from occurring. Therefore, it was necessary to identify the new flow regimes and the effect of the diameter ratio between the tank and outlet on the flow capacity and water depth inside the upper manhole to prevent overflowing of the manhole.

Fig. 1.1 Pictures of Drill Drop Manhole (DDM) in city of Edmonton, photo from Smith (2013)

By identifying new flow regimes, some design guidelines were provided to the City of Edmonton. The effect of the incoming momentum was eliminated by providing a radial water supply to a large tank and then the effect of the tank size was studied in this vertical drain. In both experimental series in DDM's and vertical drains, there was no distance between the top of the vertical pipe and the bottom of the tank. However, another application of a vertical drain can be in discharging water from reservoirs such as in shaft spillways in which there is a distance between the top of the vertical pipe and bottom of the reservoir. Therefore, the coefficient of discharge for both structures have been compared. Moreover, the required freeboard for an impinging jet has been discussed.

As a result, this thesis clarifies the flow regimes affected by the incoming momentum and drain size on the water depth-discharge variation in vertical drains that are used in stormwater manholes or spillways. Guidelines have been provided in this thesis that can be used for design purposes.

1.2 Overview of Thesis Content

Chapter 2 describes the literature of traditional water depth variation with discharge in vertical drains and then discusses flow while affected by the incoming momentum from inlets in small diameter ratios between the tank and outlet. New flow regimes that occur in small diameter ratios have been discussed besides the effect of inlet size, elevation and configuration. The characteristics of DDM's in the City of Edmonton was the motivation for this investigation. A model with a scale factor of 1:5 was built at the T. Blench Hydraulic Laboratory of the University of Alberta.

Chapter 3 presents the experimental studies of water depth variation with discharge while the effect of incoming momentum was eliminated. This was achieved by providing a radial inflow and continuously reducing the tank size. The observed water depth variation has been reported and it has been shown that a combination of vortex theories and weir control (WC) and throat control (TC) formulae can be used to explain the experimental data. These theories have been used previously in vortex drops in which a steady air core persists. A discharge equation has been presented that can be solved simultaneously with the TC and WC formulae to evaluate the head discharge curve.

Chapter 4 deals with different theories of (WC) and (TC) flows in vertical drains in the presence of circulation. The effect of the vertical pipe diameter and throat length have been

discussed. Water depth variation with time has been presented and, using the continuity equation, the outlet discharge and the coefficient of discharge have been calculated.

The effect of a protruding vertical pipe into a tank; i.e. when there is a distance between the top of the vertical pipe and the bottom of the tank, on the coefficient of discharge in the weir flow regime has been investigated in Chapter 5. A comparative study has been made with these results and the coefficient of discharge in shaft spillways.

Chapter 6 discusses a series of experiments to study the required freeboard and the observed choking condition in DDM's. Four different inlet to shaft diameter ratios have been studied and the effect of having two inlets instead of one has been discussed. For two-inlet cases that were placed at a 90-degree orientation, the height of the interaction point has been formulated and compared with the observed data. Chapter 7 presents the main conclusions of the thesis and provides some recommendations for future research.

References

Heaney, J. P., Pitt, R. & Field, R. (2000) [Introduction] In Field, R., Heaney, J. P., & Pitt, R.. "*Innovative urban wet-weather flow management systems*." CRC Press, Lancaster, Pennsylvania, pp1.

Koutsoyiannis, D., Zarkadoulas, N., Angelakis, A. N., & Tchobanoglous, G. (2008). "Urban water management in Ancient Greece: Legacies and lessons." *Journal of water resources planning and management*, 134(1), 45-54.

Smith, D., (personal communication in email format regarding City of Edmonton's drill drops manholes, March 25, 2013)

Wulff, H. E. (1968). "The qanats of Iran." *Scientific American*, *218*(4), 94-105.

Chapter 2) Experimental Study of Hydraulics of Drill-Drop Manholes[1]

2.1. Introduction

The City of Edmonton, Alberta, Canada, has a large number of Drill-Drop Manholes (DDM) in its drainage system. A drill-drop manhole is a vertical drop manhole connected to a large deep trunk sewer, which has an average diameter of 2000 mm. A DDM consists typically of an upper manhole of a diameter of 1200 mm and height of about 3 m and a lower manhole of a smaller diameter of about 600 mm and varying length, from a few meters to about 20 m (see Fig. 2.1). The lower manhole is made of corrugated steel pipe, prone to corrosion and deterioration. As a result, the City is considering inserting PVC pipes of smaller diameter inside these lower pipes. Nearly half of these drops have one inlet in the upper manhole whereas a quarter of them have two inlets. A few have more than two inlets. These DDM are used for conveying sanitary or storm flows, and would generally not be submerged at its lower end.

Drill-drop manholes have also been used in other municipalities: they were originally drilled or built to serve other purposes like conveying electrical systems or for ventilation to deeper sewers and eventually are used for conveying wastewater. The aim of this study was to investigate the hydraulics of DDM and evaluate their discharge capacity (without overflow) to assist in retrofitting efforts.

A number of studies have been performed in the past to understand the flow from a larger upper reservoir through a smaller pipe, attached either at the bottom or projecting into the reservoir (Binnie 1938; Kalinske 1941; Binnie and Wright 1941; Binnie and Hookings 1948; Anwar 1965a,

---

- [1] This chapter has been published as a paper in *ASCE Journal of Hydraulic Engineering*: Banisoltan, S., Rajaratnam, N., and Zhu, D. (2015)., 141(10), 04015021. Permanet link: http://dx.doi.org/10.1061/(ASCE)HY.1943-7900.0001042

1965b, 1966, 1969, Anwar et al. 1978; Daggett and Keulegan 1974). In these cases, the upper reservoir is relatively large and the outflow to the smaller pipe is mainly controlled by the head on the entrance to the smaller pipe. These studies indicate that as the momentum of the inflow to the upper reservoir is negligible, the flow into the small pipe resembles free flow over a circular weir, if the entrance to the lower pipe is not submerged. When the entrance is submerged, however, the flow resembles an orifice flow type. For much larger heads, the smaller pipe gets primed and flows full and this is generally referred to as full pipe flow. Blaisdell (1953) studied a case in which the smaller vertical pipe is short and is followed by a long sloping pipe, in which case there is a short pipe - controlled flow before the onset of full pipe flow.

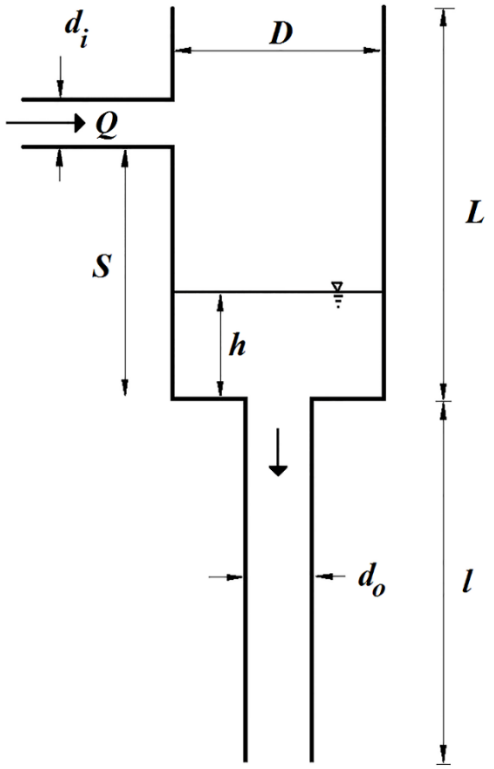

Fig. 2.1 Definition sketch of drill-drop manhole (DDM)

In some cases, the water in the upper reservoir had significant circulation. The effect of circulation on the flow through the smaller pipe has also been studied. Ma et al. (2013) reported a

significant reduction of the outflow rate through the bottom outlet of a large tank if there is significant tank circulation. Its relative importance has been expressed in the form of a dimensionless number, as ratio of the circulation around the outlet to the product of the outlet diameter and a characteristic velocity (Chang and Prosser 1987).

Our preliminary laboratory experiments with DDM indicated that since the diameter of the upper manhole D is only a few times that of the lower pipe d_o, the momentum of the flow entering the upper manhole as a jet from the inflow pipe of diameter of d_i appears to affect the flow entering the lower pipe significantly. For smaller flow rates, the upper manhole has relatively small water depths, with large velocities and the flow was also very turbulent with large eddies. Even as the inflow increases with the average depth of flow in the upper manhole increasing, the flow into the lower pipe is still affected by the momentum of the inflow. As the inflow increases further, the inflowing jet appears to dissipate in the upper manhole but because of the relatively smaller size of the upper manhole, the inflow into the smaller pipe still has noticeable momentum and was asymmetric with some circulation. Hence observations on the flow in the DDM were made, to develop an understanding of the flow features. Twenty four series of experiments were conducted to investigate the effect of the diameter ratio (D/d_o), inlet size, inlet elevation, number of inlets and different arrangements.

2.2. Experiments

The experimental arrangement was considered a scale model of a typical DDM. The diameter of the upper manhole was D= 239 mm, which would represent a prototype diameter of 1200 mm with a length scale of approximately 5. The length of the upper manhole was L=600 mm corresponding to the prototype length of 3.0 m. The discharge from the inlet pipe was measured by inline magnetic flow meters Foxboro IMT25 (±o.5 % of reading) and Foxboro M/2800 Series

(±o.25 % of reading). Video observations were made during the experiments. The main modeling similitude parameter would be the Froude number with the Reynolds number being the secondary parameter. Hydraulic modeling based on the Froudian law requires sufficiently high values of Reynolds and Weber numbers to reduce viscous effects and surface tension effects (Ettema 2000). In the current study, these numbers were sufficiently large to minimize the scale effects; minimum inlet Reynolds numbers as defined by VR_h/υ were equal to 4.6×10^3 for partially full flow and 1.6×10^4 for full pipe flow, and minimum Weber number as defined by $(\rho V^2 d_i/\sigma)^{0.5}$ was equal to 14 (Ettema 2000), where V is the mean velocity in the inlet pipe, R_h is the hydraulic radius, ρ and σ are the density and surface tension of water, respectively.

2.2.1. Primary Experiments: A-Series

In the primary series of experiments involving D/d_o=3.1, inlet diameters were different but all the inlets were located at 389 mm and the length of the lower pipe was l =557 mm. For smaller discharges from the inflow pipe, the jet impinged on either the inner wall or the bottom of the upper manhole (Fig. 2.2a). The flow depth in the upper manhole was non-uniform and the water entered the outflow pipe as a swirling jet and continued as a swirling turbulent flow. This was termed the Deflected Jet (DJ) regime. As the discharge increased, a pool was formed in the upper manhole (Fig. 2.2b) referred to as the Stable Pool (SP) regime. These two regimes may be combined into one regime, referred to as the lower flow regime.

As the discharge increases, in a transitional discharge, the outflow from the upper manhole became smaller than the inflow and the depth of water h in the upper manhole started to increase rapidly. Then suddenly the outflow pipe primed generating full pipe flow. For this condition, the outflow was more than the inflow and h in the upper manhole reduced rapidly (Figs. 2.2d and 2.2e in which inlet was at lower elevation). This cycle repeated at a certain frequency λ, and this flow

was termed the Filling and Emptying (FE) regime. At a greater discharge, the full pipe flow established itself as the only flow regime and this regime is termed as Full Pipe Flow (FPF) (Fig. 2.2f), for which the outflow was equal to the inflow and the depth of flow in the upper manhole had a certain value for every discharge. In the experiments, the water surface was uneven, especially for the DJ and SP regimes; the depth of flow h was taken as the average of depths measured at eight locations in the upper manhole, four around the outer wall and four around the rim of the outflow pipe. However, for the FE and FPF regimes, only four around the outer wall were measured.

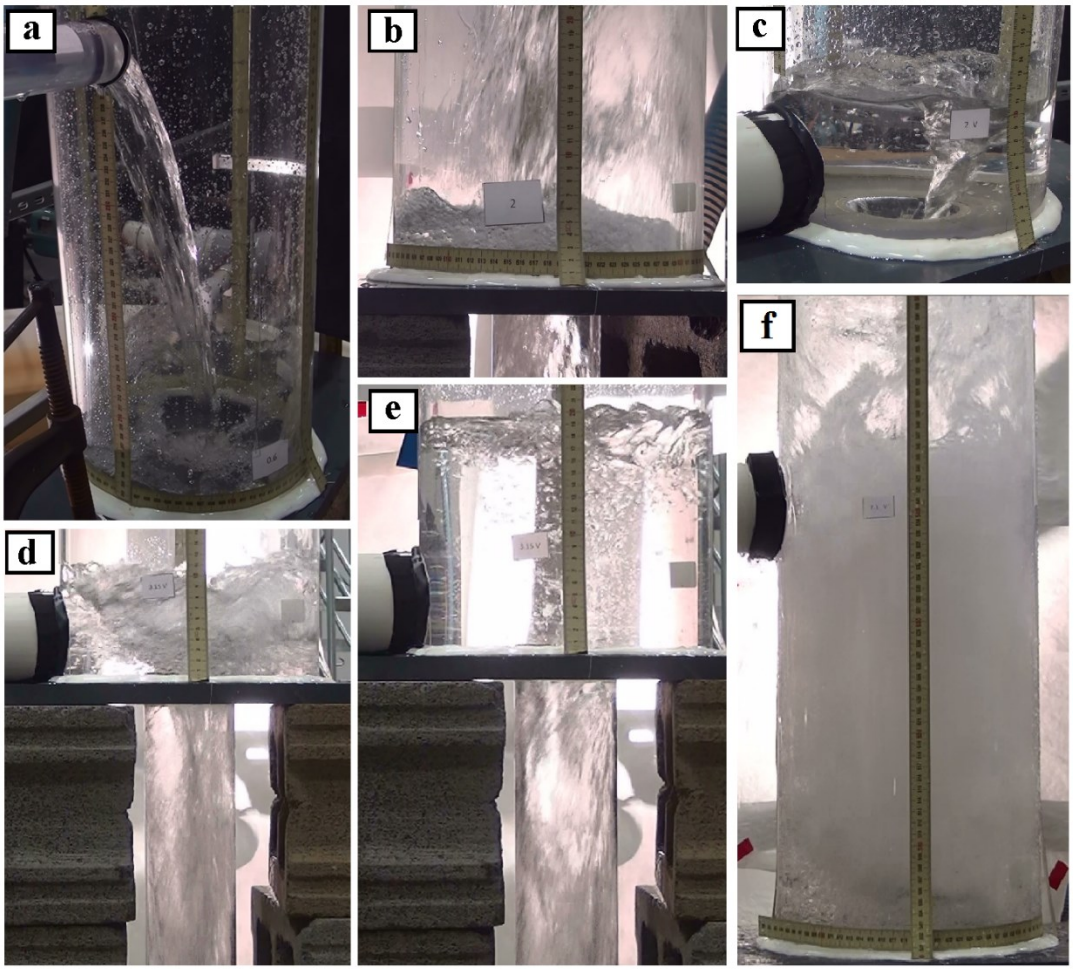

Fig. 2.2 Pictures of the different flow regimes: (a) Series A1-2, DJ regime, Q= 0.6 L/s; (b) Series A1-2, SP regime, Q= 2 L/s; (c) Series A4-3 SP regime, Q= 3.81 L/s; (d) Series A4-3, FE regime (Emptying) , Q= 6 L/s; (e) Series A4-3, FE regime (Filling), Q= 6 L/s; (f) Series A1-3, FPF regime, Q=13.5 L/s.

Since there are a number of variables, several series of experiments were performed, firstly to understand the flow of a DDM and then to find the effect of the major variables and develop definitive relations between the inflow discharge Q and h. In the A-Series, the diameter of the lower pipe was 76 mm, so that D/d_o=3.1. The diameter of the inflow pipe was d_i=40, 52 and 77 mm, whereas the height of its invert S above the bottom of the upper manhole was varied from 401 to 8 mm (Table 2.1). The maximum length l of the lower pipe was 556 mm, and was reduced in steps to a minimum value of 20 mm.

Fig. 2.3 shows a typical head-discharge (h-Q) curve, with a different symbol for each flow regime (Exp. A1-3). The DJ regime occurred for Q <1 L/s; the SP regime appeared to exist for 1<Q < 2.4 L/s. At Q=2.4 L/s, the FE regime set in and Fig. 2.3 shows the upper and lower branches of the h-Q curve. For Q=8.8 L/s, steady full pipe flow set in, indicating the start of the FPF regime.

It was observed that the h-Q curve is not significantly affected by the variation of the diameter of the inlet pipe in the DJ and SP regimes. The effect of the variation of the length of the outlet pipe l on the h-Q curve is shown in Fig. 2.4 indicating a similar type of behavior for l/d_o from 7.3 to 1.0. For l/d_o =0.3, for which the outlet acted as an orifice, the FE regime did not exist. This is in agreement with findings of Kalinske (1941) who reported small effect of pipe length when it runs partially full.

The effect of the inlet height S on the h-Q curve is shown in Fig. 2.5 wherein S was varied from 8 to 389 mm. It was observed that if the inlet was not near the bottom of the upper manhole, the variation of S did not affect the h-Q curve in the DJ and SP regimes as well as the start of the FE regime and the lower branch of the FE regime. If the inlet pipe was placed close to the bottom of the upper manhole, both branches of the h-Q curve were affected.

Table 2.1. Details of experiments

Series	d_o (mm)	d_i (mm)	l (mm)	S (mm)	D/d_o	l/d_o	Appendix Fig number	Comments
Series with one inlet								
A1-1	76	52	557	389	3.1	7.3	Fig A1.1 & Fig A1.2	One inlet at higher elevation with different inlet diameters
A1-2	76	40	557	401	3.1	7.3		
A1-3	76	77	557	383	3.1	7.3	Fig A1.3	
A2-1	76	40	557	8	3.1	7.3	Fig A1.4	One constant inlet diameter at different elevations
A2-2	76	40	557	106	3.1	7.3	Fig A1.5	
A2-3	76	40	557	207	3.1	7.3	Fig A1.6	
A3-1	76	52	506	389	3.1	6.6		One constant inlet diameter at higher elevation and varying outlet lengths
A3-2	76	52	455	389	3.1	6.0		
A3-3	76	52	379	389	3.1	5.0		
A3-4	76	52	303	389	3.1	4.0		
A3-5	76	52	227	389	3.1	3.0		
A3-6	76	52	151	389	3.1	2.0		
A3-7	76	52	76	389	3.1	1.0		
A3-8	76	52	20	389	3.1	0.3		
A4-1	76	52	557	12	3.1	7.3	Fig A1.7	One inlet at middle and lower elevations
A4-2	76	52	557	206	3.1	7.3		
A4-3	76	77	557	6	3.1	7.3	Fig A1.8	
B1-1	121	52	880	389	2	7.3		Same as A1 series but with different outlet diameter
B1-2	121	77	880	391	2	7.3	Fig A1.9	
Series with two inlets at a horizontal plane (angle:90 degree)								
C1-1	76	52	557	389, 389	3.1	7.3	Fig A1.10	a:Q_1/Q_2=1, b: Q_1/Q_2=2, c: Q_1/Q_2=3
C1-2	76	40	557	401, 401	3.1	7.3	Fig A1.11	a:Q_1/Q_2=1, b: Q_1/Q_2=2
C1-3	76	77	557	383, 383	3.1	7.3	Fig A1.12	a: Q_1/Q_2=1, b: Q_1/Q_2=2
C2-1	76	52	557	5, 12	3.1	7.3	a: Fig A1.13 b: Fig A1.14 c: Fig A1.15	a: Q_1/Q_2=1, b: Q_1/Q_2=2, c: Q_1/Q_2=3
Series with two inlets at different horizontal planes (angle:90 degree)								
C2-2	76	52	557	389, 12	3.1	7.3	Fig A1.16	a: Q_1/Q_2=1

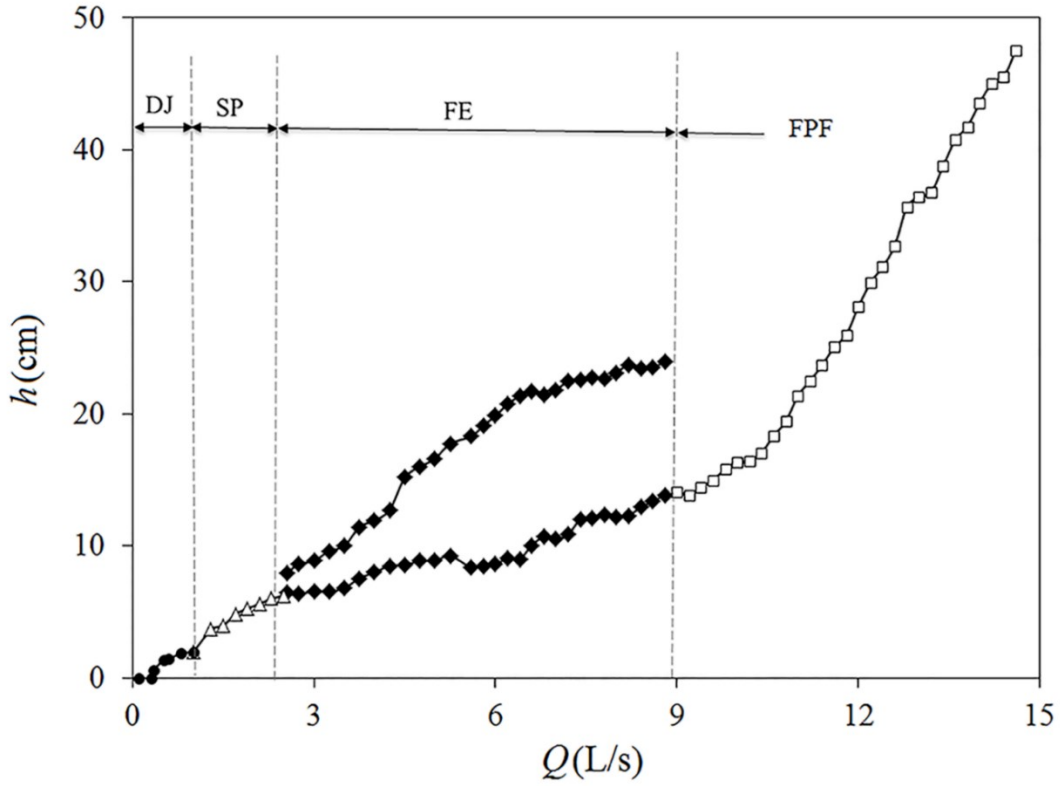

Fig. 2.3 Typical head-discharge (h-Q) curve showing different flow regimes for Series A1-3 with d_i=77mm

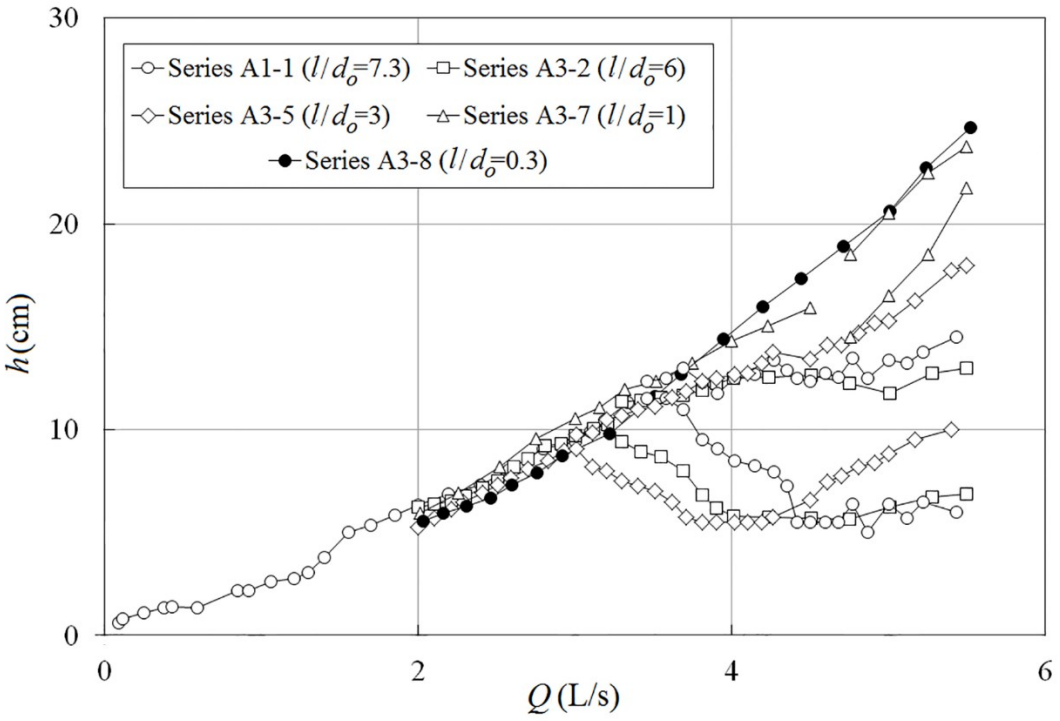

Fig. 2.4 Effect of outlet pipe length l/d_o on h-Q curves

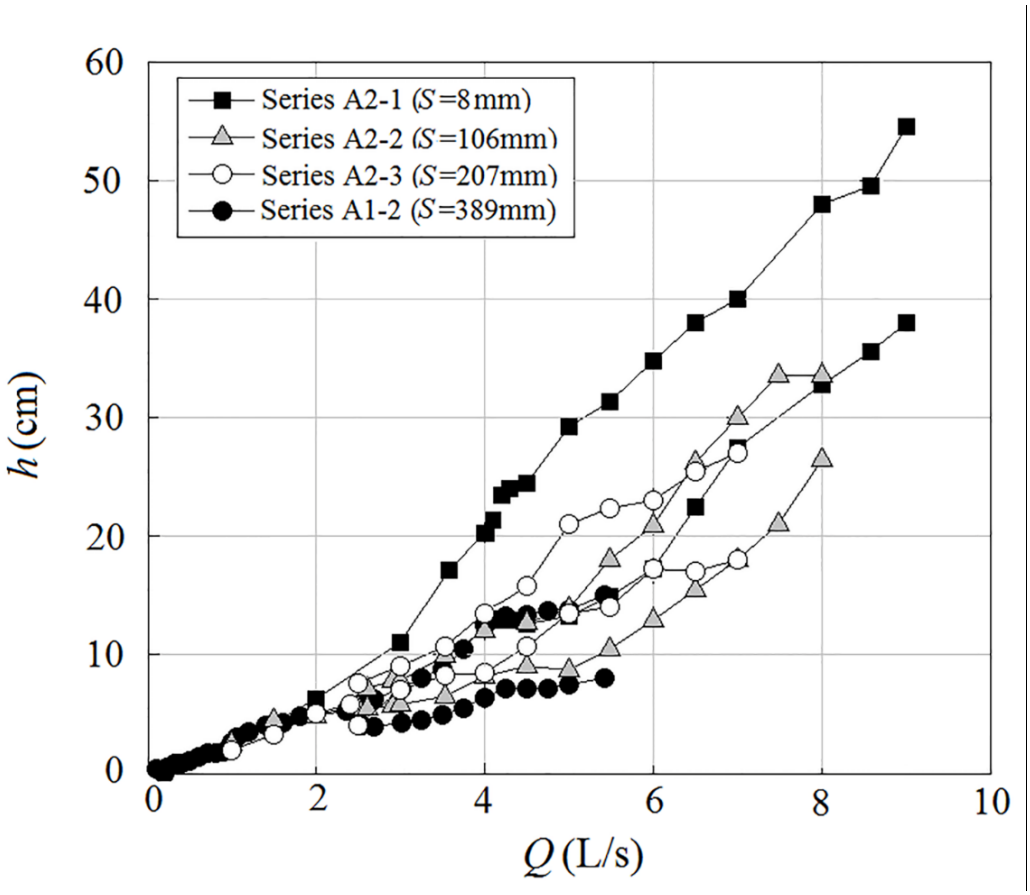

Fig. 2.5 Effect of inlet elevation S on h-Q curves

2.2.2. Further Experiments: B-Series with D/d_o=2 and C-Series with two inflow pipes

In the B-Series, the D/d_o ratio was reduced to 1.98 or approximately 2 and two different inlet sizes which were placed at high elevations were tested. Since 26% of manholes in the City of Edmonton have two inlets, four sets of experiments were done with two inlets, in the C-Series, placed at the same height or different heights and carrying equal or different flow rates. As the prototype inlet diameters vary from 200 to 1200 mm, a variety of inlets with 40 mm to 77 mm were tested. The results indicate that the flow characteristics are essentially the same as that of a single inlet with the discharge equal to the total discharge from the two inlets if both inlets were at higher elevations. Some additional experiments (C2-2) were also done with multiple inlets in order to develop proper correlations.

2.3. Results and discussion

2.3.1. Inlets at higher and middle elevations

The results of the A and B Series with D/d_o=3.1 and 2 are combined below in a dimensionless form. The diameter of the outlet pipe d_o was chosen as the length scale for the flow depth h. For the discharge, the scale is $(gd_o^5)^{0.5}$, so that the dimensionless discharge is

$$Q^* = \frac{Q}{\sqrt{gd_o^5}} \tag{2.1}$$

Fig. 2.6 shows a non-dimensional plot of the experiments A1-3 and B1-2, for which d_o= 76 and 121 mm and D=239 mm for both series. Note that the results of the two data sets involving different values of d_o almost match.

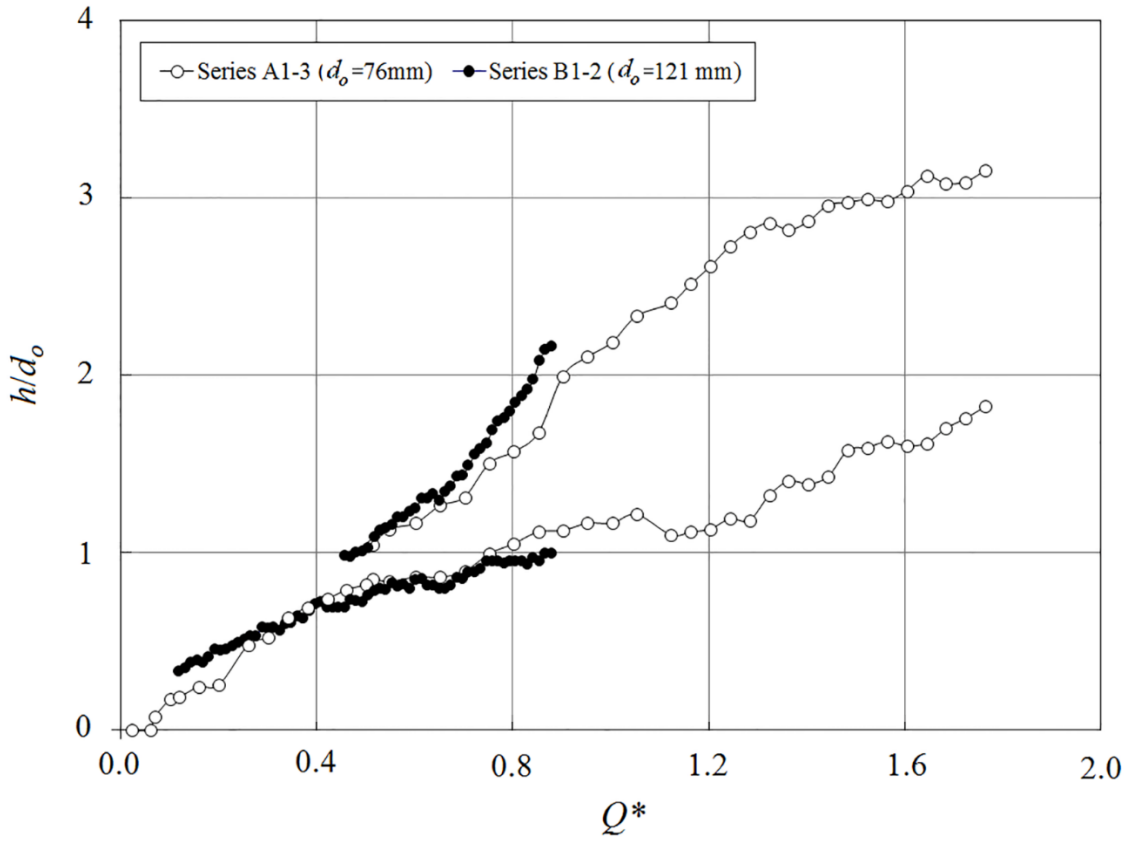

Fig. 2.6 Non-dimensional head-discharge (h/d_o-Q^*) curves for different outlet diameters

It is of interest to obtain a general relation between the discharge Q and the depth of water h in the upper manhole. Fig. 2.7 includes data from the A, B and C Series with D/d_o=3.1 and 2. The experimental results follow a straight line and most of the data are contained by the ±0.05 variation in Q^* as (R^2=0.91)

$$\frac{h}{d_o} = 1.77Q^* \qquad \text{(for DJ and SP regimes: } 0.01 \le Q^* \le 0.60\text{)} \qquad (2.2)$$

The separation between the DJ and SP regimes occurs at Q^* equal to about 0.23.

A correlation for the upper branch of the h/d_o - Q^* curve in the FE regime is shown in Fig. 2.8 It includes series with the inlet at higher and middle elevations and the mean line as (R^2=0.80)

$$\frac{h}{d_o} = 2.04Q^* \qquad \text{(for FE regime – the upper branch: } 0.61 \le Q^* \le 1.64\text{)} \quad (2.3)$$

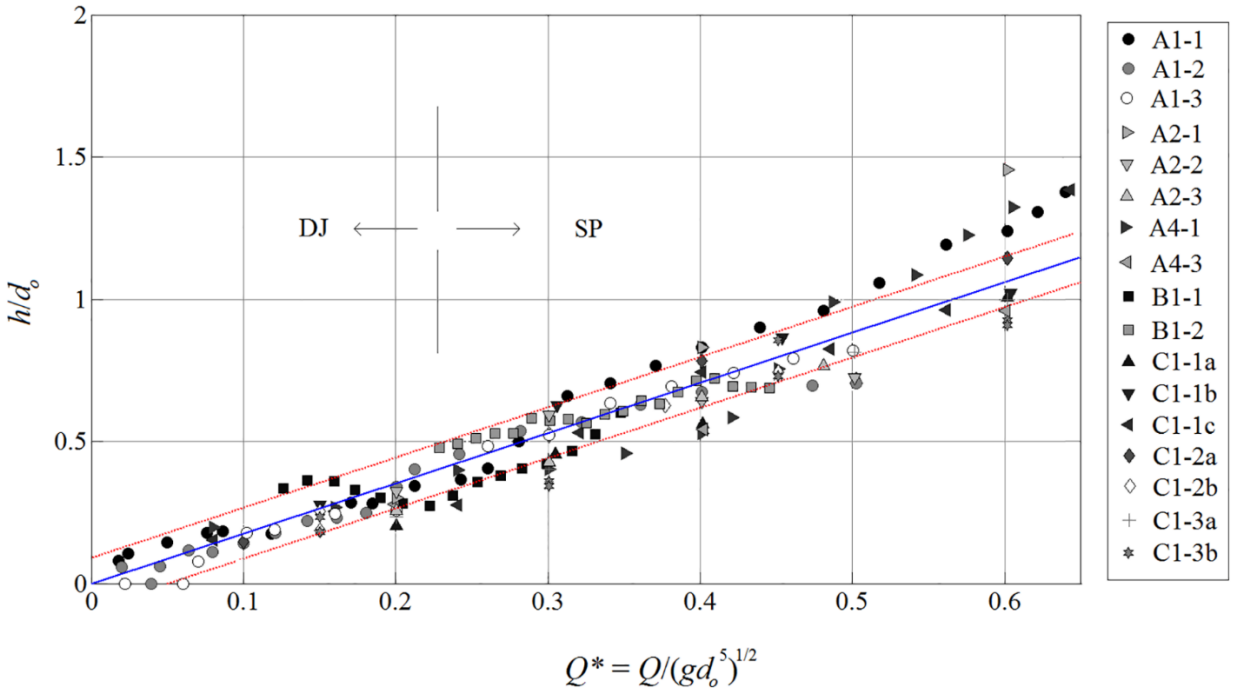

Fig. 2.7 h/d_o-Q^* curves for DJ and SP regimes. (-) fitted line, (…) with ±0.05 variation in Q^*.

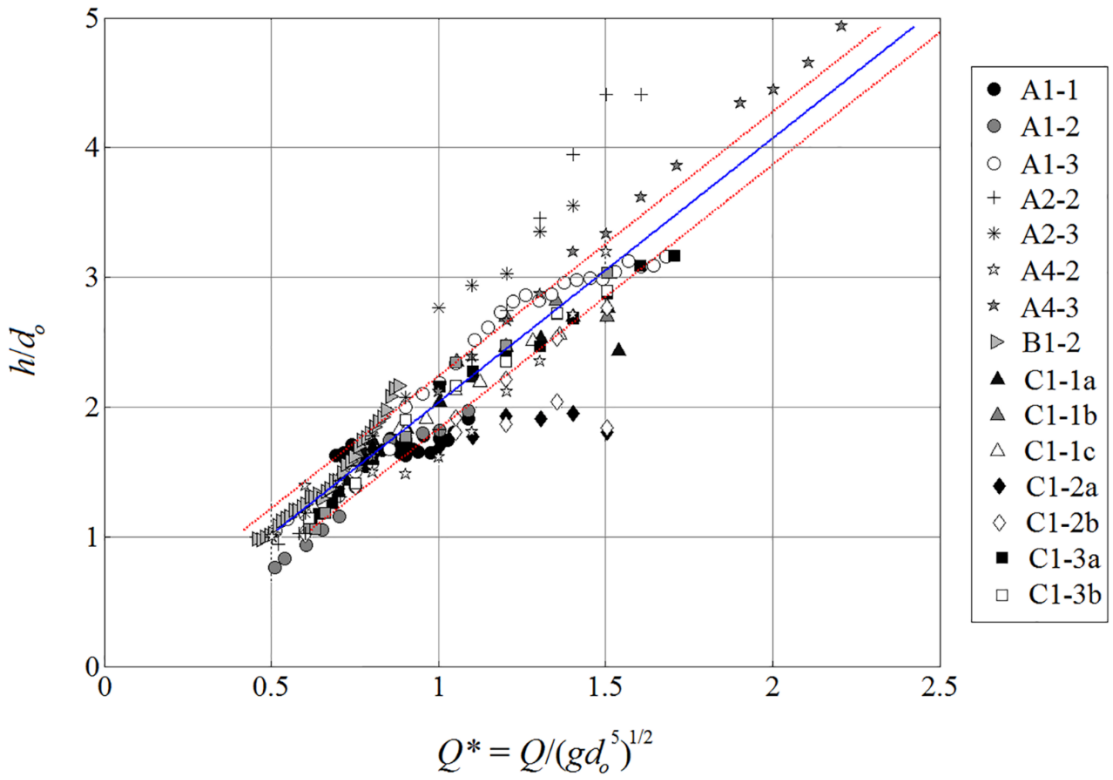

Fig. 2.8 h/d_o-Q^* curves for the upper branch of FE regime in series with one or two inlets located at higher and middle elevations. (-) fitted line, (…) ±0.10 variation in Q^*.

However an attempt to find a regression formula for the lower branch in the series with the inlet at the higher and middle elevations resulted in a poor correlation. It is believed that this is likely a result of measurement errors in reading the depth at the end of the emptying process which occurred during a short period. As the upper branch is of main concern for design purposes to prevent overflowing, such a regression equation is valuable for practical purposes.

Dimensionless discharge, at which the flow changes from the SP to the FE regime is referred as the first transitional discharge Q_{T1}^*. Similarly, the discharge at which the flow changes from the FE to FPF regime is referred as the second transitional discharges Q_{T2}^*. The start of the FE regime occurs at $Q_{T1}^* \cong 0.61$ with a standard deviation of 0.11. The end of the FE regime with the flow transition to the FPF is $Q_{T2}^* \cong 1.65$ with a standard deviation of 0.10. In the FPF regime

the total head loss including the loss in the upper manhole and at the entrance to the outlet pipe can be defined as

$$h_L = K^*(V_o^2/2g) \tag{2.4}$$

wherein V_o is the mean velocity in the outlet pipe and K^* is an empirical coefficient.

Neglecting the velocity at the water surface in the upper manhole, the energy equation between the water surface in the upper manhole and the exit of the outlet pipe states

$$l + h = \frac{V_o^2}{2g} + K^* \frac{V_o^2}{2g} + f \frac{l}{d_o} \frac{V_o^2}{2g} \tag{2.5}$$

Using the experimental data for the full pipe flow regime h and f=0.0165, the calculated K^* is plotted against Q^* in Fig. 2.9 and fitted with R^2=0.92 as

$$K^* = \frac{14.7}{\exp(Q^*)} \tag{2.6}$$

The lines indicating ±0.05 variation in Q^* is also shown in Fig. 2.9. Note that K^* is much larger than the standard value of 0.5 for a square entrance in a large upper reservoir, which is attributed to the energy loss in the upper chamber. Even for the largest value of Q^* =2.75, K^* =1. Eq. (2.5) can be re-arranged as

$$\frac{(h+l)}{d_o} = \frac{8}{\pi^2} Q^{*2} \left[1 + K^* + f \frac{l}{d_o} \right] \qquad \text{(for FPF regimes: } Q^*>1.65\text{)} \tag{2.7}$$

From Eqs. (2.6) and (2.7), h can be evaluated versus ($f\, l/d_o$). Note that if the length of the outlet pipe is large, there is the possibility of the inception of cavitation near the entrance to the outlet pipe (Anderson 1971).

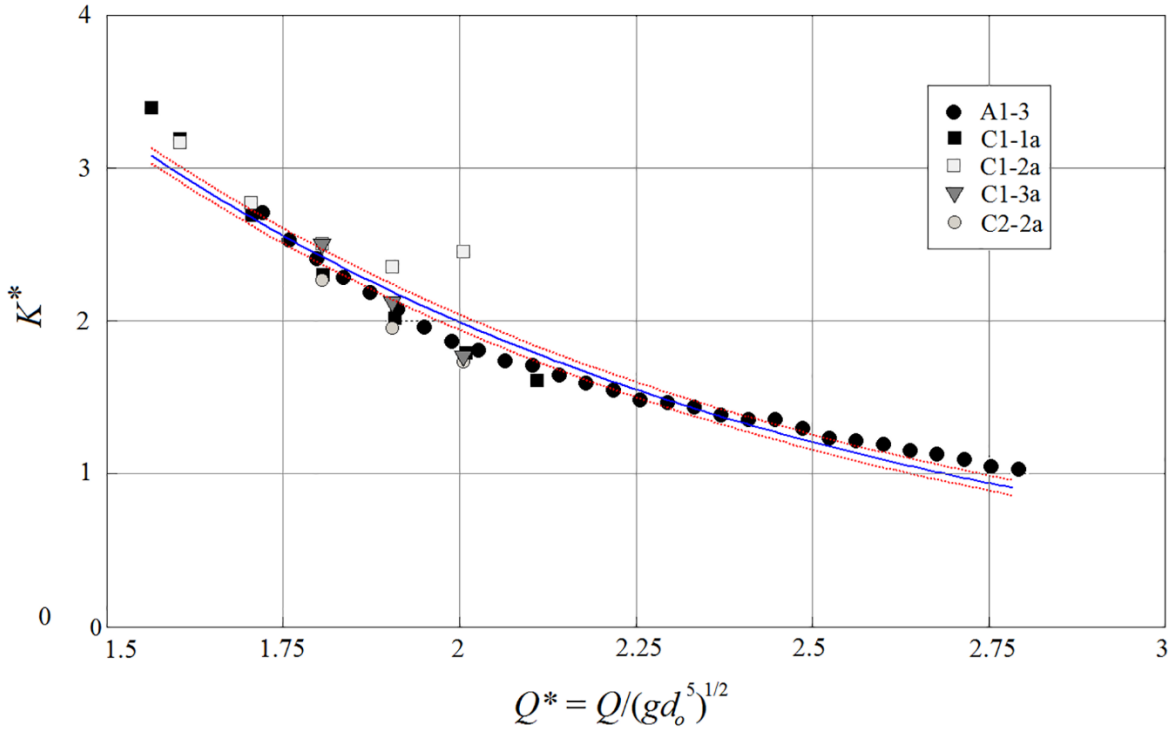

Fig. 2.9 Energy loss coefficient (K^*) versus Q^* for FPF regime. (-) fitted line, (…) ±0.05 variation in Q^*.

2.3.2. Inlets at lower elevations

The *h*-*Q* curve developed above for the DJ, SP and FE regimes are all approximately linear, thereby ruling out the corresponding weir and orifice flow types that would exist in a large upper reservoir, with negligible circulation. Note that there was a considerable amount of air entrainment in the upper manhole. Because of the presence of a large number of air bubbles and the highly turbulent nature of the flow, it was difficult to make velocity measurements.

If the one inlet was located near the bottom (A2-1, A4-1, A4-3) for small discharges, the inlet was not submerged and the flow hit the upper manhole wall, opposite the inlet. For slightly larger discharges (for example 2.25 L/s in Series A4-1), the inlet was submerged and the flow was symmetric across the centerline of the inlet. Also, the flow passed into the outlet without any vortex. With increasing discharge, an inclined vortex with an air-core formed (Fig. 2.2c). This vortex was observed to impinge on the lower pipe at a distance of 50 mm, destroying the symmetric

flow patterns in the upper manhole. As the discharge was increased, circulation also increased and the water surface became more and more turbulent, and the air-core size was decreased. A regression analysis indicated that for one inlet at lower elevation, the DJ and SP regimes, experimental results were in the band suggested above.

For the upper branch of the filling and empting regime (FE), the air-core vortex disappeared for a few seconds (Fig. 2.2e). The bubble concentration increased at the former location of the vortex and suddenly, an air column was formed and then the bubbles were evacuated. At that time, the water surface changed to the lower head (Fig. 2.2d). Shortly later, the vortex formed, causing the water surface to change to the upper head. In the upper branch of the FE regime, it was observed that larger water depths were created by smaller inlet diameters. The ratio of D/d_i multiplied by Q^* describes the water depth changes with $R^2= 0.95$ as

$$\frac{h}{d_o} = 0.68\frac{D}{d_i}Q^* \qquad \text{(for FE regime –upper branch: } 0.61 \le Q^* \le 1.64) \qquad (2.8)$$

The solid line in Fig. 2.10 shows this regression equation, whereas the dotted lines show ±0.1 variations in Q^*. For the lower branch, regression analysis as ($R^2=0.85$)

$$\frac{h}{d_o} = 0.4\frac{D}{d_i}Q^* \qquad \text{(for FE regime –lower branch: } 0.61 \le Q^* \le 1.64) \qquad (2.9)$$

Two major differences between one inlet at higher elevation and lower elevation in series A1-3 and A4-3 were delaying the formation of the FE regime from 2.56 L/s to 3.81 L/s and FPF regime from 8.58 L/s to 11.5 L/s and also decreasing frequencies.

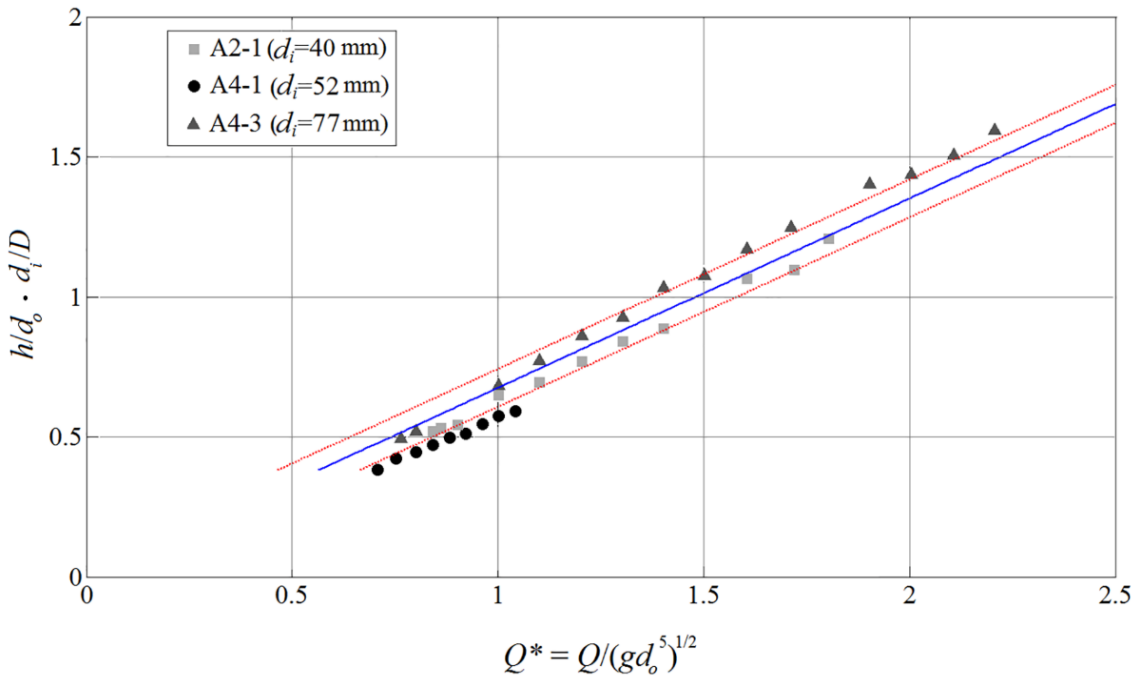

Fig. 2.10 h/d_o-Q^* curves for upper branch of FE regime in series with one inlet located at lower elevation. (-) fitted line, (…) ±0.10 variation in Q^*

When two inlets were located at lower elevations, the h-Q curves of Series C2-1 with Series A4-1 in Fig. 2.11 with d_o=76 mm show that the FPF regime does not even occur for 10 L/s, while for one and two inlets at some height, it occurs at Q=8.3 L/s.

Let Q^* be the combined dimensionless flow rate and Q_r the discharge ratio of the larger discharge to the other. Water depth in the SP regime and the upper and lower branches of the FE regime in two inlet series at the lower elevation was found to depend on Q^* and Q_r:

$$\left(\frac{h}{d_o}\right) = 2.3Q_r^{1/5}Q^* - 0.63 \qquad \text{(for SP regime, } Q^* \le 0.61,\ R^2 = 0.93) \quad (2.10)$$

$$\left(\frac{h}{d_o}\right) = 1.46Q_r^{1/3}Q^* \qquad \text{(for FE regime – upper branch: } 0.61 \le Q^* \le 1.64,\ R^2 = 0.91) \quad (2.11)$$

$$\left(\frac{h}{d_o}\right) = 0.78Q_r^{-1/3}Q^* + 0.66 \quad \text{(for FE regime –lower branch: } 0.61 \le Q^* \le 1.64,\ R^2 = 0.89) \quad (2.12)$$

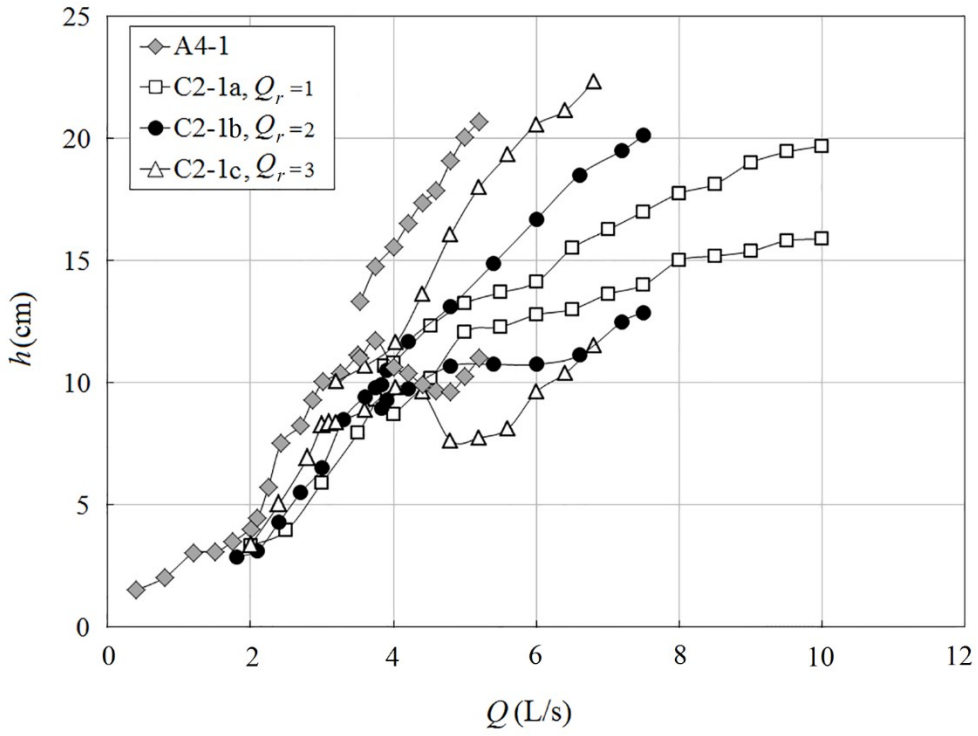

Fig. 2.11 Comparing *h*-*Q* curves for Series C2-1 (two inlets at the same plane with an angle of 90 degree and *S*= 5 and 12 mm) and Series A4-1 (one horizontal inlet with *S*=12 mm)

Considering the switching in the FE regime, the filling and emptying sequences were studied from video recordings at 30 fps with a Sony handycam (HDR-PJ580); several typical sequences are shown in Fig. 2.12.

For drain to a vertical pipe from a tank, Binnie and Hooking (1948) theoretically showed that the discharge depends on total energy, geometry and air-core diameter *a* at the throat. Ackers and Crump (1960) used Binnie and Hooking (1948) criterion and adapted it for vortex drop structures. Ackers and Crump (1960) showed that the *h*-*Q* curve for vortex drops is linear and strongly depends on air fraction (a/d_o). It is believed that linear *h*-*Q* curve in SP regimes follows this fact that air-core is also a controlling parameter in DDM. Moreover, since FE regime happens when air-core disappears, it seems that the reason for a small difference between transitional discharges for inlets at higher and lower elevation is related to the existence of a more stable air-core vortex in smaller values of a/d_o due to a less turbulent pool. Therefore, the fact that inlets at

lower elevations have smaller values of frequencies is related to a strong air-core even with a larger amount of water depth in the upper manhole.

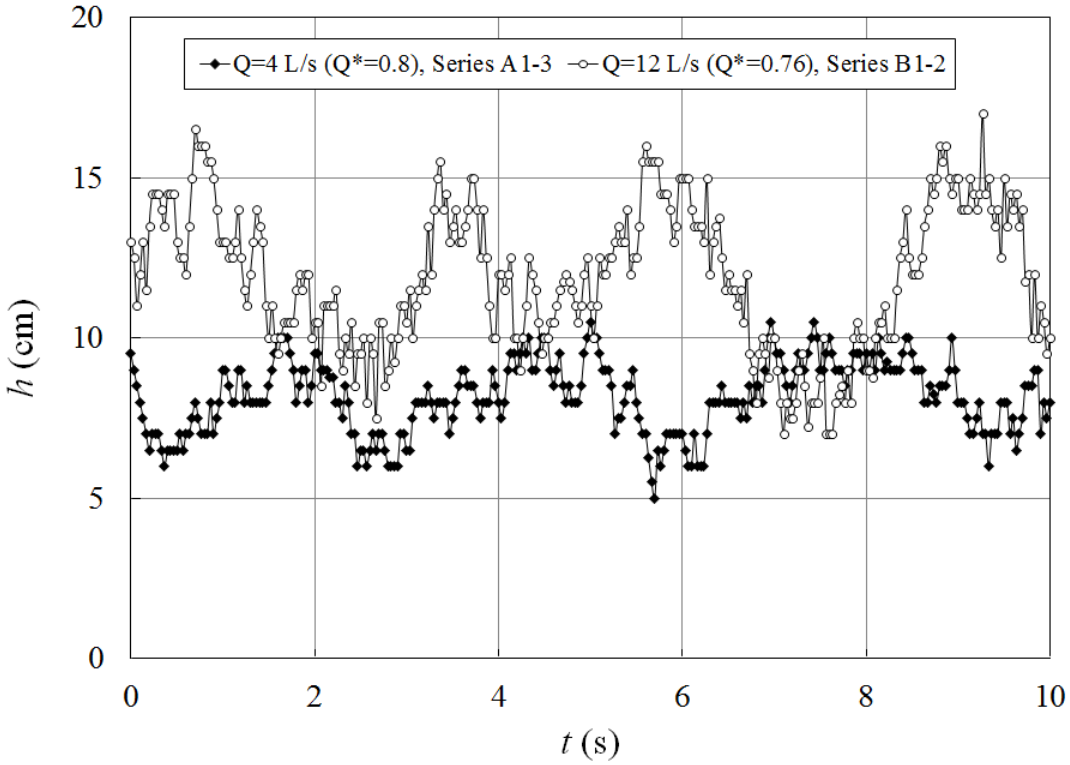

Fig. 2.12 Dimensional water depth time series in FE regime when only outlet diameter was different

Quick (1990) emphasized on the existence of a stable air-core vortex as a fundamental design parameter as found out by Binnie and Hookings (1948) and Kennedy (1988). Quick (1992) described that due to the high tendency of long pipes to drag air, entrained air will have high velocities and therefore air pressure will decrease. As a result, discharge capacity will increase and a sudden release of water depth will occur.

It is believed that in the FE regime, similar phenomenon happens during emptying. Furthermore, due to the existence of circulation, once the emptying occurs, the air-core vortex tends to form and as a result, the discharge coefficient decreases and water depth increases. In FPF regime, if inlets are at higher elevations pool is quite bubbly and turbulent. However, for inlets at lower elevations, a vortex is observed in the pool with a few bubbles. With increasing discharge,

the number of bubbles decreases, and at a discharge of 13.5 L/s, a completely clear pool with only a few bubbles is observed.

To use the findings of the current research for design purposes, first determine Q^*, inlet elevation and number of inlets. In all one inlet and two inlet cases at higher elevations, if $Q^*<0.61$, DJ or SP regimes are formed so that the inlet elevation or diameter are not important. Simply use Eq. (2.2) to find average water depth h. However, if $Q^*>0.61$, use Eq. (2.3) for inlets at higher elevations or Eq. (2.8) for one inlet case at lower elevation in which the diameter ratio of the inlet to the upper manhole is important. Moreover, if $Q^*>1.65$, FPF regime will occur for inlets at higher elevations and the length of lower pipe becomes important so Eqs. (2.6) and (7) should be applied. In cases where both two inlets are at lower elevations, use Eq. (2.10) for $Q^*<0.61$ and Eq. (2.11) for $Q^*>0.61$. Note that if inlets are at a relatively higher elevation, the number of inlets does not affect the flow regime so that the discharges are combined while for two inlet cases at lower elevations, the discharge ratio of two inlets has an effect.

2.4. Conclusions

This experimental study has shown that in the Drill-drop Manholes (DDM) of Edmonton, the flow into the outlet pipe located at the bottom of the upper manhole is dominated by the momentum of the incoming flow and as a result, weir and orifice types of flow that would occur in a relatively larger upper reservoir do not occur. Instead, there was a deflected jet (DJ) regime followed by a stable pool (SP) regime. Then, a filling and emptying (FE) regime occurs with an upper and lower branch of the h-Q curve. In this regime, for any discharge, the flow switches between two branches with a certain frequency. The FE regime is followed by a regime in which the outlet pipe runs full, referred to as the full pipe flow (FPF) regime.

For the DJ, SP and FE regimes, equations were developed between the normalized inflow rate and depth in the upper manhole, using $(gd_o^5)^{0.5}$ and the diameter of the outlet pipe d_o as scales. For one inlet, it was found that inlet size or elevation does not affect SP regime. However, FE regime formulation depends on inlet size when it is located at a lower elevation. For two inlets, if both are located at a lower elevation, discharge ratio becomes another parameter in both SP and FE regimes. A general equation has also been developed for the FPF regime, involving an expression for the sum of the losses in the upper manhole and the entrance to the outlet pipe, for inlets located at the high elevations. This study has improved current understanding of flow in DDM used by the city of Edmonton.

2.5. Notation

The following symbols are used in this chapter:

D = Diameter of upper manhole;

K^* = energy loss coefficient;

L = length of upper manhole;

Q = discharge;

Q_r = discharge ratio (of bigger discharge to another discharge);

Q_{T1} = discharge at which SP regime transits to FE regime;

Q_{T2} = discharge at which FE regime transits to full pipe flow regime (FPF);

Q^* = dimensionless discharge = $Q/(gd_o^5)^{0.5}$;

R_h = hydraulic radius;

S = elevation of the inlet pipe above bottom of upper manhole (measured to invert);

V = inlet velocity;

V_o = average water flow velocity inside lower pipe;

a = air-core diameter;

d_i = diameter of inlet pipe;

d_o = diameter of outlet pipe;

f = friction factor;

g = gravity acceleration;

h = mean water depth in upper manhole;

l = length of outlet pipe;

t = time (s);

λ = frequency of water surface changes in FE regime;

υ = viscosity of water;

ρ = density of water;

σ = surface tension of water (7.18×10^{-2} N/m);

References

Ackers, P., & Crump, E. S. (1960). "THE VORTEX DROP" *ICE Proceedings*, 16(4), 433-442*,* Thomas Telford.

Anderson, A. G., Vadiyaraman, P. P. and Chu, C. S. (1971). "Hydraulics of long vertical conduits and associated cavitation." *ST. Anthony Falls and Hydraulic Lab*, Minnesota University, Minneapolis, MN.

Anwar, H. O. (1965a). "Coefficients of Discharge for Gravity Flow in to Vertical Pipes." *J. Hydraul. Res.*, 3(1), 1-19.

Anwar, H. O. (1965b). "Flow in a Free Vortex." *Water Power*, 17, 153-161.

Anwar, H. O. (1966). "Formation of a Weak Vortex." *J. Hydraul. Res.*, 4(1), 1-16.

Anwar, H. O. (1969). "Turbulent Flow in a Vortex." *J. Hydraul. Res.*, 7(1), 1-29.

Anwar, H.O., Weller, J.A. and Amphlett, M.B. (1978). "Similarity of Free-Vortex at Horizontal Intake." *J. Hydraul. Res.*, 16(2), 95-105.

Binnie, A. M. (1938). "The Use of a Vertical Pipe as an Overflow for a Large Tank." *Proc. Royal Society of London*. Series A, Mathematical and Physical Sciences, 168, 219-237.

Binnie, A. M., and Hookings, G. A. (1948). "Laboratory Experiments on Whirlpools." *Proceedings of the Royal Society of London.* Series A, Mathematical and Physical Sciences, 194, 1038, 398-415.

Binnie, A. M and Wright, R. K. (1941). "Laboratory Experiments on Bellmouth Spillways." *J of the Institution of Civil Engrs*, 15(3), 197-219.

Blaisdell, F. W. (1953) "Hydraulic fundamentals of closed conduit spillways." *ASCE J. Hydraul. Div*., 354, 1-14.

Chang, E and Prosser, M. J. (1987). "Basic results of theoretical and experimental work" in Knauss , J. (Ed.) "Swirling flow problems at intakes". Rotterdam: A.A. Balkema.

Daggett, L. L., Keulegan, G. H. (1974). "Similitude in Free-Surface Vortex Formations." *ASCE J. Hyd. Div.*, 100(11), 1565-1581.

Ettema, R. (2000). "Hydraulic modeling: concepts and practice." *ASCE Manuals and Reports on Engineering Practice* No.97, Reston, VA.

Kalinske, A. A. (1941). "Hydraulics of vertical drain and overflow pipes." In Howe, J. W. (Ed.) "Investigations of the Iowa Institute of Hydraulic Research: Papers, abstracts of theses and research reports, and reference list of staff publications", Iowa institute of hydraulic research, 26, Iowa, IA.

Kennedy, J., Jain, S., and Quinones, R. (1988). "Helicoidal-Ramp Dropshaft." *J. Hydraul. Eng.*, 114(3), 315–325.

Quick, M. C. (1990). "Analysis of spiral vortex and vertical slot vortex drop shafts." *J. Hydraul. Eng.*, 116(3), 309–325.

Quick, M. C. (1992). Closure to "Analysis of Spiral Vortex and Vertical Slot Vortex Drop Shafts" by Michael C. Quick (March, 1990, Vol. 166, No. 3). " *J. Hydraul. Eng.*, *118*(1), 104-107.

Ma, Y., Qian, Y., and Zhu, D.Z. (2013). "Effect of air core on the shape and discharge of the outflow through a bottom outlet." *Theoretical & Applied Mechanics Letters*, 3(2), 15-022003.

Chapter 3) Experimental and Theoretical Investigation of Vertical Drains with Radial Inflow[2]

3.1. Introduction

Vertical drains involve a wide range of applications from stormwater flow in manholes to flood flow in tunnel spillways. Tunnel spillways are mostly designed and built in a way that the reservoir boundaries do not affect the flow. However, in manholes, the geometry can affect the flow regimes. In the literature, there are numerous studies that investigated the flow into vertical drains from large tanks (Binnie 1938, Kalinske 1940, Binnie and Hookings 1948, Anwar 1965). However, only a few studies are available on the vertical drain flow from smaller tanks. In chapter 2 the ratio of the tank diameter D to the vertical outlet pipe diameter d_o (D/d_o) was equal to 2 and 3. In their experiments, the flow into the drain was dominated by the incoming momentum. Therefore, it was interesting to study the effect of D/d_o for radial inflow for smaller values of D/d_o. It should be mentioned that in the experiments conducted by Anwar (1965), this ratio was 6. However, there was a 15 cm distance between the top of the vertical outlet pipe and the bottom of the tank, and in this case the outlet pipe may be referred to as an overflow pipe.

Binnie (1938) observed a normal rise of the depth h in the tank with the discharge Q which included two parts. For depths smaller than a certain critical depth, h_{cr}, smaller water depths were observed in the tank even for large discharges. However, beyond h_{cr}, water depth in the tank increased considerably even with a slight increase in Q. Moreover, Borda free and Borda full flow regimes were also observed. In the Borda free flow, there was a vena contracta and the central jet

[2] This chapter has been submitted as a paper to the *ASCE Journal of Hydraulic Engineering*

had the same diameter as that at the vena contracta. However, in the Borda full pipe flow, the annular water jet expanded in the outlet pipe.

Kalinske (1940) provided formulations for both flow regimes observed by Binnie (1938). He referred to the flow regime before the critical head as partially full pipe flow (PFP) regime, and after the critical head as full pipe flow (FPF) regime. He also suggested Eqs. (3.1) and (3.2) for these flow regimes in which C_k is the coefficient of discharge which varied with h/d_o in a complex manner. The entrance loss coefficient K_e was given an approximate value of 0.6. In these equations, l is the outlet pipe length, f is the Darcy-Weisbach friction factor and g is the acceleration due to gravity. From Eq. (3.1), it is seen that Q varies with h in a quadratic form.

$$Q = C_k g^{0.5} d_o^{0.5} h^2 \tag{3.1}$$

$$Q = (1/\sqrt{K_e + fl/d_o + 1})(\pi d_o^2/4)\sqrt{2g(h+l)} \tag{3.2}$$

Kalinske (1940) performed a few experiments in the FPF regime to observe $h_{cr.}$ Based on the interpolation of these two flow regime formulas, he predicted h_{cr}. Kalinske (1940) also mentioned that the occurrence of an orifice flow with a solid jet is probable for l <0.914m. Laushey (1952) carried out pressure measurements in the vertical shafts with different vortex inlet shapes and one radial entrance shape. For the radial entrance, negative pressures were observed at the top of the vertical outlet pipe; and he also observed some flow unsteadiness for this entrance geometry.

Rahm (1953) observed flow unsteadiness in the spillway tunnel of the Harspranget dam in Sweden. When the water depth increased to the same level as in full pipe flow, the spillway was not running full. Therefore, he carried out several experiments to understand this behavior. He described that before the critical depth, a weir flow pattern was observed with a central air core of varying diameter, causing development of various water stages. This unsteadiness could cause a rise in the water depth to form the Borda full flow. For this stage, the air core was cut off and the

pipe started flowing full. Then the process of filling and emptying repeated continuously. It was found that the h-Q curve for this flow regime could be represented by Eq. (3.3) in which C_{do} is the coefficient of discharge. Values of C_{do} were found to be larger for long pipes.

$$Q = C_{do}\left(\frac{\pi}{4} d_o^{\,2}\right)\sqrt{2gh} \tag{3.3}$$

However, a general formulation for C_{do} was not developed.

In the weir flow regime, Rahm (1953) reported that Q changes with h^2 as Kalinske (1940) predicted. Besides, in this flow regime, the Borda free flow occurred due to any accidental disturbance. This flow regime included two parts: firstly a weir flow regime (up to h/d_o=0.27) and then a bottom orifice flow that consisted of a small air core and followed Eq. (3.3) with C_{do}=0.6 for all series of experiments. At the end, Rahm (1953) analyzed the h-Q curve of the Harspranget dam and found that the observed unsteadiness was related to the occurrence of the Borda Full flow with C_{do}=0.65. Anderson (1961) also observed unsteadiness of the radial flow in the vertical drain shafts and also reported the risk of cavitation at the top of the vertical outlet pipe because of large negative pressures. Both Anderson (1961) and Laushey (1952) recommended the use of vortex inlet entrance shape to ensure the steadiness of water depth and a single h-Q curve in drop shafts.

The use of vertical drains in manholes or sewer systems is unavoidable. The use of drill drop manholes in the city of Edmonton, which were studied in chapter 2, is an example of such structures. In fact, a similar filling and emptying process as described before was observed with the difference that the filling and emptying was the only flow regime that could occur for a range of discharges. Therefore, it was called the filling and emptying (FE) regime. A normalized discharge Q^* defined by Eq. (3.4) with the normalized depth h/d_o could represent the dimensional variation of discharge with water depth.

$$Q^* = \frac{Q}{\sqrt{g d_o^{\,5}}} \tag{3.4}$$

It was found that for $0.61<Q^*<1.65$, the FE regime occurred. However, for $Q^*<0.6$, a stable pool with an air core was observed (the SP regime) and for $Q^*>1.65$, the pipe was running full (the FPF regime).

In the studies discussed above, two forms of entrance shapes were included; the drain inlet was either at the bottom of the tank or at some vertical distance above the bottom. The former was called drain pipe and the latter was called overflow pipe by Kalinske (1940). His experiments along with those of experiment in chapter 2 are the only experiments that include the *h*-*Q* curve for drain pipes. Moreover, Kalinske (1940) did not observe the Borda full flow, in contrast to Binnie (1938). Therefore, the experiments in this study were designed to cover a wider range of D/d_o ratios from 5.0 to 9.7 and provide a better understanding of the flow for radial inflow. Besides, the occurrence of the Borda free, Borda full flow and different stages of weir flow patterns were examined and *h*-*Q* formulations are presented herein

3.2. Experimental Arrangement and Experiments

The experiments were conducted in the T. Blench hydraulics laboratory at the University of Alberta. Water was pumped to a pressure tank which provided pressurized flow through a pipe of diameter of 150 mm to a manifold. The manifold with four smaller pipes with diameter of 52 mm supplied water to the bottom of a large vertical cylindrical tank with an inner diameter of D= 0.932 m and a length of L= 722 mm. These inlets were arranged 90 degrees apart (in plan) around the circumference of the tank, near the inner wall. The inlet inner diameters were d_i = 49 mm. A vertical outlet pipe with an inner diameter of d_o = 76 mm and a length l of 1219 mm was concentrically attached to the bottom of the large cylindrical tank. The entrance of this vertical

outlet pipe was a square-edge. The pipe length and diameter used were the same as those used in chapter 2 and by Kalinske (1941). Fig. 3.1 shows the definition sketch of these experimental arrangements and Fig A1.17 shows the pictures of them.

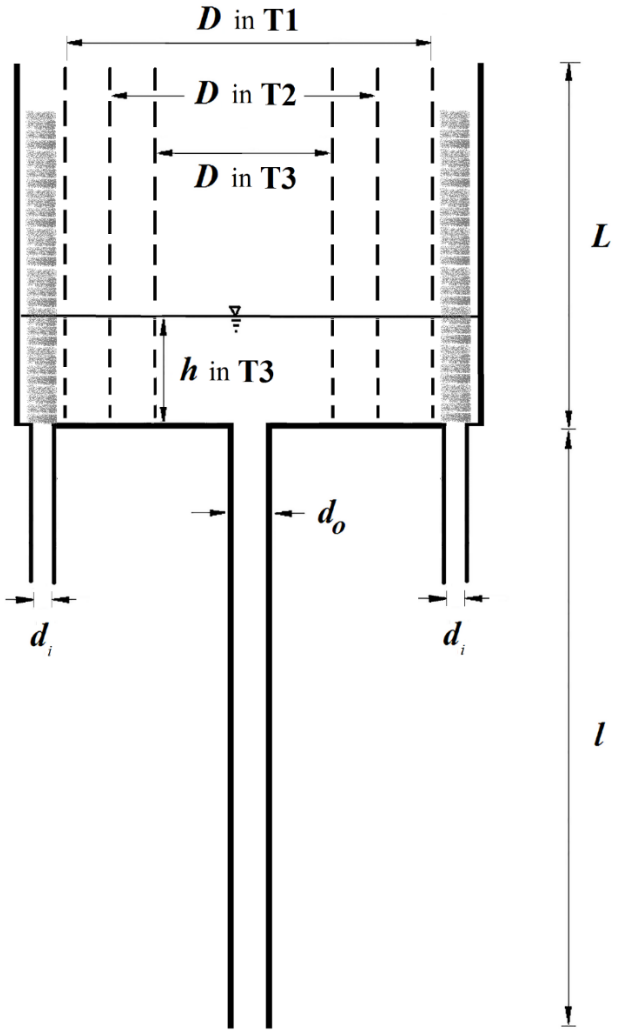

Fig. 3.1 Definition sketch of experimental setup

To study the effect of tank sizes, cylindrical perforated sheets were used with a width equal to the tank height. These sheets were 3.2 mm thick with 3.2mm diameter holes (40% porosity) and were flexible enough to bend to form cylinders of different diameters to be installed inside the large tank. For the first series of experiments (T1), a perforated cylinder with a diameter of 740mm was formed. Besides, diffusers were installed inside the gap between the inner side of the tank and

outer side of the perforated cylinder and exactly on top of the inlets to destroy the momentum of the incoming jets from the inlets and ensure a radial flow towards the outlet pipe. The D/d_o ratio in this arrangement was equal to 9.74. Then, a second perforated cylinder with a diameter of 608mm was added to the T1 setup which was called T2 (D/d_o=8). Later, a third perforated cylinder with a diameter of 380mm was added to the T2 setup and was called T3 (D/d_o=5). In each step, by adding an extra cylinder, the effective diameter of the tank was reduced. In the last series of experiments (T4), all perforated cylinders and diffusers were removed and flow was allowed to drain freely through the vertical outlet pipe (D/d_o=12.24). Table 3.1 shows the details of the experiments. Water depth in all of the setups was measured at four points inside the innermost perforated sheet.

Table 3.1 Details of experiments

Series Name	Comment	Effective *D (mm)*	D/d_o	Coefficient of discharge for OF
T1	One perforated cylinder	740	9.74	0.65
T2	Two perforated cylinders	608	8	-
T3	Three perforated cylinders	380	5	0.67
T4	Without perforated cylinder	930	12.24	-

Experiments in T1 series showed that firstly, at Q=1.04 L/s the classical weir flow existed. Then, for Q=2.15 L/s, the nappe clinged to the inner wall of the lower pipe resulting in a weir-like flow regime with an annular jet in the outlet pipe which included a central air core. Fig. 3.2a shows this flow regime. It is believed that the negative pressure at the top of the vertical outlet pipe caused this clinging. During the experiments, some frequent gulping could be observed that resulted in choking. At this time, some circulation was initiated which caused the annular jet to change to a central jet and separate from the inner walls of the lower pipe. Water depth at this stage increased until it reached a certain value h and then stayed constant. Fig. 3.2b shows this orifice flow (OF)

regime. Data analysis showed that Q varied as $h^{0.5}$ as shown in Eq. (3.3) with C_{do}=0.65. This was called the orifice flow (OF) regime. Fig A1. 18 also shows these flow regimes.

It was found that disturbing the flow field could change this flow regime into the weir-like flow and vice versa; e.g. a rod was inserted from the top to approach the air core or inserted from the bottom of the vertical outlet pipe to protrude into the air core in the central jet. Besides, it was observed that in one experiment (Q=5.7L/s), after disturbing the flow which resulted in the weir-like flow, different water stages were established.

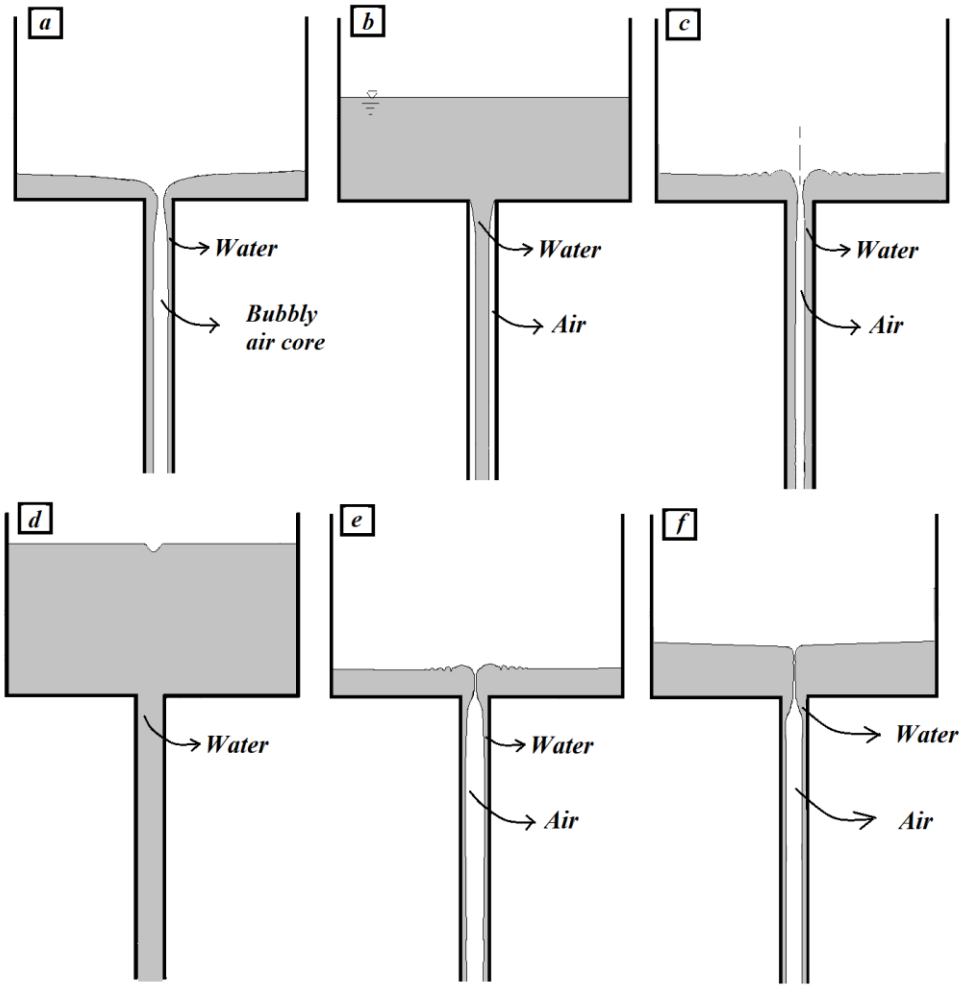

Fig. 3.2 Different flow regimes in the tank. a) Weir flow (WF) regime, b) Orifice flow (OF) regime, c) Transition flow (TF), d) Full pipe flow (FPF) regime, e) First stage of filling and emptying (FE1) process, f) First part of the third stage of filling and emptying (FE3-1) process

For 16.7 ≤ Q <19.27 L/s, a swirling air core was observed with a frequently changing diameter. The water surface was oscillating and it was found that disturbing the flow could change the air core size and the corresponding water depth by approximately 30%. Such a flow regime is shown in Fig. 3.2c. For $Q \geq 19.27$ L/s, the pipe was running full (Fig. 3.2d) with a small dimple at the water surface with or without a very thin air core. In cases where this air core was not clearly observable, dye injection was used for visualization. The *h-Q* curve for this series of experiments is shown in Fig. 3.3.

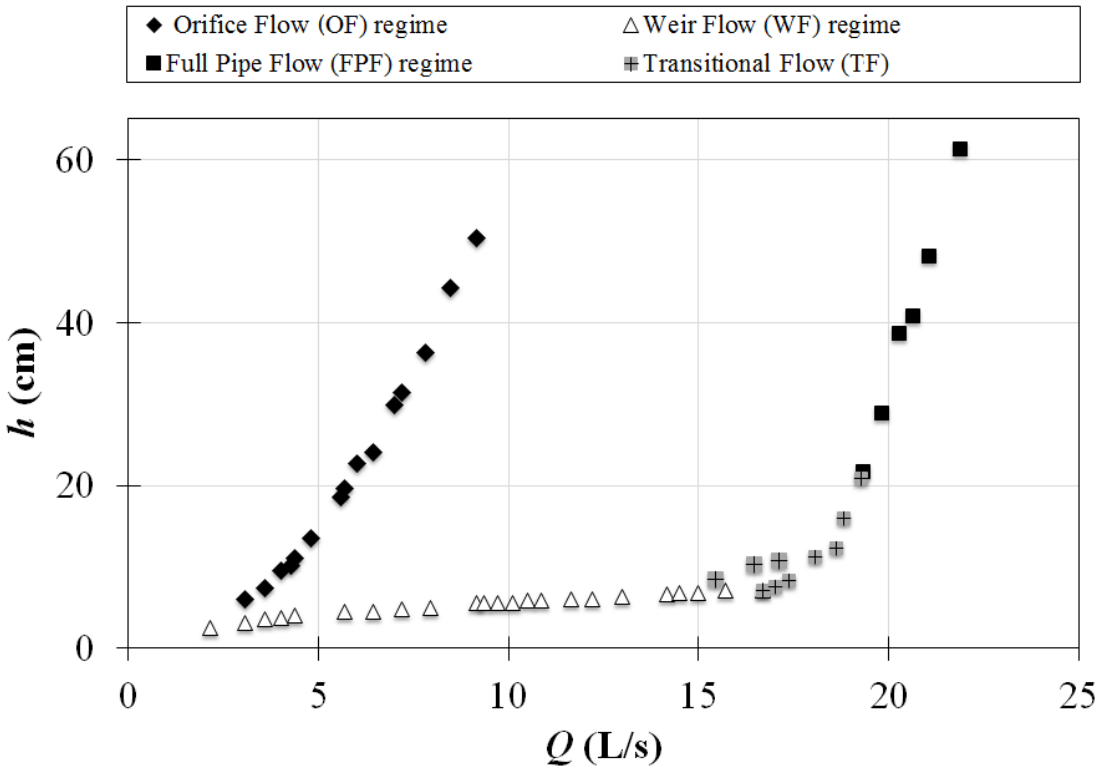

Fig. 3.3 The head discharge (*h-Q)* curve in T1 series

The experiments conducted with two perforated cylinders (T2 Series) revealed similar flow regimes that were described before for series T1 except that the OF regime will not form. Moreover, several water stages occurred for a larger range of discharges. In this series of experiments, unsteadiness in the water stages was observed which caused a Filling and Emptying (FE) process. It was found that, in general, three water stages could be distinguished in addition to

the weir flow which was the most stable one. The first stage had a depth slightly more than the weir-like flow but with a raised water depth around the top of the vertical outlet pipe due to the existence of some circulation; i.e. FE1 (Fig. 3.2e). Later this air core raised the water depth further to achieve FE2 or FE3 (Fig. 3.2f) and then the water depth changed to produce weir-like flow. In this process, the gulping noise disappeared but the flow was very unstable and water depth changed to the weir-like flow frequently. Flow in the vertical outlet pipe varied from an annular jet with entrained air in its central core to a less aerated and clear annular jet which expanded in the whole length of the pipe. It was observed that disturbing the flow could produce this process too. The *h*-*Q* curve for this series of experiments is shown in Fig. 3.4.

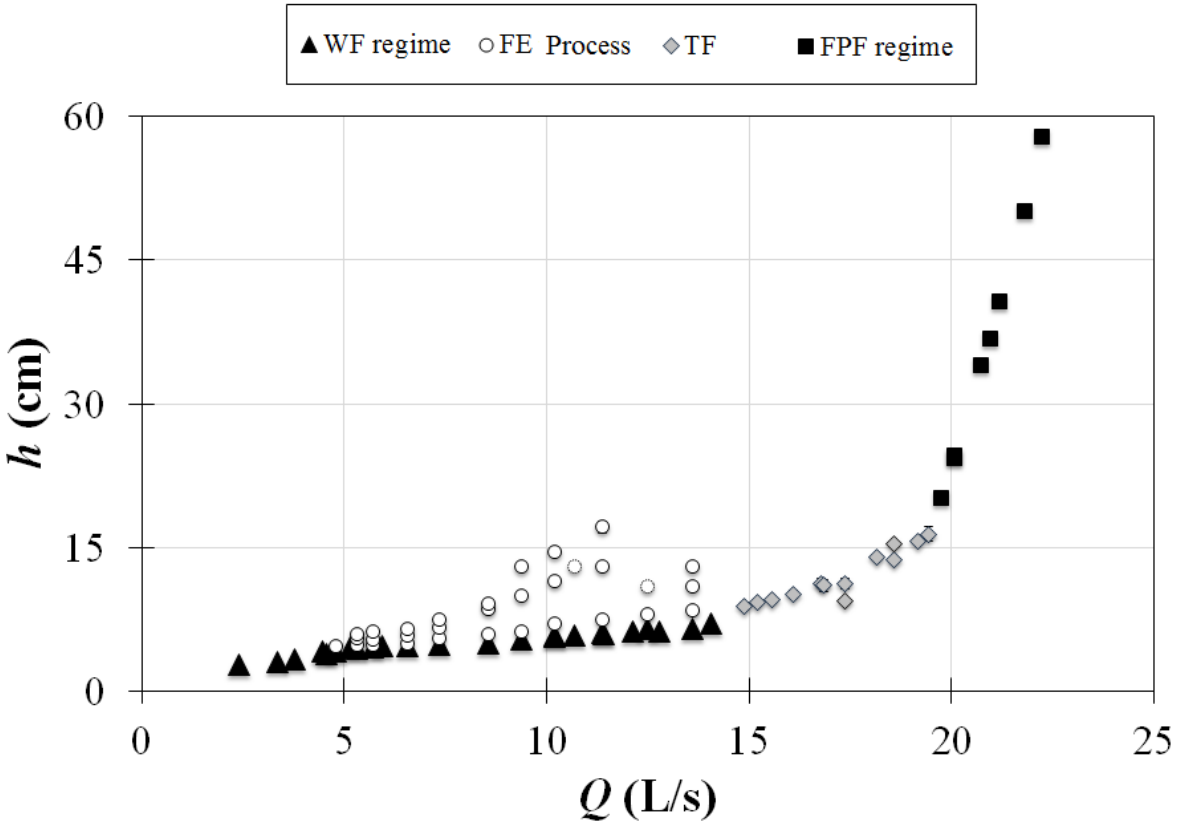

Fig. 3.4 The *h*-*Q* curve in T2 series

In the series with three perforated cylinders (T3), flow regimes similar to those observed in the T2 series were observed as shown in Fig. 3.5 with the appearance of the orifice flow regime

(C_{do}=0.67). However, the FE process was observed only in a smaller discharge range of 5.35 to 7 L/s. For Q > 7 L/s the weir-like flow was quite persistent and no swirling air core was observed. Besides, by inserting any disturbance, the weir-like flow would change to the OF flow. However, it was not as stable as in T1 and changed to the weir-like flow comparatively fast. In the last series of experiments (T4), the filling and emptying (FE) regime was observed for Q<19.23L/s as was described in chapter 2. Then, the FPF regime occurred.

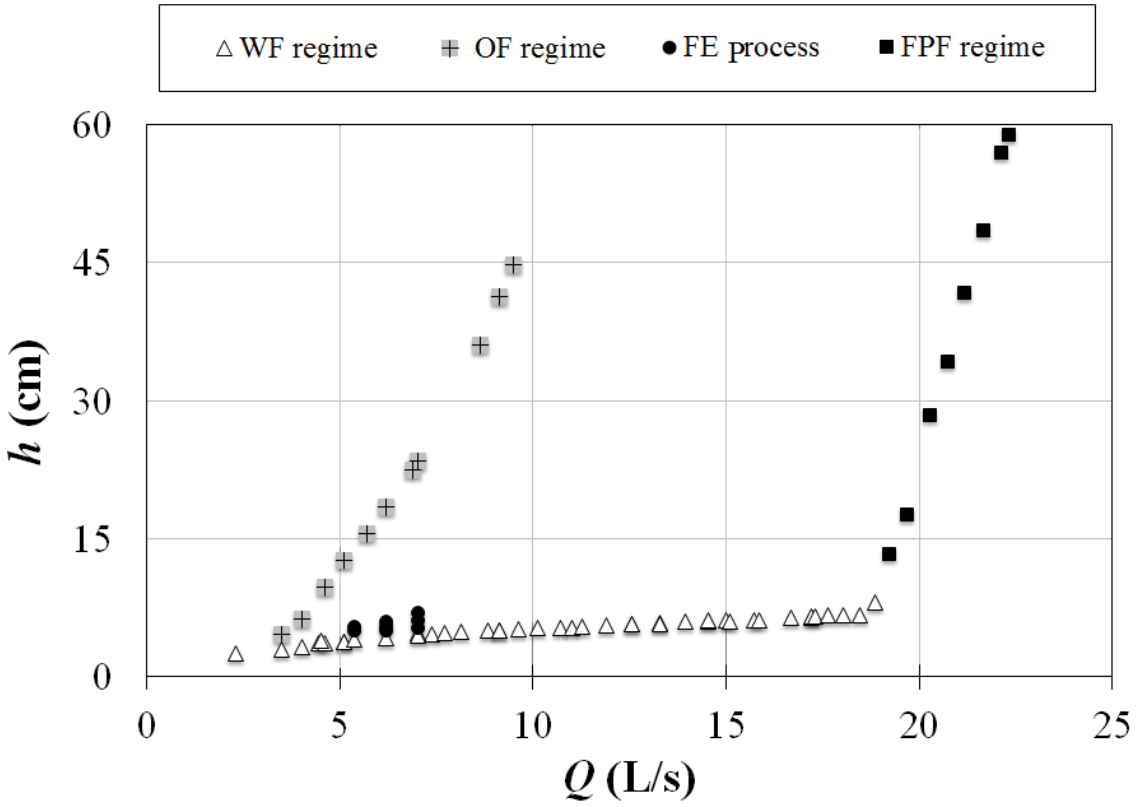

Fig. 3.5 The *h*-*Q* curve in T3 series

3.3. Analysis of the Experimental Results

3.3.1 Steady Flow Regimes

The *h*-*Q* curve in the weir-like flow was compared with the weir formula presented in Eq. (3.5) and Kalinske formula as shown in Eq. (3.1). For this purpose, the coefficient of discharge C_d

in terminal weirs with a height of p (Kandaswamy and Rouse, 1957) was used as shown in Eq. (3.6). In the current study (p=0). Therefore, C_d=1.06 was used.

$$Q = \frac{2}{3}\sqrt{2g}C_d \pi d_o h^{1.5} \tag{3.5}$$

$$C_d = 1.06(1+\frac{P}{h})^{3/2} \tag{3.6}$$

The Kalinske formulation also represented the h-Q. However, the Kalinske formula was dependent on C_k with a complex variation with h/d_o. Therefore, considering the weir formula in Eq. (3.5), the behavior of the coefficient of discharge C_d was studied. It was found that a linear relationship existed between C_d and h/d_o. This could partially explain the Kalinske formulation wherein Q varied with h^2. Combining Eq. 3.5 and 6, Q varies with $h^{2.5}$. Then, the Kalinske data for drain pipes (open symbols in Fig. 3.6) were analyzed and similar results were found. Therefore, the h-Q curve in T1 which was related to the largest D/d_o ratio of the current study and Kalinske (1940)'s data were used and C_d was calculated as Eq. (3.7) with R^2= 0.82.

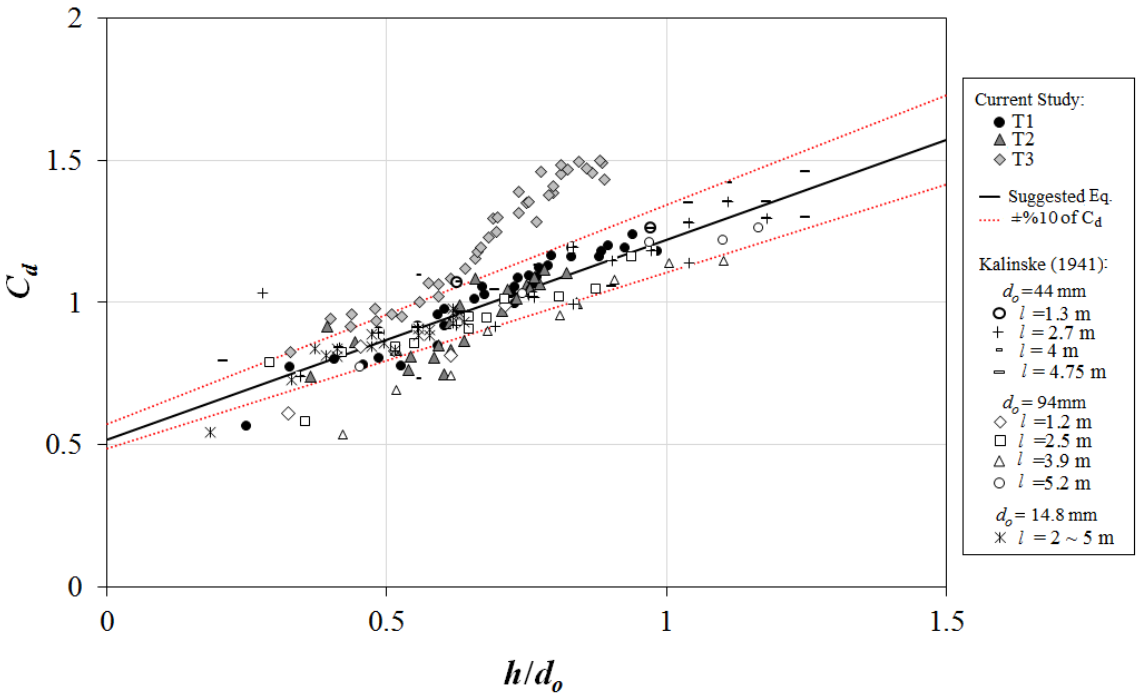

Fig. 3.6 Variation of C_d with h/d_o

It should be mentioned that the data for the T2 and T3 series were not included in this correlation. It can be seen that most of data are within the range of ±10% of C_d for each Q. As a result, for this weir flow regime, following equation is suggested for the discharge coefficient in Eq. 3.5

$$C_d = 0.7\frac{h}{d_o} + 0.52 \tag{3.7}$$

Comparison of C_d for T2 and T3 series of experiments is shown in Fig. 3.6. It can be seen that the same formula describes reasonably well the data for the T2 series. However, C_d values in T3 series were larger.

Moreover, weir equation of Eq. (3.5) could be normalized as shown in Eq. (3.8). Since C_d was a function of only h/d_o, Q^* would also be a function of only h/d_o. Such a comparison for the current data in the WF regime and the Kalinske (1940)'s data is shown in Fig. 3.7. It can be seen that except for T3 series in which water depths were smaller than the depths in the T1 and T2 series, there is good agreement between the experimental data and Eq. (3.8).

$$Q^* = \frac{Q}{\sqrt{g\, d_o^5}} = \frac{2}{3}\sqrt{2}C_d\pi\left(\frac{h}{d_o}\right)^{1.5} \tag{3.8}$$

For $Q \geq 19.23$ L/s, the FPF regime occurred without any swirling flow. However, for the T1 and T2 series, the swirling air core was observed between the WF and FPF regime. For this flow, data analysis showed that Q varied with $h^{0.5}$. This flow regime was called transition flow (TF). As a result, current series of experiments showed that Kalinske (1940) possibly missed the occurrence of this transition flow in his experiments.

In the FPF regime, Kalinske (1940) suggested the entrance loss coefficient K_e to be equal to 0.6. However, it was found that K_e was equal to 0.1, 0.125 and 0.15 in T1, T2 and T3 series. Full pipe flow can be described by applying the energy equation between the water surface in the

tank and the end of the outlet pipe with a proper value for the friction factor of the outflow pipe. Moreover, h_{cr} in Kalinske's (1940) formulation was reexamined based on his experimental data (l/d_o between 12.9 to 108) and Eq. (3.9) is suggested (R^2= 0.93). In the current study, l/d_o=16.04 so h_{cr} was calculated to be 77mm. This was actually very close to the experimental values of h=71mm in T1 at the change from WF to TF.

$$\frac{h_{cr}}{d_o} = 0.707\left(\frac{l}{d_o}\right)^{0.12} \tag{3.9}$$

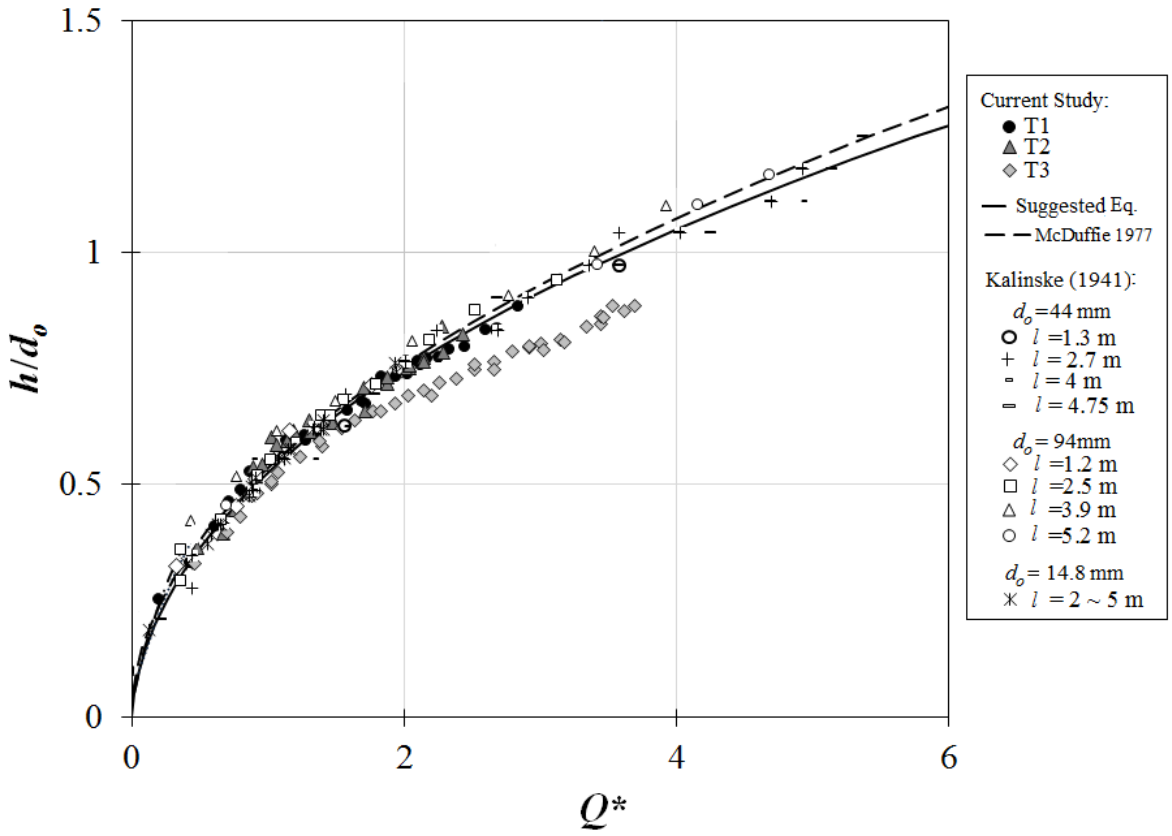

Fig. 3.7 Comparison of dimensionless h-Q curves in different series of the current study and Kalisnke (1941) experiments for weir flow (WF) regime.

3.3.2. Unsteadiness of Flow in the System

In the WF regime, gulping occurred frequently which could result in the formation of an air core while the annular flow existed in the outlet pipe. As soon as the air core formed, the water

depth in the tank increased to establish a steady depth. Such a steady depth, encompasses an irrotational vortex which is the most desirable flow regime in vortex drop manholes (VD). In VD, water is supplied tangentially in the tank. However, in this study, the water was supplied radially and could not form such a steady air core. Moreover, the steady air core requires a minimum discharge to be supplied. Therefore, other flow conditions such as a weir control section can determine the water depth.

The increased water depth under the weir control condition in which Rankine combined vortex theory applies was called FE1. If the depth increased beyond that of the FE1, two possibilities existed. For a smaller discharge Q, it was likely that the control section moved further down in the outlet pipe. The circulation in the flow increased and caused a further increase of the depth in the tank. This study shows that for a critical air core size, the control section forms at the bottom end of the outlet pipe. The flow regime under this flow condition was referred to as FE3-1. If the control section formed between the extremes, then the FE2 regime developed. At a large Q, the incoming radial flow was so dominant that it prevented the air core from moving the control section. Under this condition, the flow was controlled by the weir action and the irrotational vortex theory and called FE3-2.

In order to theoretically describe this unsteadiness, it is necessary to present the formulation for the steady irrotational vortex flow. For this purpose, consider such a flow in a setup with an identical geometry to that of the current study (Fig. 3.8).

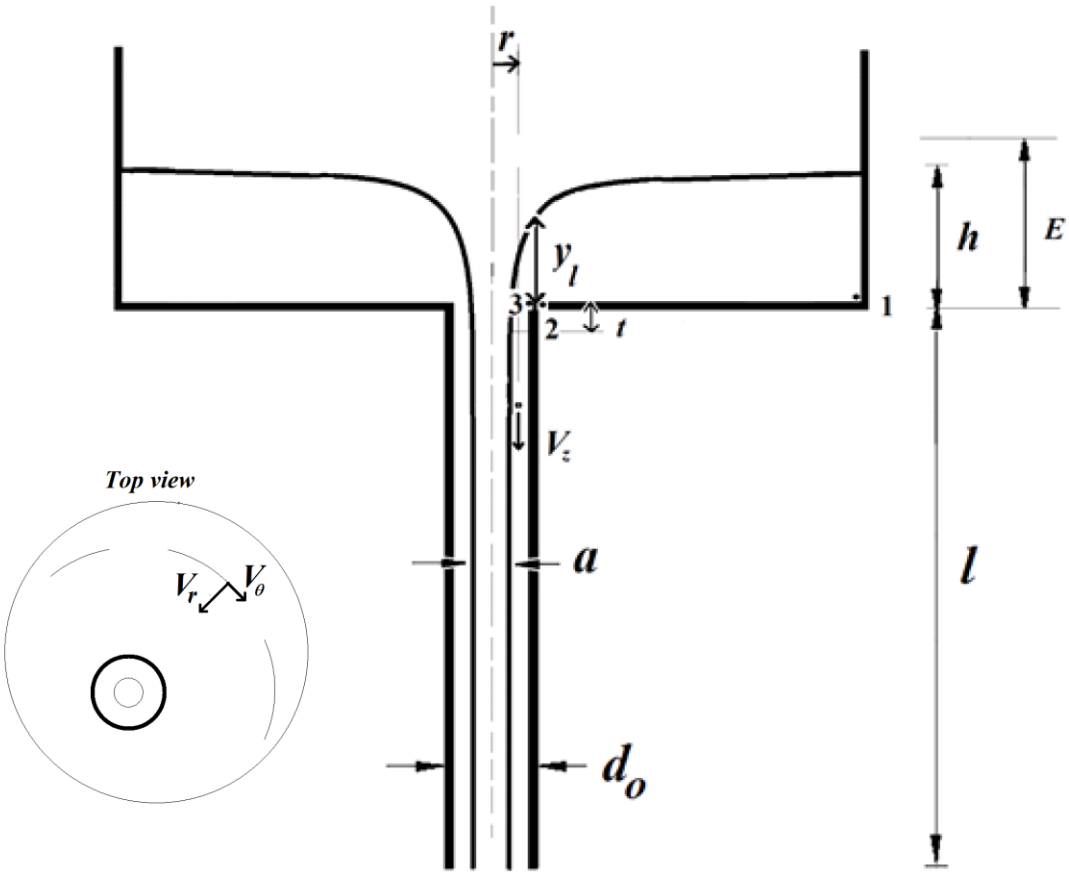

Fig. 3.8 Definition sketch for theoretical analysis

It was found that the control section is located at a small distance of t below the entrance of the outlet pipe. Such an offset distance was also observed by Rahm (1953). At this control section, the air core diameter a reaches a minimum value followed by an increase to a nearly constant value. In this irrotational vortex flow, the tangential velocity V_θ is equal to C/r where C is the vortex circulation and the Bernoulli equation can be applied to any two points in the tank. This means that the total energy E is constant everywhere and is written as

$$E = \frac{C^2}{2gr^2} + y \tag{3.10}$$

The required discharge to generate such a steady irrotational vortex Q_{rc} will be,

$$Q_{rc} = \int_{do/2}^{D/2} V_\theta y dr = \int_{do/2}^{D/2} \frac{C}{r}(E - \frac{C^2}{2gr^2})dr = EC\ln(\frac{D}{d_o}) - \frac{C^3}{g}(\frac{1}{d_o^{\,2}} - \frac{1}{D^2}) \quad (3.11)$$

From the Bernoulli equation with the datum at t:

$$E + t = \frac{P}{\gamma} + \frac{V_z^{\,2} + C^2/r^2}{2g} \quad (3.12)$$

where, P is the pressure at radius r and V_z is the vertical velocity in the annular cross section confining the air core. P can be found from the Bernoulli equation between radius r and air/water interface as

$$\frac{C^2}{2gr^2} + \frac{P}{\gamma} + \frac{V_{zr}^{\,2}}{2g} = \frac{C^2}{2g(a/2)^2} + \frac{P_{air/water}}{\gamma} + \frac{V_{zair/water}^{\,2}}{2g}$$

Since $P_{air/water}$=0 and V_z is constant in the same datum,

$$\frac{P}{\gamma} = \frac{C^2}{2g}(\frac{4}{a^2} - \frac{1}{r^2}) \quad (3.13)$$

Considering the fact that the vertical velocity V_z is equal to the $Q/(\pi/4(d_o^2\text{-}a^2))$, From Eq. (3.12) it can be shown that

$$Q = \pi(\frac{d_o}{2})^2(1 - \frac{a^2}{d_o^{\,2}})\sqrt{(2g(E+t) - \frac{4C^2}{a^2})} \quad (3.14)$$

Now, by applying the principle of maximum discharge which assumes that the maximum flow will tend to pass the drain at a minimum air core size ($\partial Q/\partial a$=0), we will have,

$$a^2 = \frac{1}{2g(E+t)}\left(C^2 + \sqrt{(C^4 + 4d_o^{\,2}C^2g(E+t))}\right) \quad (3.15)$$

Binnie and Hookings (1948) developed equations similar to Eqs. (3.12) to (3.15) to predict a and C for a specific h and Q inside a bellmouth with a length of t at the entrance of a vertical overflow pipe. It was found that Eq. (15) cannot calculate a for a small t. Later, Ackers and Crump (1960) defined $f=a^2/d_o^2$ and used ($\partial Q/\partial f$=0) to present a more general equation in a bellmouth

entrance in VD. Following Ackers and Crump (1960) in defining f and then ($\partial Q/\partial f$=0), Eq. (3.16) can be calculated.

$$E + t = \frac{C^2}{ga^2}\left(\frac{d_o^{\,2}}{a^2} + 1\right) \tag{3.16}$$

In this study, it is found that by solving Eqs. (3.11), (3.14) and (3.16), the h-Q curve and the related a and C for an irrotational vortex flow can be calculated. Values of C for a range of a/d_o (0.7 to 0.97) and t/d_o=0.2 are shown in Fig. 3.9.

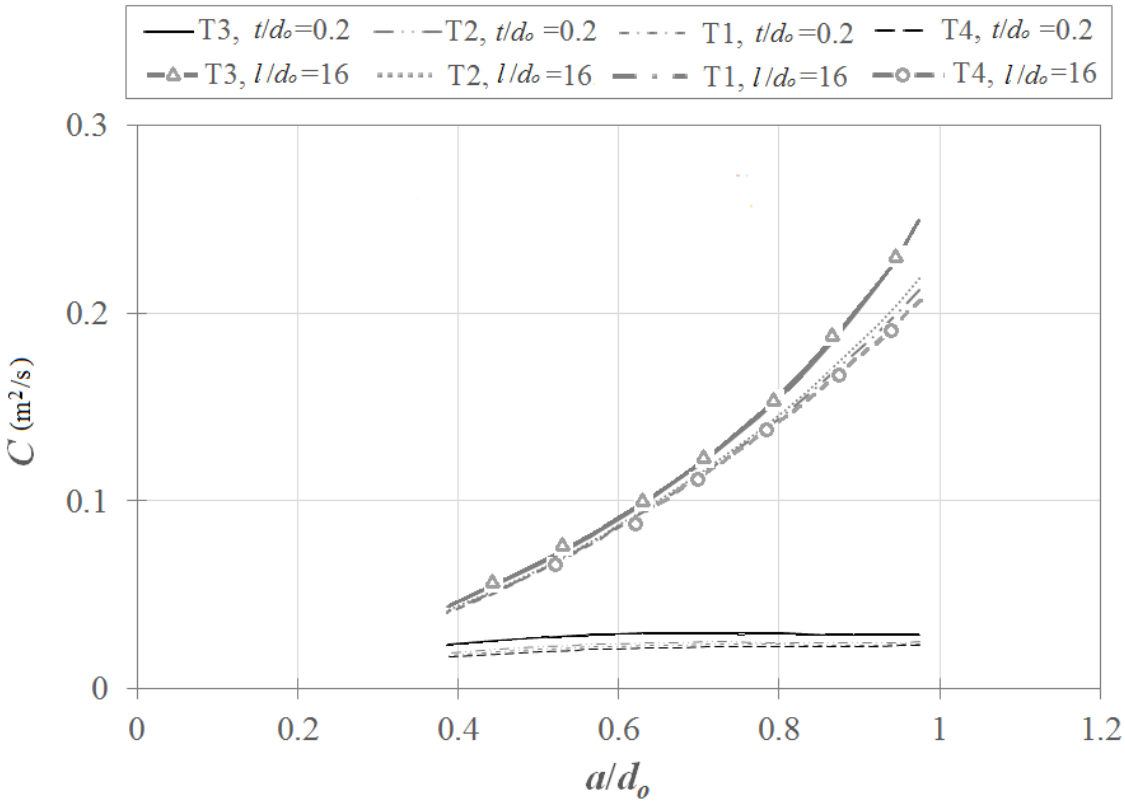

Fig. 3.9 Comparison of C in different series of the current study versus a/d_o and t/d_o or l/d_o.

It was found that for t/d_o=0.2, C remained almost constant and this distance (t=0.2d_o) is similar to the experimental observation of the smallest air core size distance. For T2, C was found to be about 0.0247 m^2/s with a standard deviation σ=2.6×10^{-4}. Besides, C was found to change only slightly with D/d_o.

As mentioned before, the steady irrotational vortex could not be observed in the tank. As soon as the air core formed, the water depth inside the tank was increased and water depth just at the top entrance of the outlet pipe y_l became larger than h ($y_l > h$). It is found that a Rankine vortex model can represent the flow in the first stage of the FE process, i.e. FE1. A Rankine vortex model states that the flow field consisted of a solid body rotation from centerline of the outlet pipe extending to $r=d_o/2$ and then an irrotational vortex. This can be followed by a transition to the radial flow in which the tangential velocity decreases with the distance.

In a solid body rotation, between every two points on a streamline, the term below (Eq. (3.17)) is constant

$$\frac{V_r^2}{2g} + \frac{P}{\gamma} - \frac{V_\theta^2}{2g} \tag{3.17}$$

where, V_θ is the tangential velocity and V_r is the radial velocity.

On the other hand, writing Bernoulli equation between points 1 and 2 ($r=d_o/2$) of Fig. 3.8 which are in the same streamline state

$$E = \frac{V_r^2}{2g} + \frac{P}{\gamma} + \frac{V_\theta^2}{2g} \tag{3.18}$$

Since the head related to the radial velocity is small, E can be replaced by h.

In Fig. 3.8, point 2 is located at $r=d_o/2$ in the irrotational vortex part and point 3 is located at $r=d_o/2$ but in the solid body rotation part. At the same streamline between point 1 and 3, E can be found to be

$$E = \frac{V_r^2}{2g} + \frac{P}{\gamma} - \frac{V_\theta^2}{2g} \tag{3.19}$$

V_θ should be constant between two points of 2 and 3 to avoid discontinuity and it can be found from irrotational vortex formulation to be equal to $C/(d_o/2)$. V_r is the radial velocity and equal to $Q/(\pi d_o y_l)$. The term (P/γ) also can be replaced with y_l by neglecting curvature as,

$$E = \frac{Q^2}{2g(\pi d_o y_l)^2} + y_l - \frac{C^2}{2g(d_o/2)^2} \tag{3.20}$$

By applying the "principle of maximum discharge" or "minimum energy" concept ($\partial E/\partial y_l$=0)

$$\frac{\partial E}{\partial y_l} = 0 \Rightarrow 0 = -\frac{2Q^2}{2g\pi^2 {d_o}^2 {y_l}^3} + 1 - 0 \quad \Rightarrow Q^2 = \pi^2 g {d_o}^2 {y_l}^3 \Rightarrow Q = \pi d_o \sqrt{g} {y_l}^{3/2}$$

$$E = -\frac{2C^2}{g d_o^2} + \frac{\pi^2 g {d_o}^2 {y_l}^3}{2g(\pi d_o y_1)^2} + y_l \Rightarrow E = -\frac{2C^2}{g d_o^2} + \frac{3}{2} y_l \Rightarrow y_l = \frac{2}{3}(E + \frac{2C^2}{g d_o^2})$$

$$Q = \frac{2\pi d_o \sqrt{2g}}{3\sqrt{3}} \left(E + \frac{2C^2}{g {d_o}^2} \right)^{(3/2)} \tag{3.21}$$

The representative h-Q curve for C=0.0247 m^2/s was calculated and plotted as shown in Fig. 3.10. It was found that this line matched the h-Q curve in FE1. Moreover, this line also represents some of the observed water depths in TF in both T1 and T2 series and the lower branch of the FE regime in T4.

If the water depth increases beyond FE1 and discharge is small enough to allow for the control section to move, then the control section can be located at the bottom of the outlet pipe. At this control section,

$$E + l = \frac{P}{\gamma} + \frac{{V_z}^2 + C^2/r^2}{2g} \tag{3.22}$$

A similar analysis of the vertical velocity, discharge and air core based on the principle of maximum discharge will result in:

$$Q = \pi(\frac{d_o}{2})^2(1-\frac{a^2}{d_o{}^2})\sqrt{(2g(E+l)-\frac{4C^2}{a^2})} \tag{3.23}$$

$$a^2 = \frac{1}{2g(E+l)}\left(C^2+\sqrt{(C^4+4d_o{}^2C^2g(E+l))}\right) \tag{3.24}$$

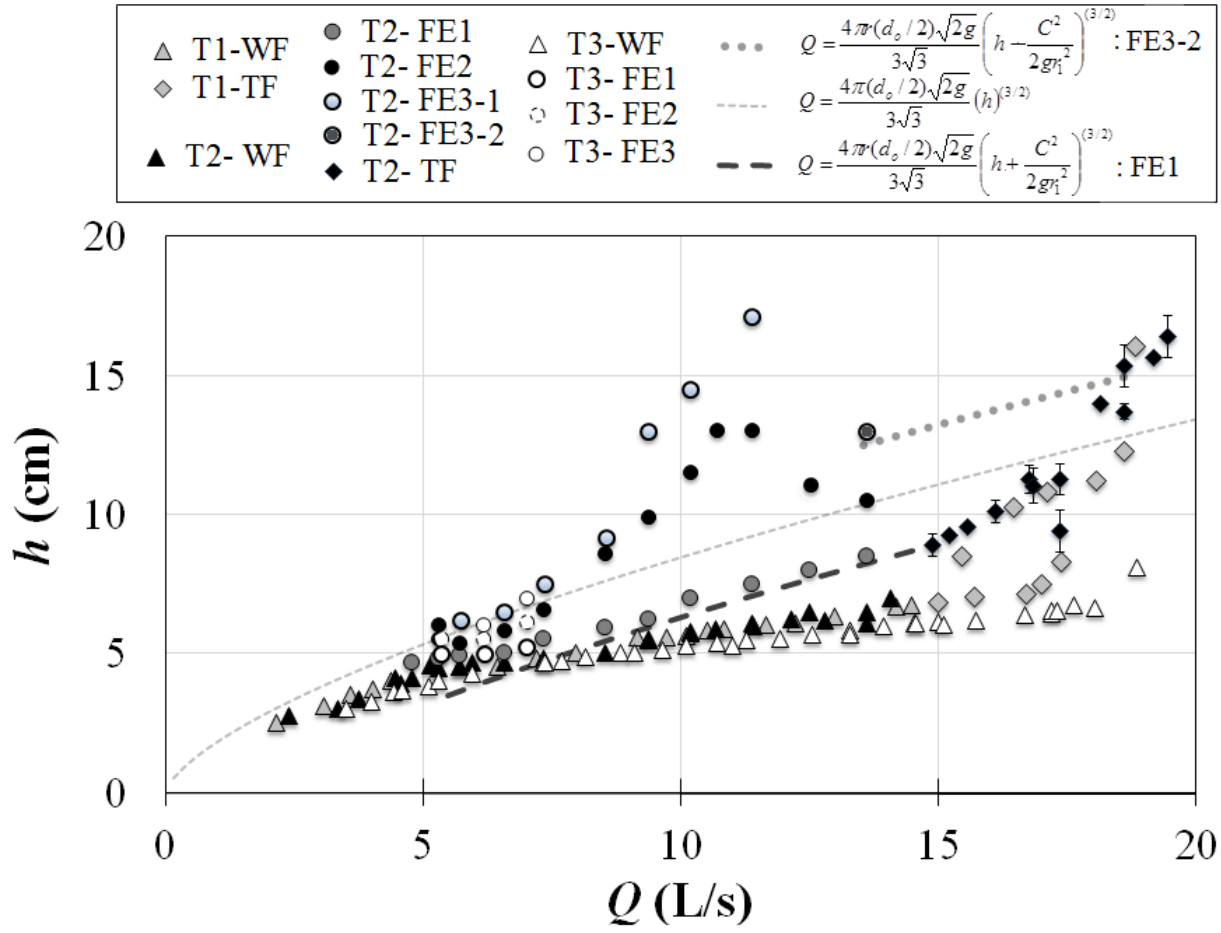

Fig. 3.10 Comparison of *h*-*Q* curves of different flow regimes in T1, T2 and T3 setups with the suggested formula

These formulas were used to evaluate the variation of a/d_o with Q^* for the water depths in FE2 and FE3-1 ($Q \leq 11.4$L/s) as shown in Fig. 3.11. Moreover, the field measurements at the Harspranget dam in Sweden as presented by Rahm (1953) as well as his own experimental data were also analyzed and are shown in Fig. 3.11.

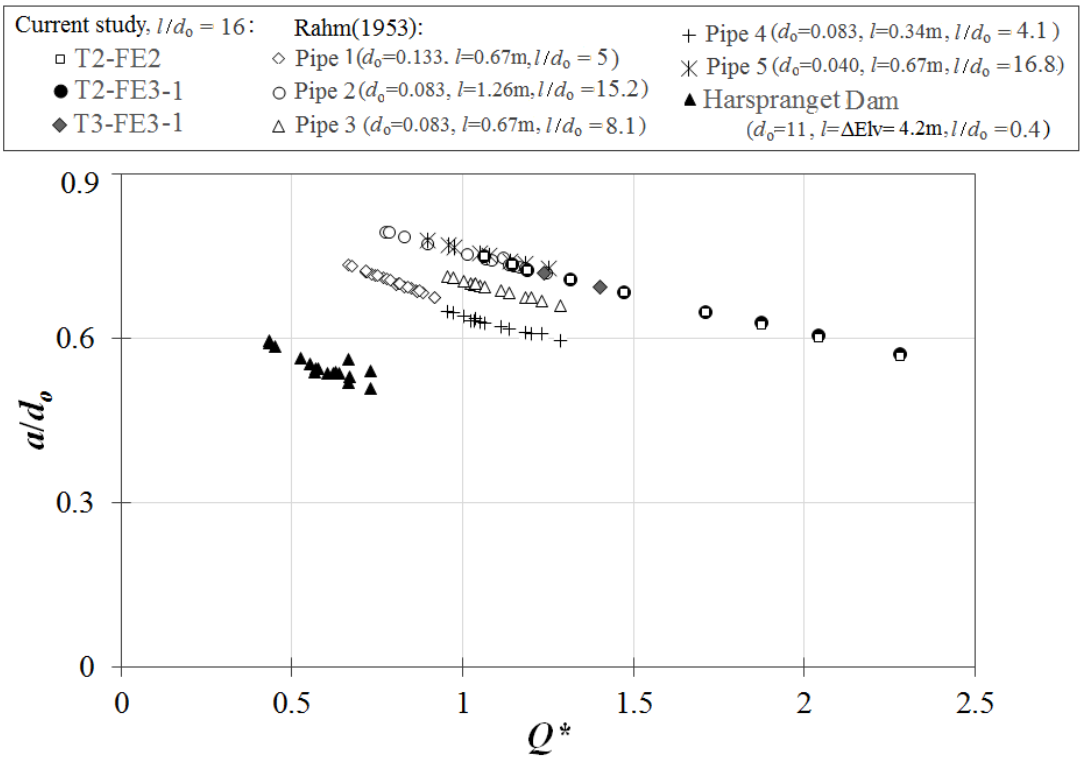

Fig. 3.11 Variation of a/d_o with Q^*

It can be seen that although the general trend is a decrease in a/d_o with increasing Q^*, an average value of 0.7 with σ=0.05 can be selected for the experimental data of Rahm (1953) and the current study. For the Harspranget dam, the bellmouth shape at the entrance resulted in an average value of critical a/d_o of 0.67 with σ=0.07. Therefore, this method provides a universal description of the maximum unsteady water depth in FE3-1 which is also known as Borda Full flow. It should be mentioned here that l/d_o for the current study was equal to 16 and in the experimental setup of Rahm (1953) varied from 4 to 16.6. Rahm (1953)'s experiments included overflow pipes at the end of a canal in which the walls could affect the flow as current experiments in T2. For the Harspranget dam, the difference in elevation of the inlet and the outlet was used as to represent l. The calculated values of C for l/d_o= 16 is also shown in Fig. 3.9.

It was found that if the discharge was large enough to prevent the complete development of the air core in the total length of the outlet pipe and relocation of the control section, a weir

control section could form in which an irrotational vortex assumption was applied. In this weir control section, h was larger than y_l and the air core was completely different in form when compared to that in FE1 and called FE3-2. A value of C equal to 0.0247 m^2/s was used to plot Eq. (3.29) as shown in Fig. 3.10. Also, this line represents the average water depths in the upper branch of the FE regime in the T4 series of experiments.

$$E = \frac{V_\theta^{\,2}}{2g} + \frac{V_r^{\,2}}{2g} + \frac{P}{\rho g} \tag{3.25}$$

$$E = \frac{C^2}{2g(d_o/2)^2} + \frac{Q^2}{2g(\pi d_o y_l)^2} + y_1 \tag{3.26}$$

By applying the "principle of maximum discharge" or "minimum energy" concept ($\partial E/\partial y_l$=0),

$$\frac{\partial E}{\partial y_l} = 0 \Rightarrow 0 = 0 - \frac{2Q^2}{2g\pi^2 d_o^{\,2} y_l^{\,3}} + 1 \quad \Rightarrow Q^2 = \pi^2 g d_o^{\,2} y_l^{\,3} \Rightarrow Q = \pi d_o \sqrt{g}\, y_l^{\,3/2} \tag{3.27}$$

$$E = \frac{2C^2}{gd_o^2} + \frac{\pi^2 g d_o^{\,2} y_l^{\,3}}{2g(\pi d_o y_l)^2} + y_l \Rightarrow E = \frac{2C^2}{gd_o^{\,2}} + \frac{3}{2} y_l \Rightarrow y_l = \frac{2}{3}\left(E - \frac{2C^2}{gd_o^{\,2}}\right) \tag{3.28}$$

Combining these two equations, we get,

$$Q = \frac{2\pi d_o \sqrt{2g}}{3\sqrt{3}} \left(E - \frac{2C^2}{gd_o^{\,2}} \right)^{(3/2)} \tag{3.29}$$

Eq. (3.29) was firstly represented by Ackers and Crump (1960) in the weir control section of VD. In Eq. (3.29), it was found that in the case of C equal to zero (as in Eq. (3.30)), the representative h-Q curve could represent the water depth in one of the experiments in FE2 and the mid line between the upper branch and lower branches of the FE regime in T4. This line is also shown in Fig. 3.10.

$$Q = \frac{2\pi d_o \sqrt{2g}}{3\sqrt{3}} h^{3/2} \tag{3.30}$$

3.4. Further Discussion

Another aspect of studying the drain in vertical outlet pipe from a large tank is the large amount of air that can be trapped. Therefore, researchers were mostly interested in predicting a minimum water depth that could prevent this air core to hit the entrance of the vertical outlet pipe. Several researchers such as Souders (1938), Harleman (1959) or Lubin and Springer (1967) studied this subject. McDuffie (1977) reanalyzed the experiments of Kalinske (1940) and predicted a conservative value as Eq. (3.31) as shown in Fig. 3.7. In this equation, Q varied by h^2 as shown by Kalinske (1940)

. It can be observed that the McDuffie (1977) equation is in good agreement with the results of the current study. However, as was shown in the analysis of the experiments, the variation of Q with h^2 was not a proper way to represent the data and this flow regime was actually a weir flow regime in which C_d increased with h/d_o.

$$\frac{Q}{\sqrt{g d_o^{\,5}}} = 4.9\left(\frac{h}{d_o}\right)^2 \tag{3.31}$$

Flow regimes for discharges larger than the weir flow regime have been referred to using different terminology in overflow pipes. Some researchers such as Kalinske (1940), reported only one flow regime, referred to as the full pipe flow (FPF). In this flow regime, Q varied with $(h+l)^{0.5}$. The same h-Q relation was called the orifice flow by Anwar (1965) for an overflow pipe. However, some other researchers, reported the occurrence of two flow regimes. For example, USBR (1960) reported orifice flow and then pipe control for morning glory spillways, Humphreys et al. (1970) reported vortex flow and then full pipe flow for overflow pipes and Leopardi (2014) reported throat control flow regime and then tunnel control flow regime for morning glory spillways. This study

showed that for $D/d_o \geq 8$, the TF flow forms. Moreover, Eq. (3.11) cannot represent h_{cr} in TF in T2 series, therefore, Eq. (3.11) should be applied in large D/d_o only. However, for $D/d_o=5$, the suction was very dominating and prevented the occurrence of the TF. This suction actually prevented the occurrence of the FE process in T3 for $Q>7$ L/s.

This fact that average water depths in the lower and upper branches of the FE regime of T4 were approximately similar to FE1 and FE3-2 was very interesting. Moreover, since both branches were parallel to the h-Q curve represented by Eq. (3.31) in which $C=0$, it can be concluded that the control section was at the top of the outlet pipe while free vortex or solid body rotation vortex could form. Furthermore, water depth resulting from disturbing TF in T1 was also similar to TF in T2 and both occurred in the extension of FE1 in which most of the air core in the outlet pipe was replaced by water.

3.5. Conclusions

Different regimes of the flow from a large cylindrical tank through an outlet pipe were experimentally investigated. Water was supplied radially to a tank that was 9.74 times larger than the outlet pipe ($D/d_o = 9.74$). The diameter of the tank was reduced in several steps (to achieve $D/d_o = 8$ and 5) and the effect on the head-discharge curves was studied. Moreover, the experimental measurements of Kalinske (1940) and Rahm (1953) were reexamined and compared with the current experimental data. Also, the head-discharge curve of the Harspranget dam in Sweden as presented by Rahm (1953) were also considered in this analysis.

It was found that the partial full pipe flow regime of Kalinske (1940) was in fact a weir flow (WF) regime in which the coefficient of discharge C_d varied linearly with h/d_o. It was shown that for $D/d_o=5$, this C_d increased. It is believed that this was because of the pipe length that became more important in smaller tank diameters.

The full pipe flow (FPF) regime was also observed in which the entrance loss coefficient was equal to 0.1 and was found to be very smaller than the suggested value of 0.6 by Kailinske (1940). Reducing the tank size, resulted in a slight increase in this coefficient. Moreover, it was shown that for D/d_o equal to 8 and larger, in addition to the weir flow and full pipe flow, there was another flow with a swirl air core in which the discharge varied with the square root of water depth. This flow was called the transition flow (TF). For D/d_o=5, suction was strong enough to prevent the occurrence of it.

If the WF regime was established, it was possible to observe some gulping. These gulping resulted in the occurrence of the air core. In case of D/d_o= 9.7 and 5, the air core caused an increase of the water depth in the tank until it reached to a steady depth. In this phenomenon, the annular jet changed to a central jet. This flow regime was called the orifice flow (OF) regime. This flow regime was not observed for D/d_o= 8. Instead, the circulation resulting from this gulping, caused the annular flow to be extended in the pipe length and water depth to be increased to a certain level. Then, water depths returned to the weir flow regime. This process was called the filling and emptying (FE) process. It was found that three water depths were possible in this process. In order to predict the head-discharge curves for all three stages of this process, principle of maximum discharge and vortex theories have been used. The control section was either at the top or bottom of the outlet pipe. The Rahm's (1953) experiments and measurements in the Harspranget dam were used for developing a critical condition in the last stage of this process which occurs in relatively small discharges and mostly have been known as Borda full flow. Moreover, the results of this study were compared with the formulation of the minimum water depth that can prevent the intrusion of the air core to the top of vertical outlet pipe.

3.6. Notation

The following symbols are used in this chapter:

a = Air-core diameter

C = Vortex circulation

C_d = Coefficient of discharge for weir flow in Eq. (3.5)

C_{do} = Coefficient of discharge for orifice flow in Eq. (3.3)

C_k = Coefficient of discharge for Kalinske (1941) study in Eq. (3.1)

D = Diameter of the upper manhole

d_o = Diameter of the outlet pipe

d_i = Inlet diameter

E = Total energy of the flow

f = a^2/d_o^2

g = Acceleration due to gravity

h = Mean water depth in the tank

h_{cr} = Critical head in which TF happens

K_e = Entrance loss coefficient for full pipe flow regime in Eq. (3.2)

l = Length of the vertical outlet pipe

L = Depth of the tank

P = Pressure

p = Approach flow depth

Q = Discharge

Q^* = Dimensionless discharge = $Q/(gd_o^5)^{0.5}$

Q_{rc} = Required discharge for a steady irrotational vortex

t = Distance of air core control section from the entrance of the outlet pipe, Bellmouth height in Binnie and Hookings (1948) study

V_θ = Tangential velocity equal to C/r

V_z = Vertical velocity

V_r = Radial velocity

y = Water depth at r

y_l = Water depth at the top of the outlet pipe

σ = Standard deviation

References

Ackers, P., and Crump, E. S. (1960). "The vortex drop." *ICE Proceedings*, 16(4), 433-442.

Anderson, S. H. (1961). "Model studies of storm-sewer drop shafts." *ST. Anthony falls hydraulic laboratory*, Technical paper No. 35, Series B, University of Minnesota.

Anwar, H. O. (1965). "Coefficients of Discharge for Gravity Flow into Vertical Pipes." *Journal of Hydraulic Research*, 3(1), 1-19.

Banisoltan, S., Rajaratnam, N., and Zhu, D. Z. (2015). "Experimental Study of Hydraulics of Drill-Drop Manholes." *Journal of Hydraulic Engineering*, 04015021.

Binnie, A. M. (1938). "The use of a vertical pipe as an overflow for a large tank." *Proceedings of the Royal Society of London. Series A, Mathematical and Physical Sciences*, 219-237.

Binnie, A. M., and Hookings, G. A. (1948). "Laboratory Experiments on Whirlpools." *Proceedings of the Royal Society of London*. Series A, Mathematical and Physical Sciences, 194, 1038, 398-415.

Kalinske, A. A. (1941). "Hydraulics Humphreys, H. W., Sigurdsson, G., and Owen, H. J. (1970). "Model test results of circular, square, and rectangular forms of drop-inlet entrance to closed-conduit spillways." *State Water Survey Division.*." *Iowa Institute of Hydraulics Research*.

Kandaswamy, P. K., and Rouse, H. (1957). "Characteristics of flow over terminal weirs and sills." *Journal of the Hydraulics Division*, *83*(4), 1-13.

Laushey, L. M. (1952). "Flow in vertical shafts." *Carnegie Institute of Technology*, Department of Civil Engineering.

Leopardi, M., (2014) "Experimental study and design aspects of morning glory spillways." *New developments in dam engineering, Proceedings of the 4th International Conference on Dam Engineering, 18-20 October, Nanjing, China* (p. 461). CRC Press.

McDuffie, N. G. (1977). “Vortex free downflow in vertical drains.” *AIChE Journal*, *23*(1), 37-40.

Rahm, L. (1953). “Flow of water discharged through a vertical overflow pipe” in “Flow problems with respect to intakes and tunnels of Swedish hydro-electric power plants.” *Trans. Roy. Inst. Tech.*, Stockholm, No. 71. 71-117.

Chapter 4) A Theoretical Study of the Hydraulics of Drill Drop Manholes

4.1. Introduction

Drill Drop Manholes (DDM) have been used in the drainage system of the City of Edmonton for several years. In a drill drop manhole (see Fig. 4.1a,) two vertical manholes are attached concentrically, in which the diameter of the lower manhole d_o is two to three times smaller than the upper manhole diameter D. In the DDM, the flow can be significantly impacted by the momentum of the inlet jets. The inlets are placed at different distances above the bottom of the upper manhole and have various sizes and different arrangements. Chapter 2 studied experimentally the hydraulics of these drill drop manholes in a 1:5 scale model and observed several flow regimes depending on the value of the dimensionless discharge $Q^*=Q/(gd_o^5)^{1/2}$ where Q is the total discharge from the inlets, and g is acceleration due to gravity. For $Q^*<0.23$ a deflected jet (DJ) regime formed. For $0.23<Q^*<0.6$, a stable pool regime with a air core was observed. For $0.6<Q^*<1.65$, an unsteady flow regime was observed in which the water depth changed between two values for the same discharge and this was referred to as the filling and emptying (FE) regime. For $Q^*>1.65$, the outlet pipe was running full and it was called the full pipe flow (FPF). Chapter 2 developed empirical equations for predicting the h-Q curves of these flow regime, where h is the depth of water in the upper manhole.

In this chapter, the hydraulic characteristics of the DDM are predicted by a theoretical model based on the free vortex flow and the findings of Binnie and Hookings (1948) and Ackers and Crump (1960).

Binnie and Hookings (1948) studied vertical drains from a large tank and showed how the existence of circulation in the approach flow can affect the h-Q curve. Binnie and Hookings (1948) conducted several experiments with different entrance shapes and established a theoretical method

to predict the air-core diameter *a* inside a bellmouth-shaped overflow pipe. In their theoretical method, Binnie and Hookings (1948) calculated *a* at two possible control sections, at the crest or the throat and assumed that the air core size changes to a minimum value to pass the maximum discharge.

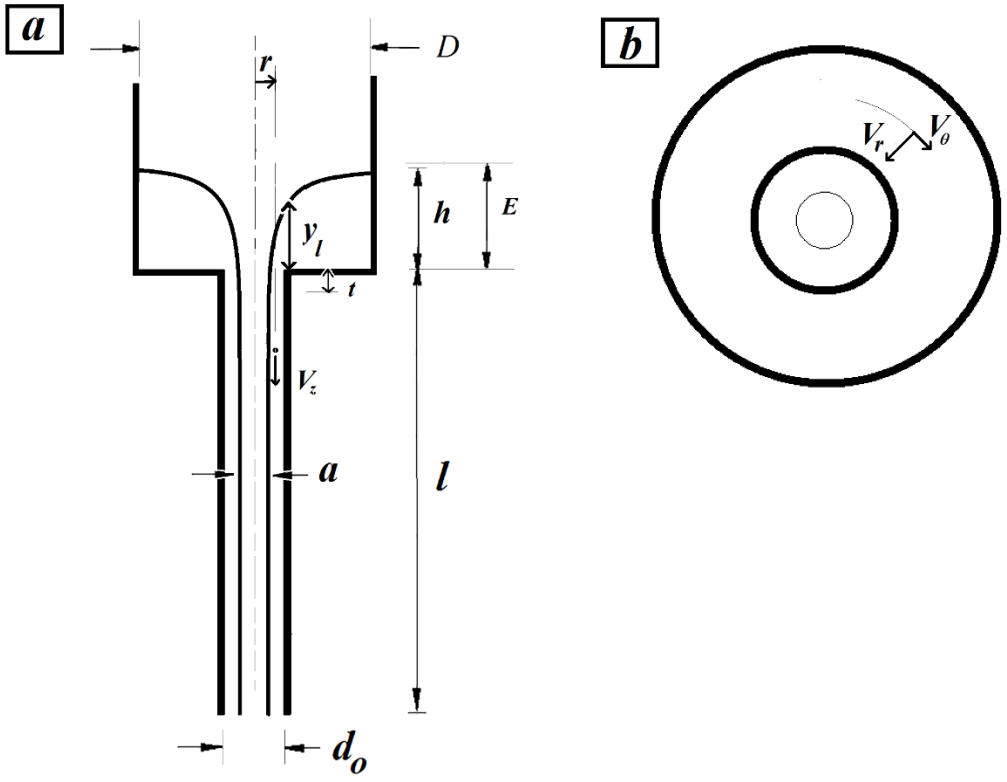

Fig. 4.1 Definition sketch of the parameters: a) section, b) top view

Table 4.1**.** Details of experiments (D = 239 mm)

Series	d_o (mm)	d_i (mm)	l (mm)	S (mm)	D/d_o	l/d_o	Comments
Series with one inlet							
A1-1	76	52	557	389	3.1	7.3	One inlet at higher elevation with different inlet diameters
A1-2	76	40	557	401	3.1	7.3	
A1-3	76	77	557	383	3.1	7.3	
A2-1	76	40	557	8	3.1	7.3	One constant inlet diameter at different elevations
A4-1	76	52	557	12	3.1	7.3	One inlet at middle and lower elevations
A4-3	76	77	557	6	3.1	7.3	
B1-1	121	52	880	389	2	7.3	Same as A1 series but with different outlet diameter
B1-2	121	77	880	391	2	7.3	

Ackers and Crump (1960) applied the theoretical method of Binnie and Hookings (1948) to vortex drops (VD). In these drop structures, instead of a large inlet tank, a well-designed chamber was used to form a stable air core vortex. Ackers and Crump (1960) provided additional formulation for the discharge considering the inlet geometry. Ackers and Crump (1960) also classified the flow in the VD's into two flow regimes. In the first regime which formed for small discharges, the lip at the top of the drain controlled the flow. In the second regime, the throat below the lip controlled the flow based on the magnitude of the air fraction $f_a = a^2/d_o^2$.

4.2. Theoretical Method

To describe the theoretical method, it is necessary to formulate a free vortex flow in a geometry of DDM as shown in Fig. 4.1. Such a steady free vortex flow contains a steady air core and the circulation C is constant everywhere in the flow and the tangential velocity V_θ is equal to C/r where r is the radial distance from the vertical axis in the DDM. In this flow, the total energy E is constant everywhere in the domain and is written as

$$E = y + \frac{C^2}{2gr^2} \tag{4.1}$$

where y is the water depth at radius r and g is the acceleration due to gravity. This form of energy equation is also mentioned by Ackers and Crump (1960). The discharge for such a flow is,

$$Q_{req} = \int_{do/2}^{D/2} V_\theta y dr = \int_{do/2}^{D/2} \frac{C}{r}\left(E - \frac{C^2}{2gr^2}\right)dr = CE\,Ln\left(\frac{D}{d_o}\right) + \frac{C^3}{g}\left\{\frac{1}{D^2} - \frac{1}{d_o{}^2}\right\} \tag{4.2}$$

In Ackers and Crump (1960) formulation for discharge, the limits of integration were inlet radiuses. Moreover, in this free vortex flow, there is a control section at which the air core size is minimum to pass a maximum discharge. This control section is found to be at the throat of the bellmouth entrance of the vertical pipe in the setups of Binnie and Hookings (1948) and Ackers and Crump (1960). In the DDM, the entrance has a sharp-edge. However, it was observed that the

air core impacted the inner wall of the lower pipe at a distance below the entrance, which varied between $0.2d_o$ and d_o.

If the throat controls the flow, the total energy equation E at the control section is written as

$$E + t = \frac{V_\theta^{\,2}}{2g} + \frac{V_z^{\,2}}{2g} + \frac{P}{\rho g} \tag{4.3a}$$

where t is the throat length, V_z is the vertical velocity at the throat given by $Q/((\pi/4)(d_o^2-a^2))$, ρ is the density of water and P is the pressure at radius r in the annular cross section confining the air core. This is referred to as the Throat Control (TC) flow. From the Bernoulli equation between radius r and air/water interface, P can be found as

$$\frac{C^2}{2g(a/2)^2} + \frac{P_{air/water}}{\gamma} + \frac{V_{z\,air/water}}{2g} = \frac{C^2}{2gr^2} + \frac{P}{\gamma} + \frac{V_z}{2g} \tag{4.3b}$$

V_z is constant in the same datum and $P_{air/water}=0$. Therefore,

$$\frac{P}{\gamma} = \frac{C^2}{2g}\left(\frac{4}{a^2} - \frac{1}{r^2}\right) \tag{4.4}$$

Combining Eqs. 4.3 and 4.4, it can be shown that,

$$Q = \pi\left(\frac{d_o}{2}\right)^2\left(1 - \frac{a^2}{d_o^{\,2}}\right)\sqrt{2g(E+t) - \frac{4C^2}{a^2}} \tag{4.5}$$

The above equations (4.3 to 4.5) were developed by Binnie and Hookings (1948). They also showed that at the control section, discharge is maximized, $\partial Q/\partial a=0$ (as shown in Eq. 4.6) and the two equations can be solved to estimate a and C for a specific h and Q. In this analysis, it is assumed that E can be replaced with h.

$$a^2 = \frac{1}{2g(E+t)}\left(C^2 + \sqrt{C^4 + 4d_o^{\,2}C^2g(E+t)}\right) \tag{4.6}$$

For a very small t, the application of Eqs. 4.5 and 4.6 is not possible. To present a more general equation in a bellmouth entrance of VD, Ackers and Crump (1960) defined $f=a^2/d_o^2$ and then used ($\partial Q/\partial f=0$) to obtain Eq. 4.7. Both Eqs. 4.5 and 4.7 should be solved simultaneously to estimate a and C.

$$E+t=\frac{C^2}{ga^2}\left(\frac{d_o^{\,2}}{a^2}+1\right) \tag{4.7}$$

In the VD, if the discharge was not enough for the occurrence of TC flow, the lip controlled the flow and weir flow developed. This flow regime will be referred to as the weir control (WC) flow in this study. In the DDM, the lip of the bellmouth entrance does not exist and the top end of the vertical pipe which is a sharp-end pipe controls the flow ($r=d_o/2$). In the WC flow, E is written as,

$$E=\frac{V_r^{\,2}}{2g}+\frac{V_\theta^{\,2}}{2g}+\frac{P}{\rho g}+h \tag{4.8}$$

where V_r is the radial velocity equal to $Q/(\pi d_o y_l)$, y_l is the water depth at $r=d_o/2$. If the flow curvature is neglected, $(P/\rho g + h)$ can be replaced with y_l. Then,

$$E=\frac{Q^2}{2g(\pi d_o y_1)^2}+\frac{2C^2}{gd_o^2}+y_1 \tag{4.9}$$

Eqs. 4.8 and 4.9 were presented by Ackers and Crump (1960). They also used the "principle of maximum discharge" or "minimum energy" concept (i.e. $\partial E/\partial y_l=0$) to find Eqs. (4.10) to (4.12),

$$\frac{\partial E}{\partial y_l}=0\Rightarrow 0=0-\frac{2Q^2}{2g\pi^2 d_o^{\,2} y_l^{\,3}}+1 \quad \Rightarrow Q^2=\pi^2 g d_o^{\,2} y_l^{\,3}\Rightarrow Q=\pi d_o\sqrt{g}\,y_l^{\,3/2} \tag{4.10}$$

$$E=\frac{2C^2}{gd_o^2}+\frac{\pi^2 g d_o^{\,2} y_l^{\,3}}{2g(\pi d_o y_l)^2}+y_l\Rightarrow E=\frac{2C^2}{gd_o^{\,2}}+\frac{3}{2}y_l\Rightarrow y_l=\frac{2}{3}\left(E-\frac{2C^2}{gd_o^{\,2}}\right) \tag{4.11}$$

Combining Eqs. 4.9 and 4.10:

$$Q = \frac{2\pi d_o \sqrt{2g}}{3\sqrt{3}} \left(E - \frac{2C^2}{g d_o^{\,2}} \right)^{(3/2)} \tag{4.12}$$

4.3. Application of the WC and TC flow theories to predict h-Q curves in DDM

In the DDM, D was equal to 0.382 m and for $D_r = D/d_o$=2 and 3.1, d_o was equal to 0.121 m and 0.076 m, respectively. Both of these diameter ratios are used in the theoretical methods and compared in this study. For example, Fig. 4.2 shows the comparison of both WC and TC flows in D_r=2 and 3.1 with the experimental data in Series A1-3 and Series B1-2. It can be seen that for Q^*>0.45, the WC formulation for D_r= 3.1 can describe the experimental data of the lower branch of the FE regime very well. For D_r=2, the difference is about 10%. Therefore, the application of WC flow in DDM is related to the lower outflow discharge. The circulation C in Eq. 4.12 was found using the free vortex theory as described before assuming t=0.2d_o. Comparison of C for different a/d_o and t/d_o in case of D_r= 3.1 is shown in Fig. 4.3.

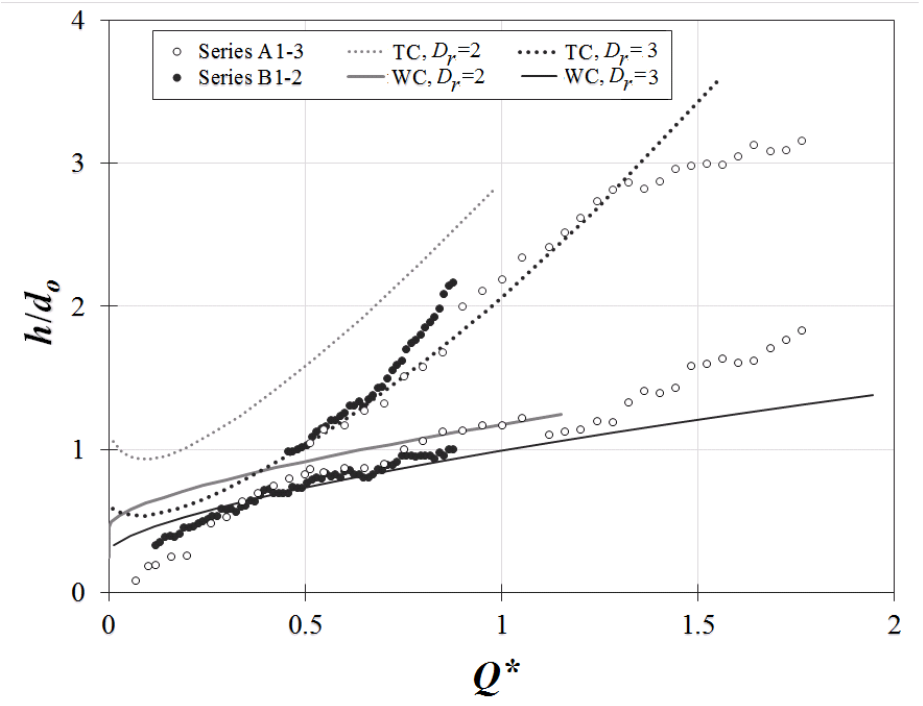

Fig. 4.2 Comparison of experimental values of h/d_o versus Q^* for series A1-3 and B1-2 (experimental data of chapter 2) with theoretical results of throat control (TC), weir control (WC)

For a range of a/d_o between 0.975 to 0.7, it was found that C will remain approximately constant and equal to about 0.0262 m^2/s with a standard deviation of σ=0.0006. This range of a/d_o was also used by Ackers and Crump (1960). In case of D_r= 2, the average C for the same range of a/d_o was found to be equal to 0.064 m^2/s with σ=0.0035.

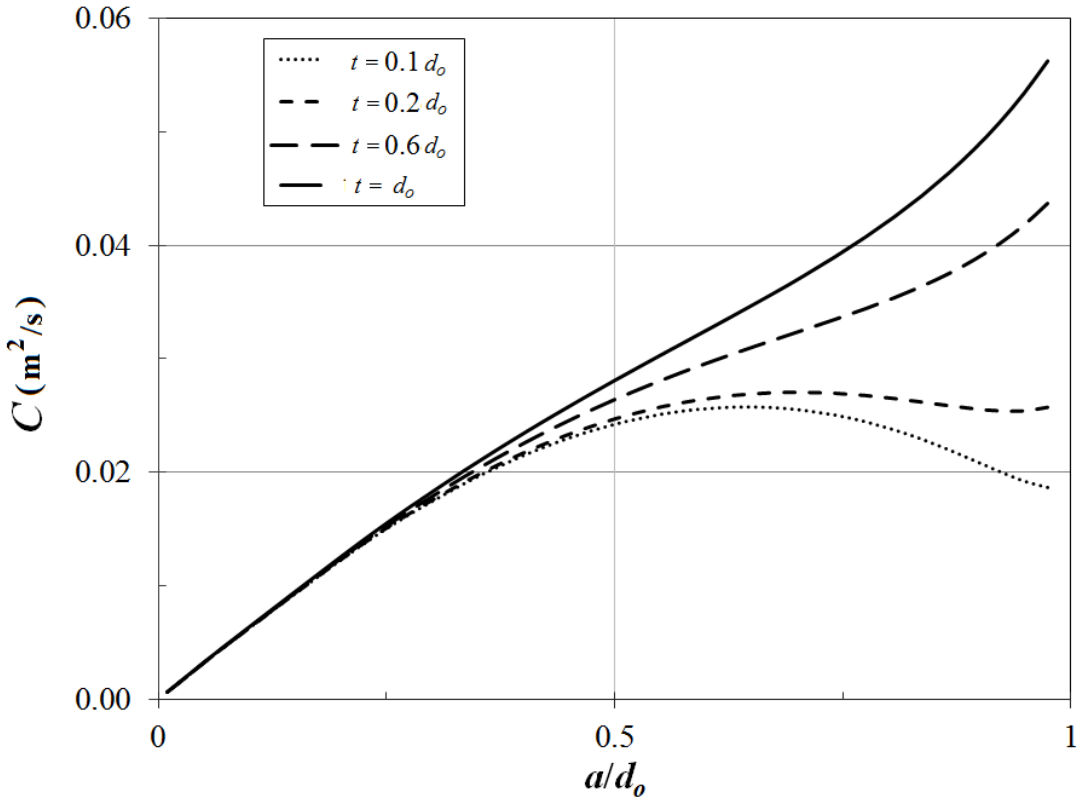

Fig. 4.3 Variation of circulation C (m^2/s) with ratio of air core diameter to lower pipe diameter (a/d_o) for the geometry of DDM in case of D_r=3.1

In Fig. 4.3, the comparison of TC formulation assuming $t=d_o$ and the experimental data also showed that there is better agreement in the case of D_r=3.1 as called TC, D_r=3.1 rather than TC, D_r=2. In case of TC, D_r=2 formulation, there is a considerable difference between the equation and the experimental data at the beginning of the FE regime but at Q^*=0.88, this difference is about 15%. It is believed that for such large diameters of the outlet, which makes $D/2$-$d_o/2$ very small (about 6 cm), the jet inside the upper pipe was not strong enough to reach to the h-Q curve

for the free vortex. With increasing discharge, the jet became more strong and became close to the *h*-*Q* curve associated with it.

Chapter 2 presented the regression analysis for all of the DJ, SP and FE regimes in the experiments. Experimental data have been compared with the proposed theoretical methods of this study as shown in Figs. 4.4 and 4.5. Fig. 4.4 shows that in the DJ and SP regimes of DDM, the TC method with $t=d_o$ describes the SP regime and the TC method with $t=0.2d_o$ describes the DJ regime. Separation between DJ and SP regime is at $Q^*=0.23$. It was also found that the WC methods are not in good agreement with the experiments. This supports the theory of a tendency for formation of a free vortex flow as discussed before.

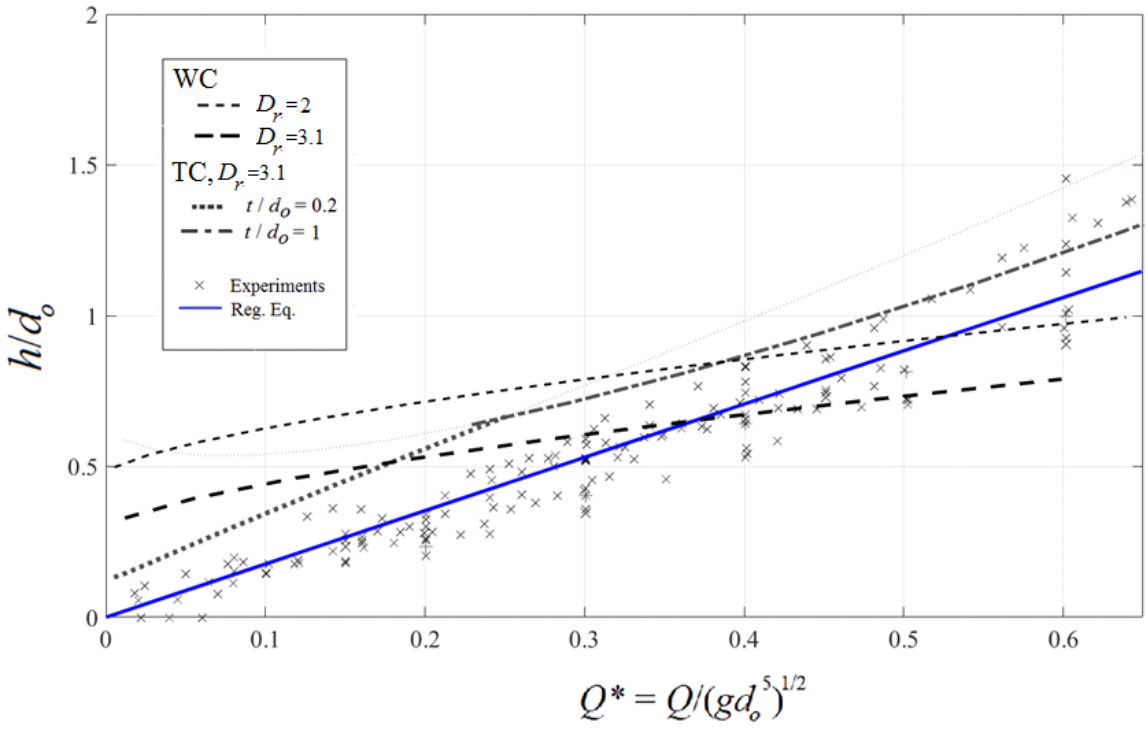

Fig. 4.4 Comparison of experimental values of (h/d_o-Q^*) for the SP regime in DDM (experimental data of chapter 2)and the theoretical results of (WC and TC) with the application of different values of D_r and t/d_o

Fig. 4.5 shows the comparison of the theoretical method and the experimental data in the FE regime. Two values of t/d_o equal to 1 and 0.2 have been used in TC, D_r=3.1 analysis. It can be

seen that while the curve of t/d_o=1 is a good match for the regression formula of chapter 2), the curve of t/d_o=0.2 also can represent some other experimental data in which the inlet was located away from the bottom and top. Moreover, although TC, D_r=2 was not in good agreement with the experimental data, the WC-JT method, D_r=2 could represent them very well. In WC-JT, D_r=2, t_j was equal to 8 mm and C was equal to 0.064 m^2/s which is the average of C for t/d_o=0.2 for a range of a/d_o between 0.975 to 0.7.

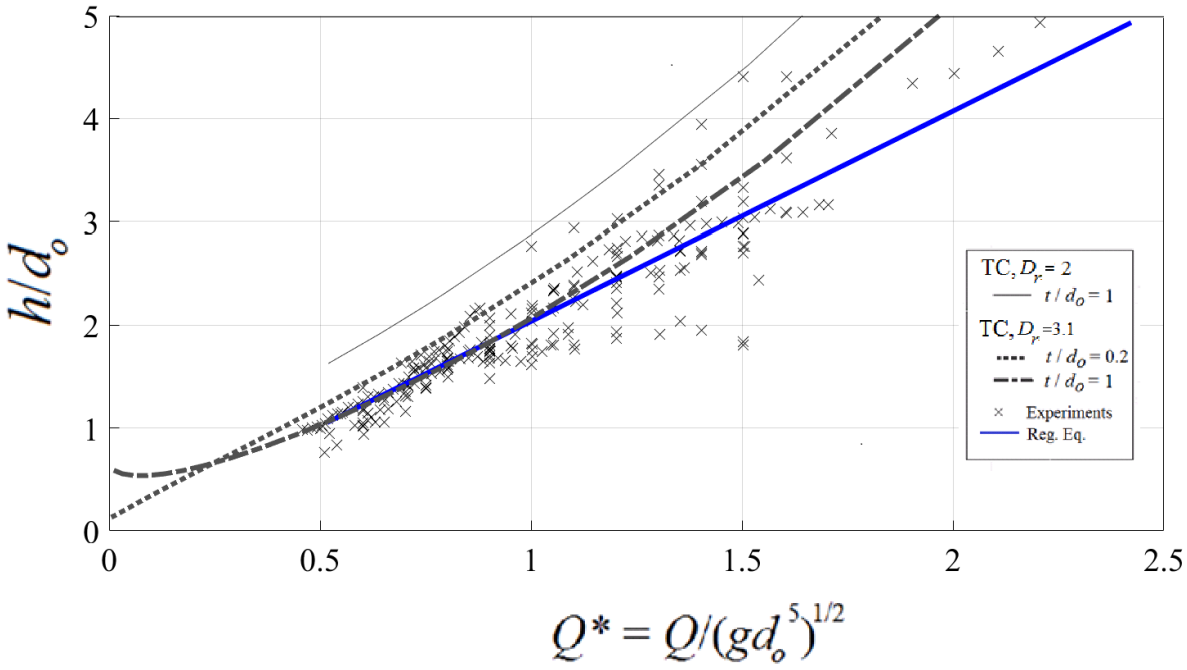

Fig. 4.5 Comparison of experimental values of the h/d_o-Q^* curves for the FE regime in DDM (experimental data of chapter 2) with the theoretical results of (TC, WC and WC-JT) for different values of t/d_o .

4.4. Analysis of the FE regime of DDM

In the SP regime of the DDM, the outlet discharge Q_{out} is equal to the inflow rate Q. However, in the FE regime, the outlet discharge was not the same as the incoming discharge. In the experiments of DDM in chapter 2, the variation of h with time t was recorded with a Sony Handycam (HDR-PJ580) at 30 fps. This h-t variation provided the velocity of the water surface variation in the FE regime (dh/dt). Then, using the continuity equation

$$Q_{out} = Q - \frac{dh}{dt}\left(\frac{\pi}{4}D^2\right) \tag{4.19}$$

For filling: $Q_{out}<Q$ and h increases with time, for emptying, $Q_{out}>Q$ and h decreases.

As an example, consider the water depth time series in the FE regime for a discharge of 5.9 L/s in Series A1-3 of DDM (with d_o= 0.076 m, D=0.2388 m and Δt=1/30 s). In Fig. 4.6a. the variation of the measured h with t is shown with the filled symbols. The solid line shows the smoothed line of the h-t curve using the *smooth function* in MATLAB (Loess method with 10 percent span). Fig. 4.6b shows Q_{out} versus t. It can be seen that with an incoming discharge of 5.9 L/s, the outlet discharge varied between 3 L/s to 10 L/s. Moreover, it showed that the minimum outlet discharge occurred when the lower branch was changed to the upper branch and in return, the maximum outlet discharge occurred when the upper branch switched to the lower branch. Discharge coefficient (C_{dt}) can be defined based on h at any given time as Eq. 4.20.

$$Q_{out} = C_{dt} A\sqrt{2gh} \tag{4.20}$$

Using MATLAB and Eq. 4.23, C_{dt} was calculated and plotted as shown in Fig. 4.6c. It was observed that at C_{dt}=0.65, water depths were at maximum and minimum levels.

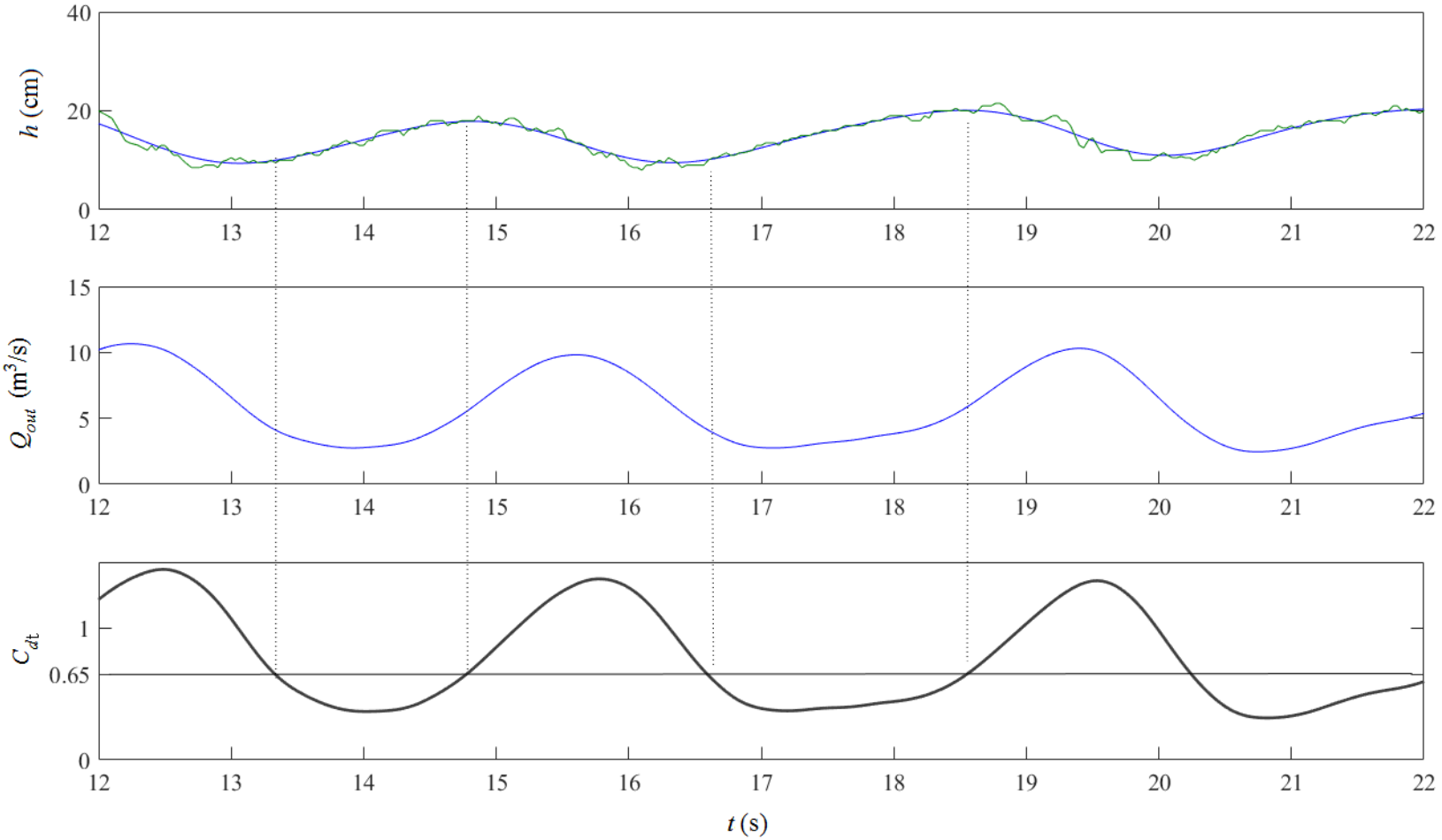

Fig. 4.6 a: Water depth variation h (cm) with t (s), b: outlet discharge variation Q_{out} (m^3/s) with t (s), c: discharge coefficient variation (C_{dt}) with t (s) for the FE regime in Series A1-3 with Q=5.9L/s

For the short tube flow regime, Blaisdell (1953) presented Eq. 4.21 in which, C_s is the coefficient of discharge and H_s is the head from the water surface to the end of the vertical pipe connecting to the inclined pipe. C_s was found to have values of 5.28, 5.31 and 5.31:

$$Q_{out} = C_s A H_S^{1/2} \tag{4.21}$$

However, by rewriting Eq. 4.21 as Eq. 4.20, Since $C_s=C_{dt}(2g)^{0.5}$, C_{dt} in Blaisdell (1953) for maximum and minimum discharges was found to be equal to 0.65.

Fig. 4.6c shows that the values of C_{dt} exceeded the value of one in which it was related to the changes of maximum level to the minimum level. In fact, the pipe was primed and application of h in $(2gh)^{0.5}$ is not right. It could be concluded that, V_{out} was larger than $(2gh)^{1/2}$for $C_{dt}>1$

Variation of Water depth h variation with time has been used to analyze the frequency changes (f) of the oscillation in the FE regime where f is $1/T$ and T is the period of the oscillation. For this purpose, 10 periods for each discharge were considered. Fig. 4.7 compares the calculated average period T (s) with Q (L/s) in different series of the experiments. Black symbols show the series with the one inlet at the top. It can be seen that there is general trend of increasing T with Q. However, if one inlet was located at a lower elevation which has been shown with the gray symbols in Fig. 4.7, the general trend was a decrease in T with Q. Dimensional analysis showed that the frequency can be expressed as a Strouhal number to be related to the ratio of oscillation amplitude (the difference between the maximum and minimum levels of the FE regime) to the inlet diameter, $\Delta h/d_i$ as presented in Eq. 4.22 with $R^2=0.84$ and shown in Fig. 4.8. In this Strouhal number, the characteristic length is related to the diameter of the upper pipe and the characteristic velocity is the inlet velocity.

$$\frac{\Delta h}{d_i} = 0.257\left(\frac{fD}{U_i}\right)^{-0.625} \tag{4.22}$$

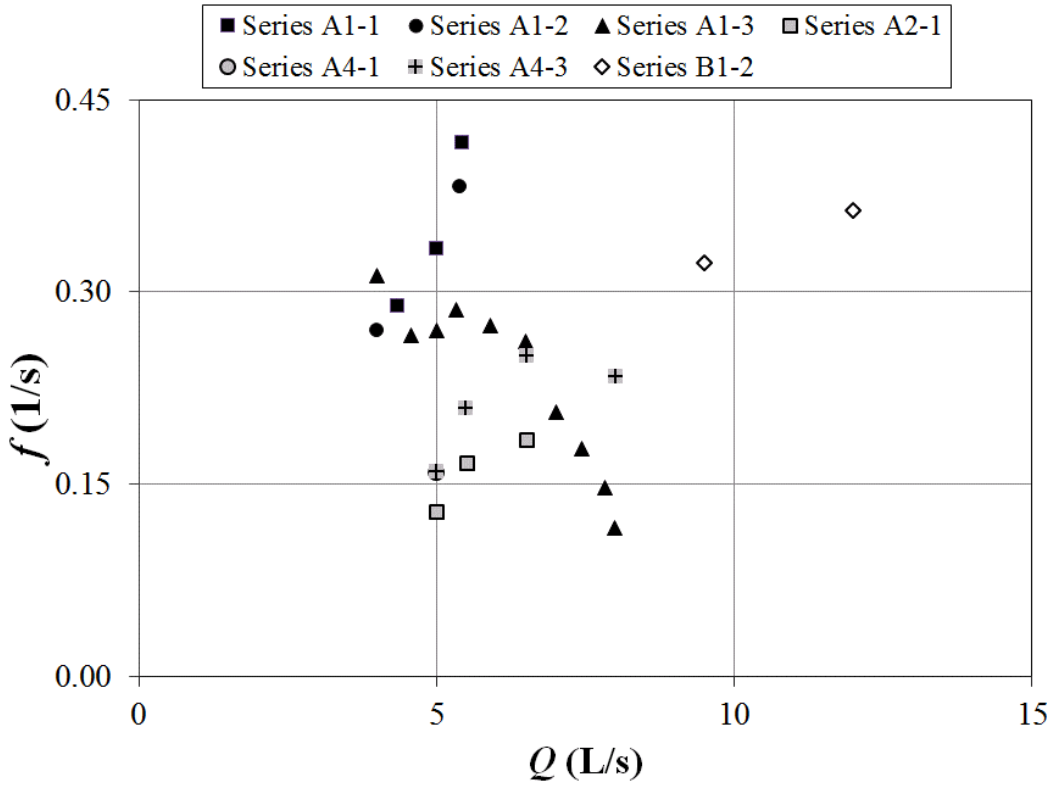

Fig. 4.7 Variation of frequency of the oscillations in the FE regime f (1/s) with Q (L/s)

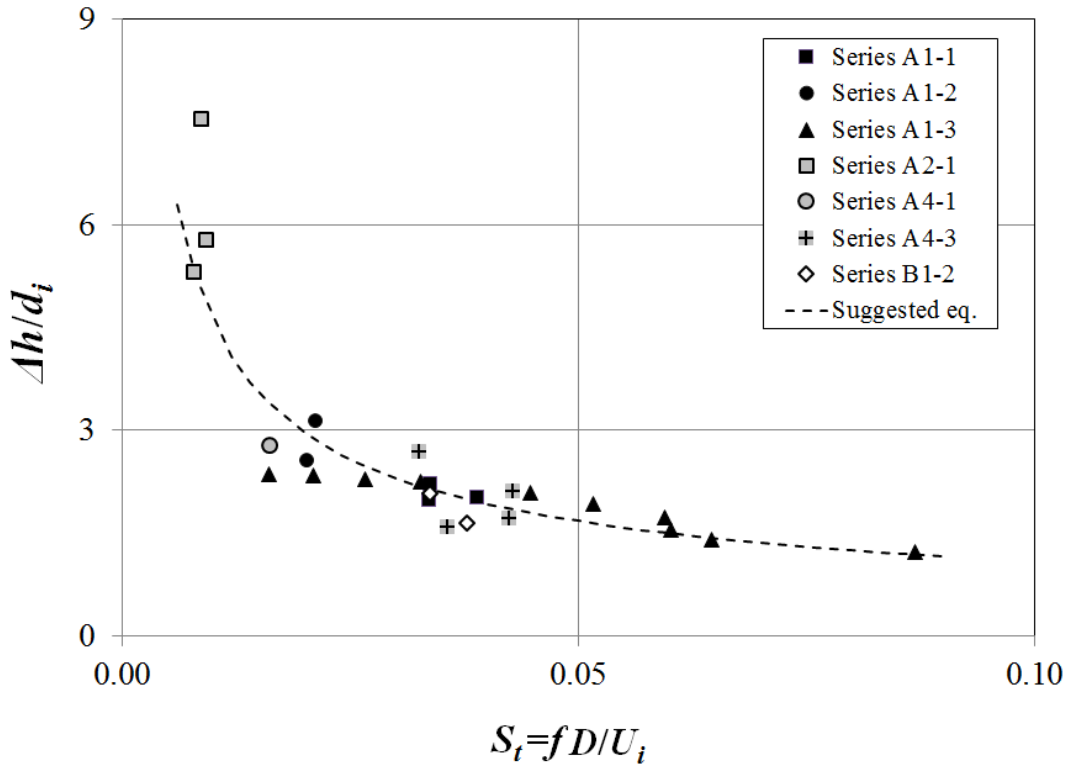

Fig. 4.8 Variation of dimensionless frequency as Strouhal number with $\Delta h/d_i$

4.5. Further Discussions and conclusions

The regression formulation of the DJ and SP in chapter 2 experiments was valid for one and two inlets located at different elevations. Therefore, the formulation of TC-D_r=3.1 which represented both of these flow regimes will be also valid for experiments in different elevations. In the FE regime, it has been found that TC-D_r=3.1 formulation is in a very good agreement with the inlet size of 77 mm as shown in Fig. 4.9. It was observed that the increased water depth in the upper pipe destroyed the incoming momentum after a few circulation. However, for the smaller inlet sizes, the incoming momentum of the jet was so strong that the assumption of the required discharge for a free vortex could not follow Eq. 2. In fact, the jet blocked the entrance of the vertical pipe and then hit the opposite wall which caused a separate jet to form inside the upper pipe.

The direct results of the application of the TC formulation and the continuity equation is that the maximum level in the FE regime is the result of a balance between the circulation, air core and incoming discharge. At this balanced water depth, the circulation was destroyed in the pool. Then, all of the water in the upper tank was discharged following an orifice flow formula. To calculate the equilibrium water depth from the WC-JT formulation, the thickness of the water jet was assumed constant for all discharges. This is because of the observation that in the FE regime, the jet curtain covered the whole circumference of the upper pipe such that both wings reached again in the inlet side and formed a falling jet. With an increase in discharge, it was observed that this falling jet became thicker. This suggested that t_j could be assumed constant.

In this study, application of free vortex theory in different flow regimes of DDM's has been discussed. It was found that there is a tendency for the water depth to form a stable free vortex in which the throat controlled the flow regime. However, some other limitations such as a very small

distance for the formation of a free vortex, could cause some differences. In the stable pool flow regime, the incoming momentum was enough to hold this stable air core. However, in the FE regime, the incoming flow was insufficient for holding the stable air core. As the result, the air core was not stable and the pool drained following an orifice flow formula based on the outlet discharge.

Formulations of Ackers and Crump (1960) for a stable free vortex inside a vortex drops (VD) have been developed for this analysis. It was found that in DDM unlike the VD in which the throat control was constant, the throat length t could vary between 0.2 to 1 times the outlet diameter d_o. To use the weir control section, it was found that the average circulation C based on t/d_o=0.2 could be used. Experimental data of chapter 2 was used for comparing the theoretical predictions.

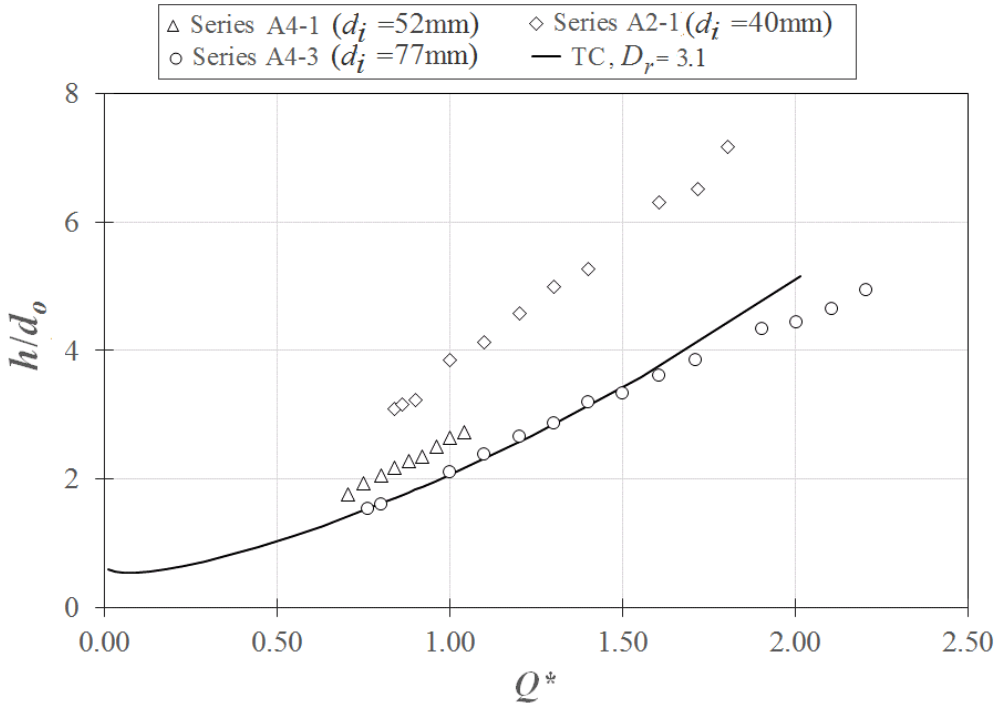

Fig. 4.9 Comparison of the TC, D/d_o=3 formulation with the experimental results of one inlet located at the lower elevation

4.7. Notation

The following symbols are used in this chapter:

a = Air-core diameter

A = Area of the lower pipe.

C = Circulation

C_{dt} = Coefficient of discharge for FE regime in Eq. 4.29

C_s = Coefficient of discharge in short tube flow regime by Blaisdell (1958)

D = Diameter of the upper pipe

D_r = Diameter ratio of upper pipe to lower pipe diameters = D/d_o

d_i = Diameter of the inlet pipe

d_o = Diameter of the outlet pipe

E = Total energy of the flow

f_a = fractional air-core section=a^2/d_o^2

g = Acceleration due to gravity

H_s = Total head over the crest of shaft spillway or overflow pipes

h = Mean water depth in the upper pipe

P = Pressure

Q = Inlet discharge

Q_{out} = Outlet velocity in a specific time

Q^* = Dimensionless discharge = $Q/ (gd_o^5)^{0.5}$

S = Inlet elevation

ST = Strouhal Number

t = Throat length

t_j	=	Thickness of the annular jet in DDM setups if the inlet was located at the upper elevation
U_i	=	Inlet velocity
V_θ	=	Tangential velocity equal to C/r_1
V_z	=	Vertical velocity
V_{out}	=	Outlet velocity in each specific time
V_r	=	Radial velocity
V_j	=	Velocity of the annular jet in DDM setups if inlet located at the upper elevation
y	=	Water depth at radius r
y_1	=	Water depth at the entrance of the vertical pipe ($r=d_o/2$)
Δh	=	The amplitude of the oscillation in the FE regime
ρ	=	Density of water

References

Ackers, P., & Crump, E. S. (1960, August). "The vortex drop". *In ICE Proceedings* (Vol. 16, No. 4, pp. 433-442). Thomas Telford.

Banisoltan, S., Rajaratnam, N., & Zhu, D. Z. (2015). "Experimental study of hydraulics of drill-drop manholes". *Journal of Hydraulic Engineering*, 04015021.

Binnie, A. M., and Hookings, G. A. (1948). "Laboratory experiments on whirlpools." *Proceedings of the Royal Society of London*. Series A, Mathematical and Physical Sciences, 194, 1038, 398-415.

Blaisdell, F. W. (1953) "Hydraulic fundamentals of closed conduit spillways." ASCE J. Hydraul. 295 Div., 354, 1-14.

Quick, M. C. (1990). "Analysis of spiral vortex and vertical slot vortex drop shafts". *Journal of Hydraulic Engineering*, *116*(3), 309-325.

Chapter 5) A Comparative Study of Discharge Coefficient in Overflow Pipes and Shaft Spillways

5.1. Introduction

Vertical drains are often used in the design of manholes in municipal drainage systems. Vertical drainsare also used as the basic element in the design of shaft or morning glory spillways. In these cases, a radial flow is provided. If the shaft is running partially full, the operation of the spillway is limited to $0.2<h/d_o<0.5$ where h is the head and d_o is the shaft diameter in shaft spillways or the crest diameter in morning glory spillways (Vischer et al., 1998). Otherwise, the flow could become unsteady. Fig 5.1a shows this flow condition as reported by Wagner (1956).

To avoid this unsteadiness in stormwater manholes or sewer systems, Anderson (1961) and Laushey (1952) recommended the use of vortex inlet entrance shapes to ensure a steady water depth and a unique curve of depth-discharge (h-Q), where Q is the discharge. However, there are many manholes in which the entrance has a shape different from a vortex inlet and the flow is not radial. For example, chapter 2 studied a case of manholes called Drill Drop Manholes (DDM) in which the flow was affected by the incoming momentum from the inlets and an unsteady flow pattern exists. In another study by chapter 3, the unsteadiness was studied in a perfectly radial flow and it was found that the tank size can affect the type and the magnitude of the oscillations. Understanding the pattern and magnitude of the oscillating water depths can provide a safe operation of the vertical drain with radial inflow in manholes. For this purpose, it is necessary to review some of the previous studies and conduct a comparative analysis.

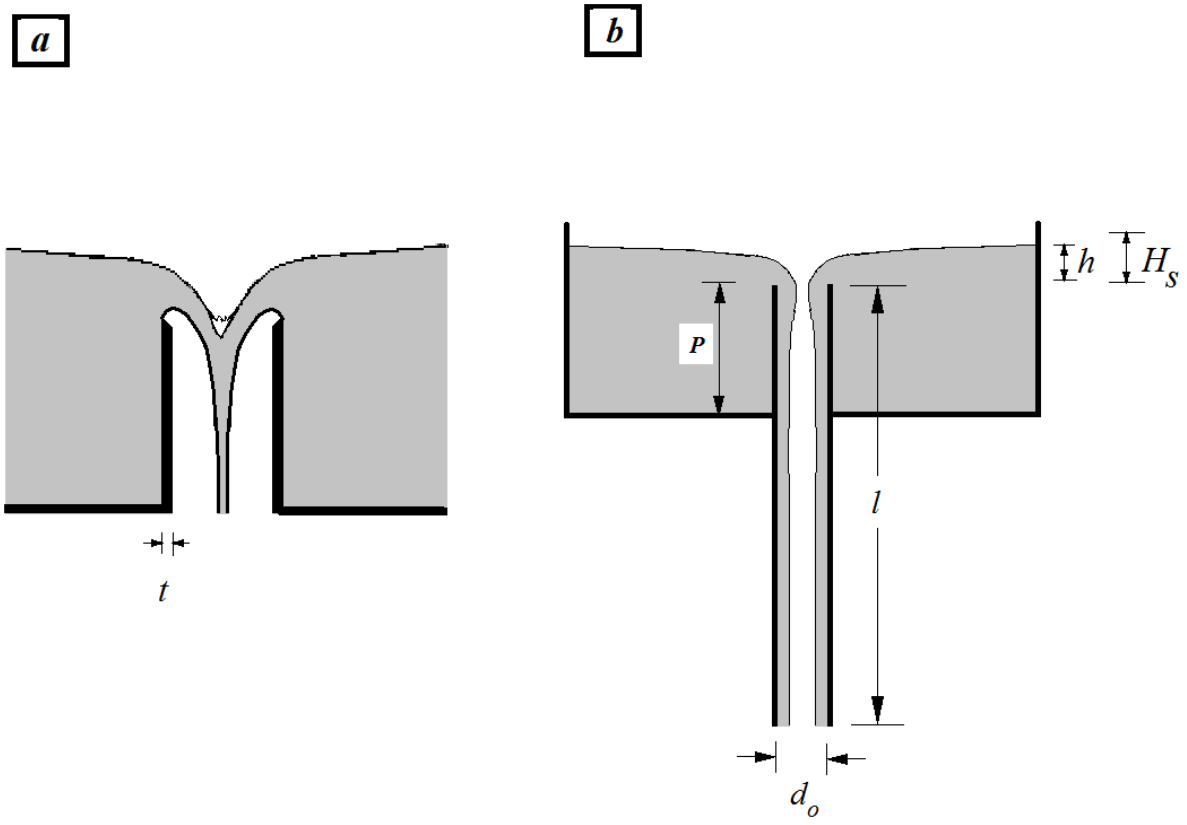

Fig. 5.1 Comparison of water surface profile in overflow pipes: a) the lower nappe is aerated (it is a simplified from Wagner 1956), a) the lower nappe clinged to the inner wall of the outlet pipe (it is simplified from Rahm 1953)

5.2. Analysis of Previous Studies

Effect of entrance shape (flat-ended, sharp-ended and bellmouth) on the *h*-*Q* curve in vertical outlet pipes with a radial inflow was investigated by Binnie (1938). The normal rise of the *h*-*Q* curve included two parts. Before a critical depth, h_{cr}, the water depth only increased slightly for a considerable increase in *Q* and the outlet pipe was running partially full. The experiments by Kalinske (1941) provided a *h*-*Q* relationship formula for it as shown in Eq. 5.1 and Kalinske (1941) called it partially full pipe flow (PFPF) regime. In this equation, C_k is the coefficient of discharge for PFPF and varied with h/d_o in a complex form. For depths greater than $h_{cr,}$ the pipe ran full and full pipe flow (FPF) regime was established as represented by Eq. 5.2.

$$Q = C_k g^{0.5} d_o^{0.5} h^2 \tag{5.1}$$

$$Q = (C_e \pi d_o^2 / 4)\sqrt{2g(h+l)} \tag{5.2}$$

where, C_e is the discharge coefficient for FPF, g is acceleration due to the gravity and l is the length of the pipe. In the experiments of Binnie (1938), there was a distance P between the top of the vertical pipe and the bottom of the tank, and this arrangement is referred to as the overflow pipe in this study. However, Kalinske (1941) also studied the h-Q curve for P=0 and this arrangement was referred to as the drain pipe. Table 5.1 shows the geometrical details of the experimental arrangements of Binnie (1938), Kalinske (1941) and other setups that will be referred to later.

In the study of the effect of tank size on the h-Q curves for vertical drains with radial inflow (P=0) in chapter 3, it was found that the PFPF regime in Kalinske (1941) is in fact a weir flow (WF) regime (Eq. 3.5) in which the lower nappe was clinging to the inner wall of the vertical pipe and C_d increased linearly with h/d_o. In chapter 3, Kalinske (1941) experimental results have been reexamined for drain pipe and suggested a C_d formulation as shown in Eq. (3.6).

$$Q = \frac{2}{3}\sqrt{2g} C_d \pi d_o h^{1.5} \tag{3.5}$$

$$C_d = 0.7\frac{h}{d_o} + 0.52 \tag{3.6}$$

For the overflow pipe experiments of Kalinske (1941), variation of the C_d in Eq. (3.5) is shown in Fig. 5.2. It is found that the linear relation as shown in Eq. 5.3 with R^2=0.785, can predict C_d with h/d_o. Fig. 5.2 also shows that the formula for drain pipes is within a ±%10 range of C_d for overflow pipes and the overflow pipes have slightly larger values of C_d. In fact, the difference in C_d between the drain and overflow pipes increased with h/d_o.

$$C_d = 0.82\frac{h}{d_o} + 0.487 \tag{5.3}$$

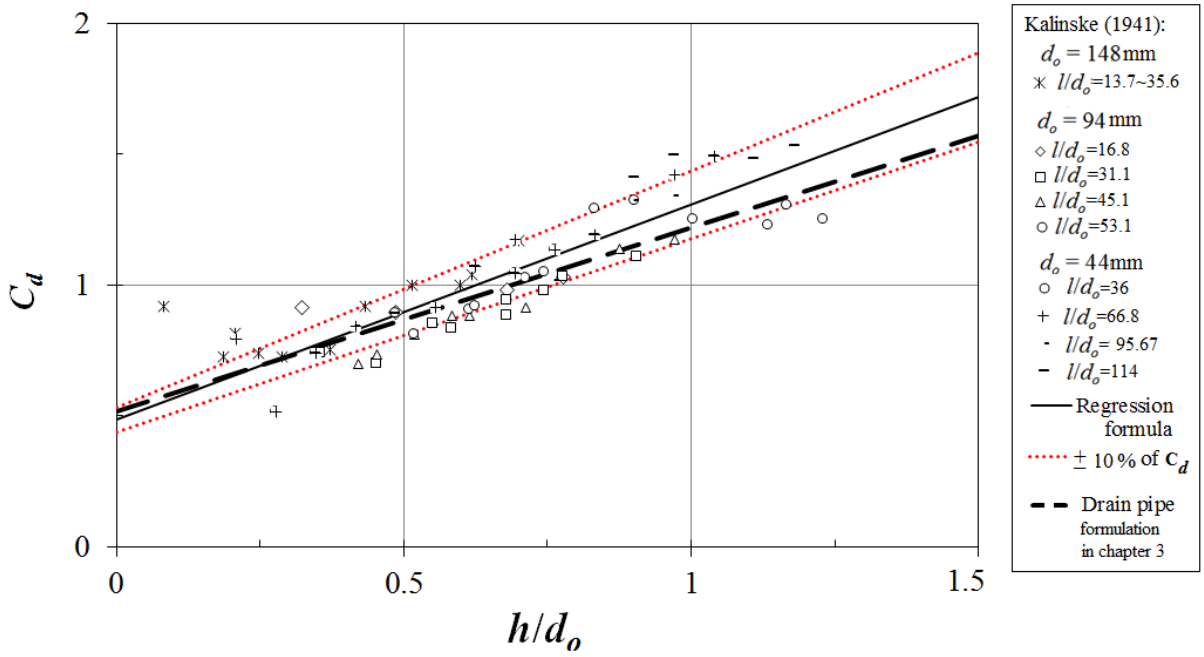

Fig. 5.2 Comparison of C_d versus h/d_o for overflow pipes of Kalinske (1940) experiments (empty marks), black plain line shows the suggested equation for overflow pipes and dotted line shows ±%10 of C_d, dark dotted black line shows Eq. 3.7 (in chapter 3 for drain pipes).

Table 5.1 Experimental details of literature

	P (m)	d_o (mm)	P/d_o	l (m)	t (mm)
Binnie (1938)	0.52	25.4	20.5	0.61	1.6
Kalinske (1941)	0.254	148 94.1 43.9	1.7 2.7 5.8	1.6,2.9,4.2,5	3.2
Rahm (1953)	0.6	Pipe 1: 133 Pipes 2 to 4: 83 Pipe 5: 40	4.5 7.2 15	0.67 1.26, 0.67, 0.34 0.67	3.4 1.6 1.3
Wagner (1956)	0.0381	508	0.075	0.508	12.7
Anwar (1965)	0.15	152.9 38.4 101.6 66.3	0.98 3.9 1.5 2.26	0.609	9.7 6.5 9.2 5

In investigating unsteady water depths in overflow pipes, Rahm (1953) observed that for h/d_o<0.3, the flow had steady h-Q curve similar to the formulation of the WF flow with C_d=0.9. However, for h/d_o>0.3, unsteadiness set in and it seemed that Q changed with h^2 instead of $h^{1.5}$. Similar investigation of Kalinske (1941) for developing C_d versus h/d_o has been confirmed using Rahm (1953) experimental data as well. Fig. 5.3 shows the results of this analysis. The shape of this flow regime as was photographed by Rahm (1953) was shown in Fig. 5.1b.

As mentioned before, Fig. 5.1a also shows flow in an overflow setup where the lower pipe was open to the atmosphere (this figure is adapted from Wagner 1956). The characteristic of this flow regime was investigated by Wagner (1956). Two flow regimes of free flow, Eq. 5.4, and submerged flow, Eq. 5.5, were stablished

$$Q = CLH_s^{3/2} \tag{5.4}$$

$$Q = C_o A_o \sqrt{2gH_s} \tag{5.5}$$

where C is the coefficient of discharge in free flow, H_s is the total head of the flow approaching the outlet, L is the crest length, C_o is the coefficient of discharge in the orifice formulation and A_o is the cross sectional area of the outlet. Wagner (1956) showed that C changed with H_s/d_o and also mentioned that a decrease in the approach flow depth (P), will increase discharge by up to 8%. The results of Wagner (1956) have been widely used in the design of circular shaft spillways and morning glory spillways (USBR, 1990 and Khatsuria, 2004). To compare C with C_d of other studies as shown in Fig 5.3, Eq. 5.6 has been used where g is in the imperial system (i.e., 32.2 ft/s^2),

$$C = \frac{2}{3} C_d \sqrt{2g} \tag{5.6}$$

Effect of pipe thickness on the WF regime was investigated by Anwar (1965) in overflow pipes. He showed that an increase of pipe thickness t, reduced C_d in all flow regimes as shown in Fig 5.3. This fact that in the WF regime of overflow pipes, the water depth is affected by the thickness, can justify that pipe thickness might have an effect in small discharges. However, it was interesting to see how it affects C_d for higher discharges as will be discussed later.

In the drop inlet entrance to closed conduit spillways, Humphreys et al. (1970) showed that C_d varies with h/d_o in two different forms. It was dependent on the values of h/d_o. For h/d_o smaller than 0.475, Eq. 5.7 was used and beyond that, Eq. 5.8 was used. In these equations, d_o is the diameter of the drop and not the diameter of the inclined tunnel. Both of these formulations are also shown in Fig. 5.3.

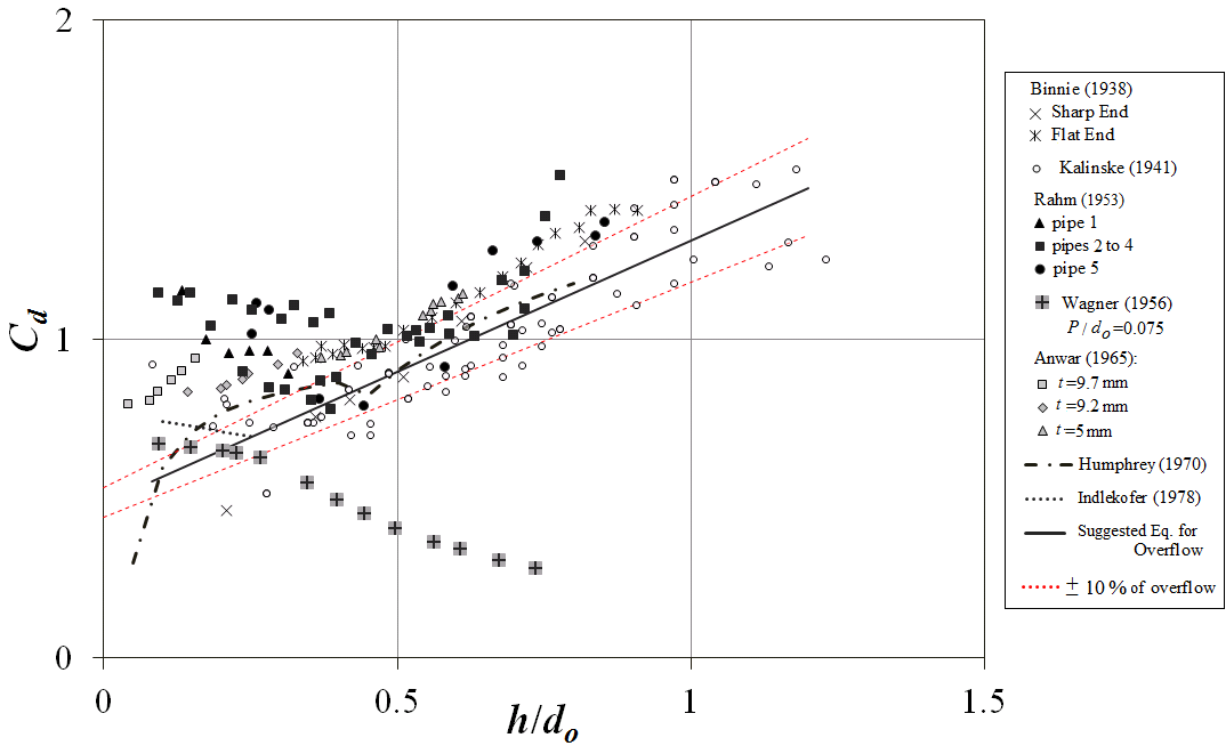

Fig. 5.3 Comparison of C_d variation versus h/d_o for overflow pipes in literature and suggested equation based on the overflow for Kalinske (1941)

$$C_d = 0.957(1-\frac{0.027}{h/d_o})^{3/2} \quad (5.7)$$

$$C_d = 1.68(1-\frac{0.17}{h/d_o})^{3/2} \quad (5.8)$$

Vischer and Hager (1998) referred to Indlekofer (1978), where Eq. 5.9 is used in Germany to find the coefficient of discharge, C_d, for shaft spillways (applicable for $0.1<h/d_o<0.25$). Shaft aeration is also emphasized in those studies. Vischer and Hager (1998) also emphasized the effect of boundaries such as topographic conditions of dams which might produce rotational conditions.

$$C_d = 0.515(1-0.4\frac{h}{d_o}) \quad (5.9)$$

5.3. Discussion

The comparison of variation of C_d with h/d_o is presented in Fig. 5.3 and it is seen that for a range of $h/d_o<0.47$, not only the suggested formulation in Eq. (5.5) is not a good fit to the experimental data, but also the Humphrey et al. (1970) formulation cannot represent them. In fact, it was found that C_d with an average value of 0.89 and standard deviation of $\sigma=0.14$, can represent them. For $h/d_o\geq0.47$, the suggested formulation in Eq. (5.5) and the Humphrey et al. (1970) experiments are very close and most of the data are in the ±10% range of the suggested equation.

It was attempted to compare the effect of t in the previously mentioned studies as well. It was found that Kalinske (1941) presented the same thickness for all of the pipes in his experiments with various lengths and diameters. These results did not follow the trend of the other series with the various thicknesses and therefore, they were eliminated from the analysis. It was found that C_d

is nearly constant for $h/(d_o+2t)<0.47$ with an average value of 0.94 and standard deviation of $\sigma=0.14$. For $h/(d_o+2t)\geq 0.47$, C_d varies as Eq. (5.10) with $R^2=0.73$.

$$C_d = 1.19\frac{h}{d_o + t} + 0.44 \tag{5.10}$$

Rahm (1953) mentioned that for $h/d_o>0.3$, unsteady flow was started and Vischer and Hager (1998) referred to Indlekofer (1978) and mentioned that $0.1<h/d_o<0.25$ is applicable for insuring a steady flow. In chapter 3 it has been found that the first unsteady water depth was observed at $h/d_o=0.4$. Therefore, it seems that a range of $0.1<h/d_o<0.25$ represents the steady range. However, this range is very small and in fact providing such a design condition in manholes is not always possible. Therefore, it is necessary to provide not only more understanding of those unsteadiness in the flow but also to improve the design to carry water safely in higher heads.

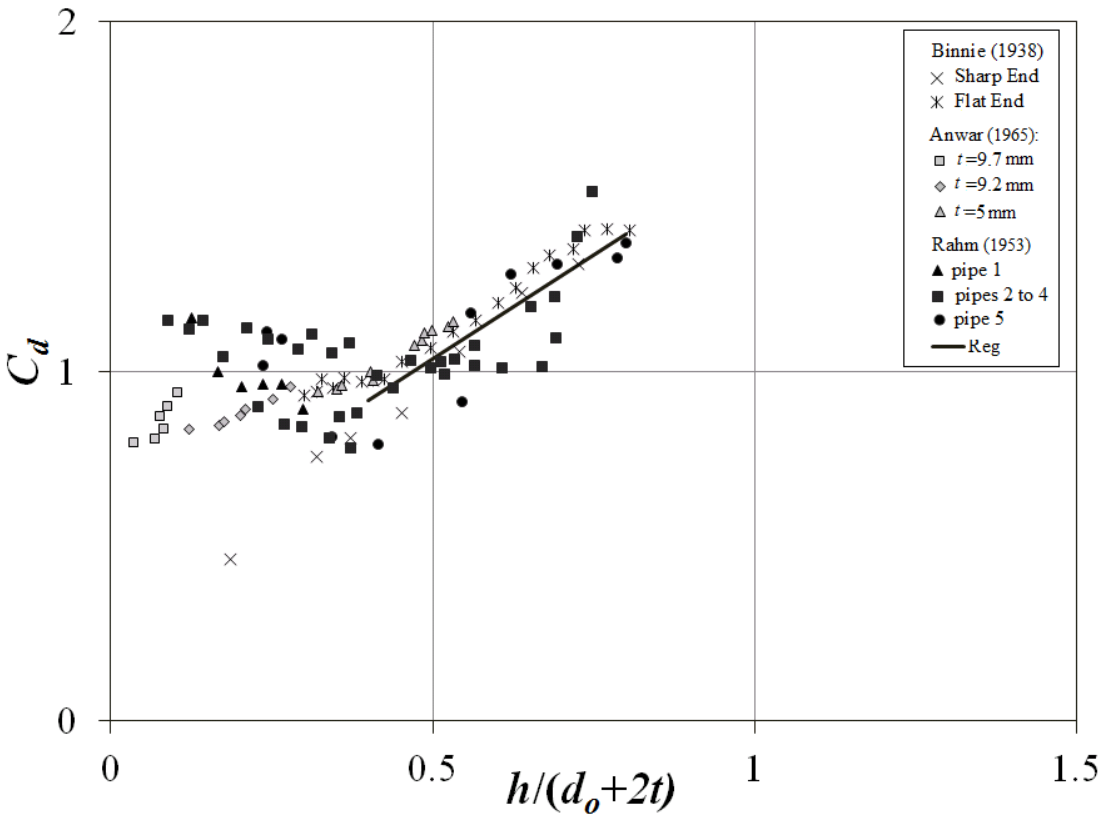

Fig. 5.4 Comparison of C_d variation versus $h/(d_o+t)$

5.4. Conclusions

Experimental data of vertical drains from a large tank have been compared to the data for overflow pipes with radial inflow. Since most of design books (e.g., USBR 1973, Khatsuria, 2004) refer to Wagner (1956) for finding the coefficient of discharge in circular shaft spillways which had an aerated nappe, his formulation is compared with the overflow pipe setups. For shaft spillways, the jet is aerated while in overflow pipes of this study, the lower nappe clung to the inner wall of the vertical pipe. This study shows that the difference between C_d in an aerated and non-aerated nappe is considerable. It has been discussed that since the thickness of the vertical outlet pipe in the weir flow regime is in contact with water, its effect has to be considered and some formulations are provided.

5.5. Notation

The following symbols are used in this chapter:

A_o = Cross sectional area of the outlet

D = Diameter of the upper pipe

C = Coefficient of discharge in Wagner (1956) formulation

C_d = Coefficient of discharge

C_e = Entrance loss coefficient

C_o = The coefficient of discharge in the orifice formulation

C_k = Coefficient of discharge in Kalinske (1941) formulation

d_o = Diameter of the outlet pipe

g = Acceleration due to gravity

h = Mean water depth in the upper pipe

h_{cr} = Critical water depth in which before it, the weir flow was observed

H_s = water depth and velocity head

P = Distance of the vertical outlet pipe from the bottom of the tank

Q = Water discharge

L = Length of the crest in the shat spillways

l = Length of the vertical outlet pipe

ρ = Density of water

References

Anwar, H. O., (1965). "Coefficients of discharge for gravity flow into vertical pipes." Journal of Hydraulic Research, 3:1, 1-19.

Banisoltan, S., Rajaratnam, N., and Zhu, D. Z. (2015). "Experimental Study of Hydraulics of Drill-Drop Manholes." *Journal of Hydraulic Engineering*, 04015021.

Banisoltan, S., Rajaratnam, N., and Zhu, D. Z. (2016). "Experimental and Theoretical Investigation of Vertical Drains with Radial Inflow." *Submitted to the ASCE journal of Hydraulic Engineering*.

Binnie, A. M. (1938) "The use of a vertical pipe as an overflow for a large tank." *Proceedings of the Royal Society of London. Series A, Mathematical and Physical Sciences*, 219-237.

Humphreys, H. W., Sigurdsson, G., & Owen, H. J. (1970). "Model test results of circular, square, and rectangular forms of drop-inlet entrance to closed-conduit spillways." State Water Survey Division.

Indlekofer, H. (1978), "The computation of crest profiles of cup-shaped dam spillways." *Bautechnik*, 55 (11), 368-371 [in German]

Kalinske, A. A. (1941). "Hydraulics of vertical drain and overflow pipes." *Papers abstracts of theses and research reports, and reference list of staff publications,* J. W. Howe, ed., Iowa Institute of Hydraulic Research, Iowa City, IA.

Khatsuria, R. M. (2004). "Hydraulics of spillways and energy dissipators." CRC Press.

US Army Corps of Engineers (1990–92), "Hydraulic design of spillways." EM1110-2-1603, Department of the Army, Washington DC.

Laushey, L. M. (1952). "Flow in vertical shafts." *Carnegie Institute of Technology*, Department of Civil Engineering.

Rahm, L. (1953). “Flow of water discharged through a vertical overflow pipe” in “Flow problems with respect to intakes and tunnels of Swedish hydro-electric power plants.” *Trans. Roy. Inst. Tech.*, Stockholm, No. 71. 71-117.

Vischer, D. L. , Hager, W. H (1998). “Dam hydraulics.” Wiley, Chichester.

Wagner, W. E. (1956). “Morning-glory shaft spillways: A Symposium: Determination of Pressure-Controlled Profiles.” *Transactions of the American Society of Civil Engineers*, *121*(1), 345-368.

Chapter 6) Freeboard for flows inside a dropshaft with one and two inlets

6.1. Introduction

Any city or land development agency needs rethinking of current stormwater controlling systems to ensure a safe operation under new conditions. This means that if some new inlets are added to the existing dropshaft, overflowing should be checked and if corrosion has been reported, necessary steps in rehabilitation should be taken. In the City of Edmonton, one type of stormwater controlling structure called drill drop manhole (DDM) faces erosion and corrosion problems. These DDM's are essentially two attached manholes in which the diameter of the upper manhole, D (equal to 1200 mm) is only about twice that of the diameter of the lower manhole, d_o (equal to 600 mm). Stormwater flow is conveyed to the upper manhole by several inlets with various sizes and configurations. Corrosion is known to occur in the lower manhole which is a corrugated pipe and City of Edmonton has decided to insert new PVC pipes with a diameter of 384 mm inside the corrugated pipes to ensure safe operation of these structures. With this proposed rehabilitation design, D/d_o will change to 3.

Chapter 2 studied different flow regimes in these DDM and developed dimensionless graphs to predict the water depth in the upper manhole for different discharges and inlet numbers and also for high and low inlet elevations. If one inlet was located at a higher elevation, the incoming jet from the inlet hit the opposite wall, and formed a rolling curtain of water around the inner wall of the upper pipe. Fig. 6.1 shows a schematic sketch of this jet impingement and Fig. 6.2a shows one experiment with Q=2 L/s. Maximum water elevation of this water curtain has been shown as J_1 (see Fig. 6.1). It was found that J_1 occasionally exceeded the height of the upper pipe L.

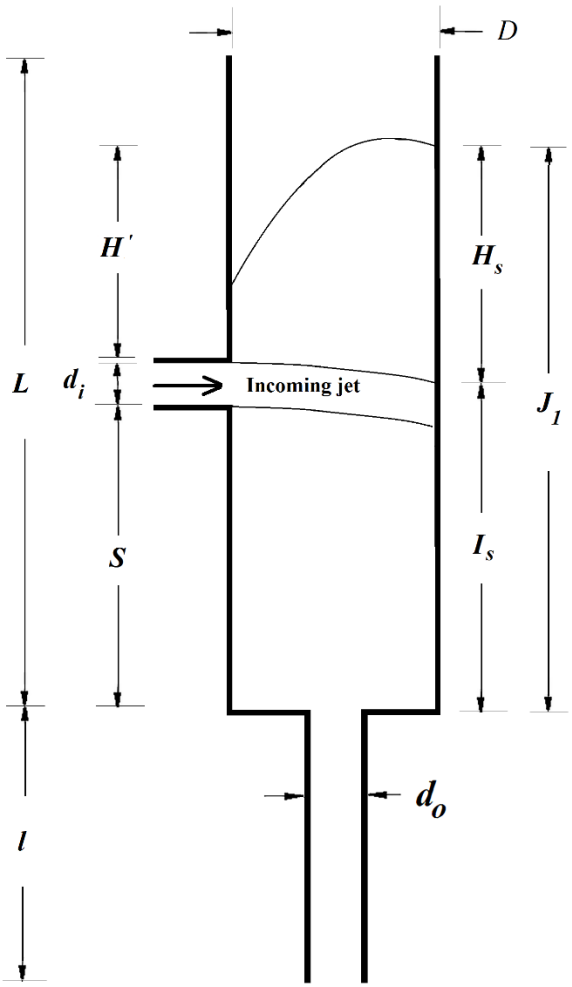

Fig. 6.1 Sketch of the experimental setup

In a recent study by Camino et al. (2014), it has been emphasized that the adequate free board plays an important role in the capacity of dropshafts. Camino et al. (2014) provided dimensionless graphs for a constant value of the shaft to inlet diameter equal to 2 (D/d_i=2). In this study, their study was expanded to a range of diameter ratios, also the effect of two inlets (instead of one) was evaluated. The effect of the D/d_i ratio in determining the maximum water elevation J_1 was studied and the corresponding required free board was compared with the velocity head. For this purpose, four different inlet sizes have been used for one inlet setup and the comparison of J_1 in a two inlet setup with the one inlet setup has been presented.

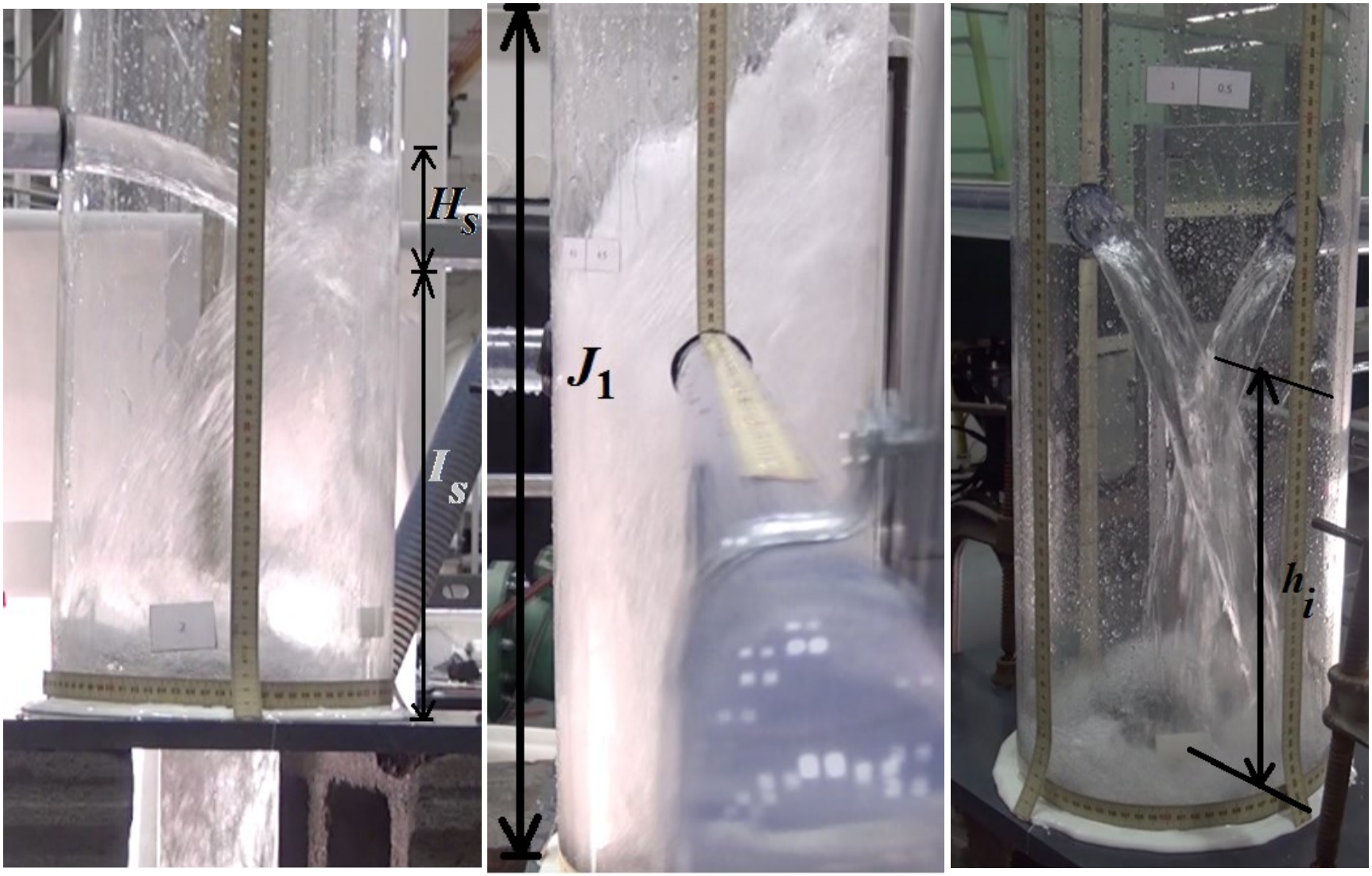

a b c

Fig. 6.2 Incoming jet from inlet, a) Q_1= 2L/s, b) Q_1=Q_2=4.5L/s c) Q_1= 1L/s, Q_2=0.5L/s

6.2. Experiments and Experimental Analysis

The experiments were conducted in the T. Blench hydraulic Laboratory at the University of Alberta. A physical model scale of 5 was selected with different inlet sizes. The experimental details are shown in Table 6.1. Because of the oscillatory nature of water elevation in the dropshaft, the maximum value was recorded and reported as J_1 in this study. Four different inlet diameters have been used with the smallest one representing the smallest inlet diameter in the DDM's in City of Edmonton equal to 200 mm. Therefore, the D/d_i ratio in this study varies between 2.2 and 6. The inlet elevation S was approximately equal for all of the experiments. The height of the upper pipe L was equal to 600 mm corresponding to the smallest manhole length in the city equal to 3 m. Although it was expected that the lower pipe diameter or length have no effect on J_1 (in the flow regime considered), a varying outlet length with a diameter was also included in the experiments.

Table 6.1 Details of experiments

Series	d_o (mm)	d_i (mm)	S (mm)	D/d_o	D/d_i	Comments
A1-1	76	52	389	3.1	4.6	One inlet at higher elevation with different inlet diameters and l=557mm
A1-2	76	40	401	3.1	6	
A1-3	76	77	383	3.1	3.1	
A1-4	76	107	391	3.1	2.2	
A3-2	76	52	389	3.1	4.6	One constant inlet diameter at higher elevation and l=455mm
B1-1	121	52	389	2	4.6	Same as A1 series but with different outlet diameter
B1-2	121	77	391	2	3.1	
Series with two inlets at a horizontal plane (angle:90 degree)						
C1-1	76	52	389, 389	3.1	4.6	a:Q_1/Q_2=1, b: Q_1/Q_2=*2*, c: Q_1/Q_2=3
C1-2	76	40	401, 401	3.1	6	a:Q_1/Q_2=1, b: Q_1/Q_2=2
C1-3	76	77	383, 383	3.1	3.1	a: Q_1/Q_2=1, b: Q_1/Q_2=2

Note: D = 239 mm.

The elevation of the impingement point I_s has been recorded separately and can be calculated using Eq. 6.1.

$$I_s = J_1 - H_s \tag{6.1}$$

Here, H_s is the height of water surface above the impingement point. Water depth above the crown of the inlet, H', has been recorded following Camino et al. (2014). The variation of H'/D with dimensionless discharge Q_i*, as presented in Eq. 6.2, was studied. Here, Q is the flow discharge. Such a comparison is shown in Fig. 6.3. It was found that although the results of series A1- 4 and Camino et al. (2014) which both have approximately equal D/d_i ratio, follow a similar trend, the experiments of other D/d_i ratios suggested the importance of this ratio in the prediction of H'. The dimiensionless discharge is written as

$$Q_i^* = \frac{Q}{\sqrt{g d_i^{\,5}}} \tag{6.2}$$

Similar results were observed for the variation of $H'/(V_i^2/2g)$ with Q_i* as presented by Camino et al. (2014) where V_i is the inlet velocity. Therefore, it became necessary to look for general dimensionless parameters that can represent the observed changes. For this purpose, instead of H', the maximum water elevation J_1 was expanded as H_s and I_s to be analyzed in further detail.

It was found that $H_s/(V_i^2/2g)$ versus Q_i* has the same decreasing trend for all of the experimental data of the current study in which the inlets are located at the same elevation. Besides, H_s in the series with the largest inlet diameter (the smallest Q_i* and V_i), was quite larger than the incoming velocity head as shown in Fig. 6.4. Accordingly, H_s was found to highly depend on d_i and varies with Q_i* as shown in Fig. 6.5. The regression analysis showed that Eq. (6.3) can be represented by the following fitted curve with R^2=0.94.

$$\frac{H_s}{d_i} = 2.5Q_i^* - 1.06 \qquad \text{(For } D/d_i \text{ between 2.2 to 6)} \quad (6.3)$$

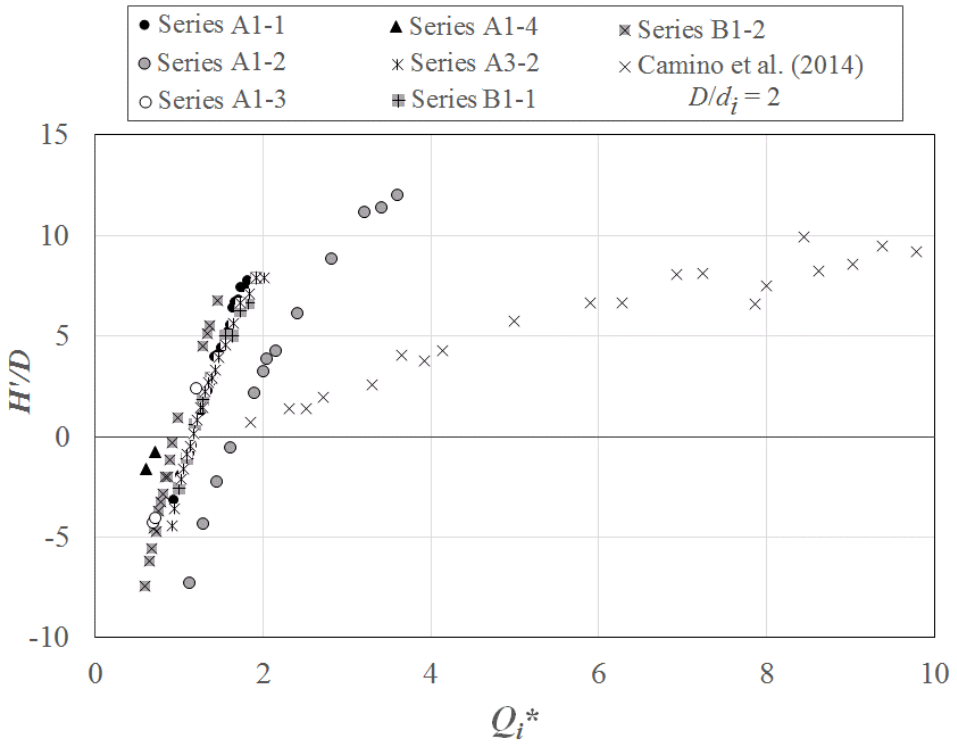

Fig. 6.3 Comparison of current study results with Camino et al. (2014)

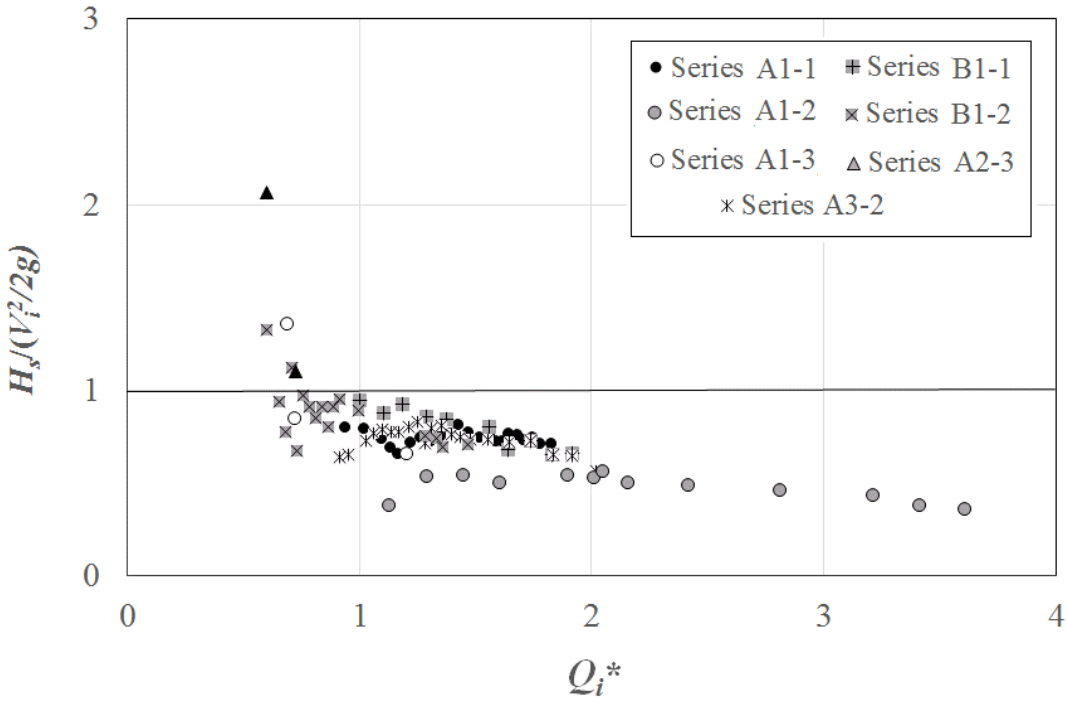

Fig. 6.4 Variation of ratio of water height to the velocity head with Q_i*

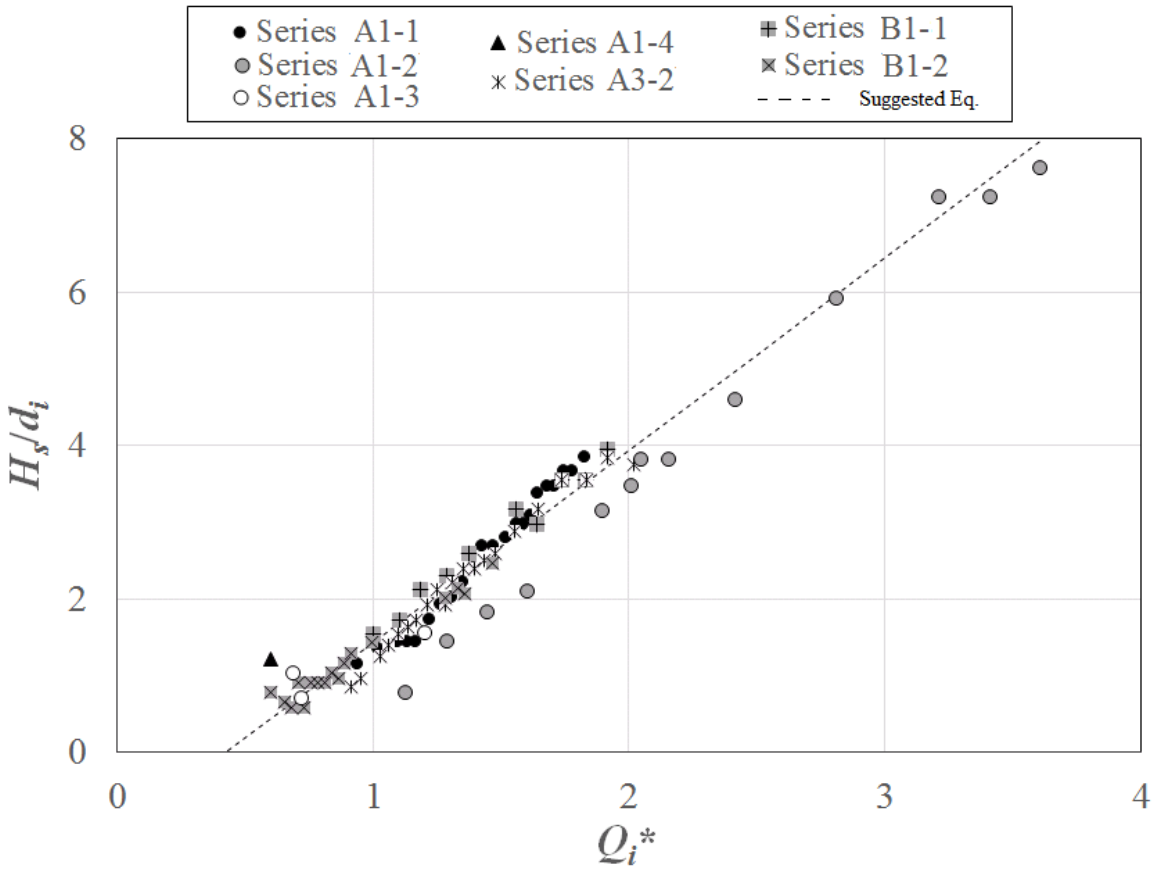

Fig. 6.5 Variation of dimensionless H_s with Q_i*

Similar dimensional analysis for J_1 showed the importance of D/d_i ratio as shown in Fig. 6.6. This curve could be represented by Eq. (6.4) with R^2=0.9. For a larger D/d_i (smaller d_i/D) ratio, J_1 has a smaller value. Therefore, the freeboard H' can be calculated indirectly.

$$\frac{J_1 - S}{S} = 3Q_i^* \frac{d_i}{D} - 0.67 \tag{6.4}$$

If two inlets were located at a 90 degree orientation, and at the same elevation, it was found that J_1 does not depend on the discharge ratio between the inlets Q_1/Q_2. However, it is considerably smaller than J_1 in the one inlet setup with the same inlet size which is located at the same inlet elevation. This difference increased with the increase in discharge as shown in Fig. 6.7.

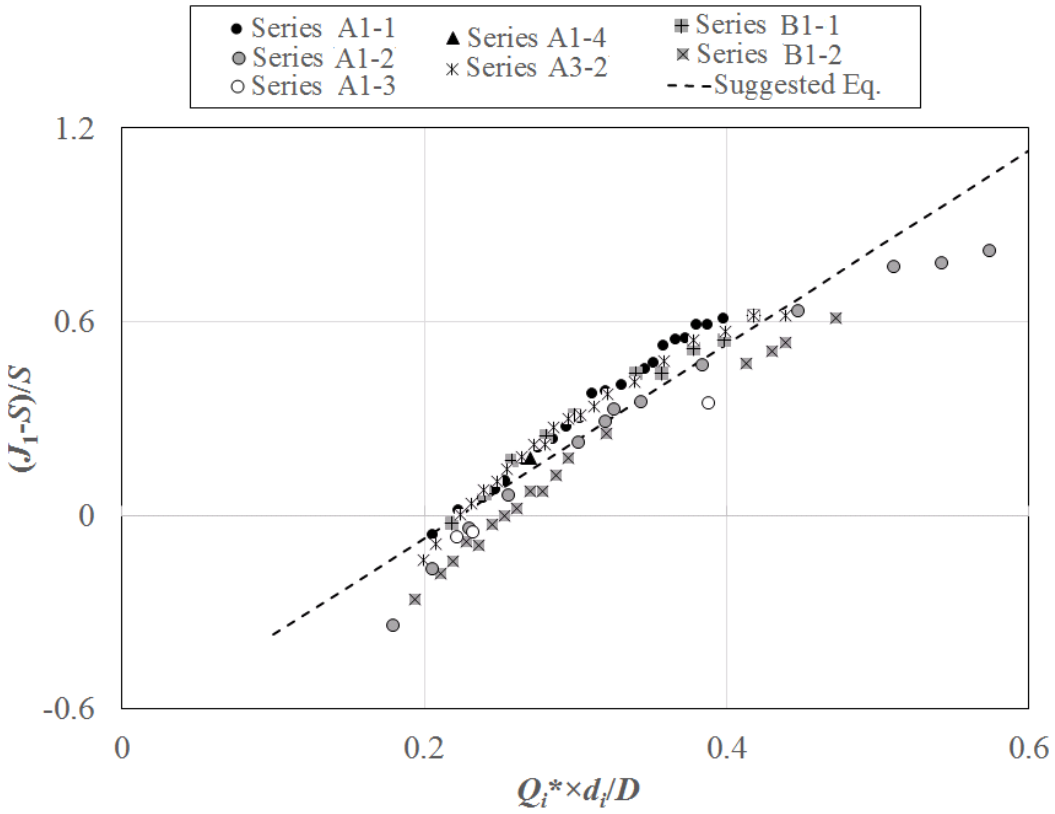

Fig. 6.6 Dimensionless variation of J_1 with the discharge

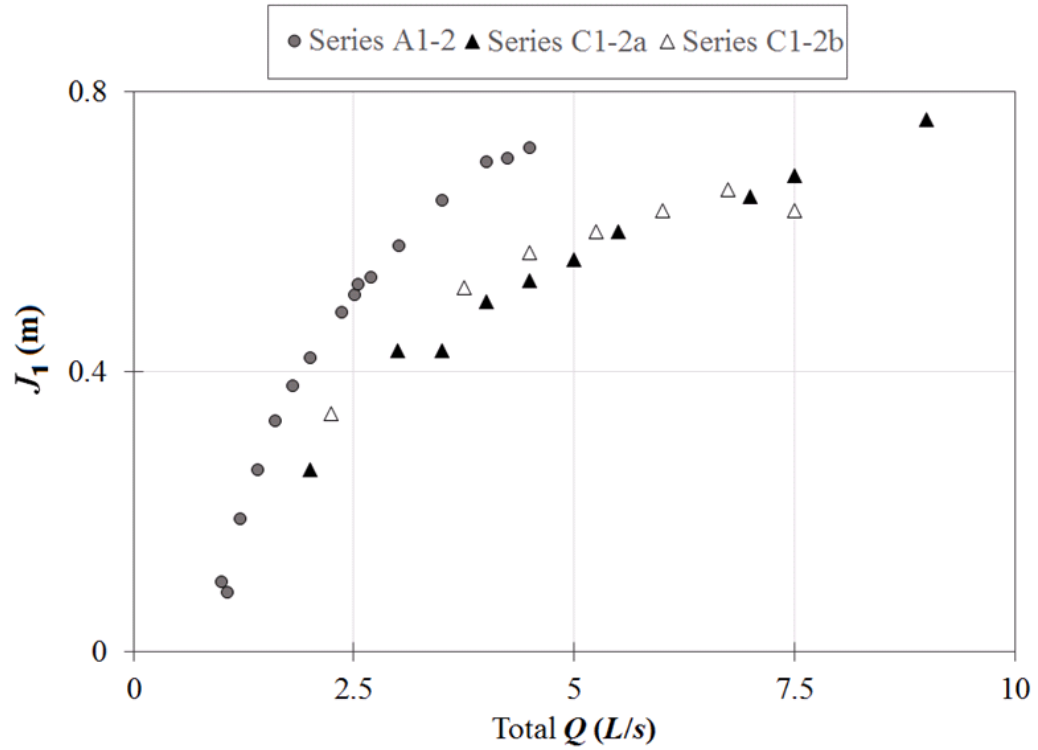

Fig. 6.7 The effect of number of inlets in J_1 with the discharge

6.3. Interaction of Incoming Jets from Inlets

In two inlet series of experiments, the interaction point of the two incoming jets was very discharge-dependent and it was attempted to measure the elevation of the highest impact point h_i as shown in Fig. 6.2c. From the theory of water jet trajectories, for horizontal inlet velocities of V_1 and V_2,

$$y_1 = \frac{g}{2}\frac{x_1^2}{V_1^2} \quad \text{and} \quad y_2 = \frac{g}{2}\frac{x_2^2}{V_2^2}$$

where x is the distance along x-axis in the direction of inlet and y is the vertical downward distance from y-axis. Both of x and y axis are shown in Fig. 6.1. At the point of interaction, $y_1=y_2$, therefore:

$$\frac{x_1}{x_2} = \frac{V_1}{V_2} \tag{6.5}$$

For trajectories for two horizontal inlets located 180 degree apart at a height of S,

$$x_1+x_2=D \tag{6.6}$$

Therefore,

$$y_2 = \frac{g}{\left(\frac{V_1}{V_2}+1\right)^2}\frac{D^2}{2V_2^2} \quad \text{or} \quad \frac{y_2}{D} = \frac{0.5}{\left(\frac{V_1}{V_2}+1\right)^2}\frac{gD}{V_2^2}$$

Since $S=y_2+h_i$, $d_{i1}=d_{i2}$, $Q_1/Q_2=r$: $$\frac{h_i}{D} = \frac{S}{D} - \frac{0.5}{(r+1)^2}\frac{gD}{V_2^2} \tag{6.7}$$

The comparison of Eq. 6.7 with the experimental data as h_i/D with $V_2/(gD)^{0.5}$ did not show a good agreement. Therefore, a similar trend for 90 degree has been followed with considering the thickness of jet as is shown in Fig 6.8.

$$D/2 - x_2 = t_1/2$$

$$D/2 - x_1 = t_2/2$$

Therefore, combination of both of the above equations will result in:

$$D - x_1 - x_2 = (t_1 + t_2)/2 \tag{6.8}$$

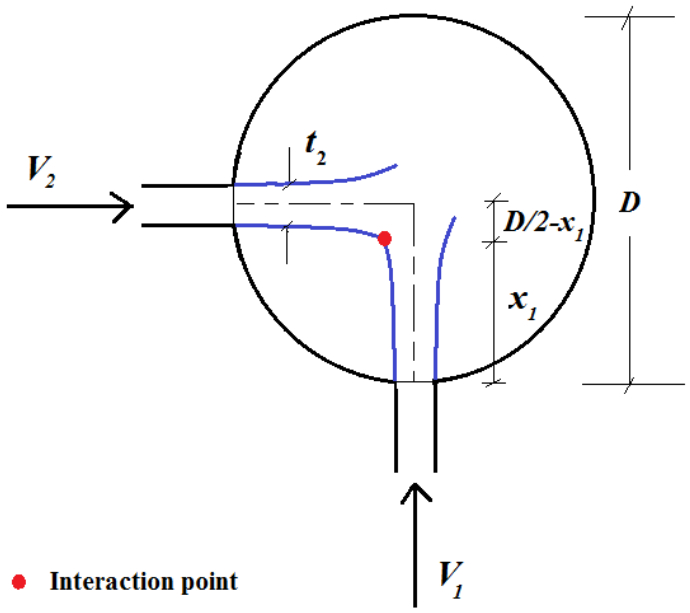

Fig. 6.8 Simplified two-dimensional plan view of the interaction point.

For the upper nappe trajectory of partial full inlets, Hager (2010) presented the vertical thickness of the jet t_i as Eq. 6.9 In this study, it has been assumed that the same thickness can be used for the horizontal thickness.

$$T = \frac{t}{h_0} = 1 + 0.06\left(\frac{x}{h_0}\right)F_0^{-0.8} \tag{6.9}$$

where h_0 is the head ($y_i + V_i^2/2g$), $F_0 = Q/(g d_i h_0^4)^{0.5}$ and d_i is the inlet diameter in Hager (2010).

For this study in which h_i has been measured for the full inlets, several form of "Froude Number" has been examined. It was found that Eq. 6.10 represents the results somewhat better. The head h_0 was also considered as ($d_i + V_i^2/2g$)

$$F_0 = \frac{Q}{\sqrt{g h_0^{\,5}}} \tag{6.10}$$

Therefore, inserting Eq. 6.9 in Eq. 6.8, will conclude

$$D - x_2(\frac{V_1}{V_2} + 1) = \frac{1}{2}(h_{01} + 0.06x_1 F_{01}^{-0.8} + h_{02} + 0.06x_2 F_{02}^{-0.8})$$

$$D - x_2(\frac{V_1}{V_2} + 1) = \frac{1}{2}(h_{01} + h_{02}) + 0.03(x_2 \frac{V_1}{V_2} F_{01}^{-0.8} + x_2 F_{02}^{-0.8})$$

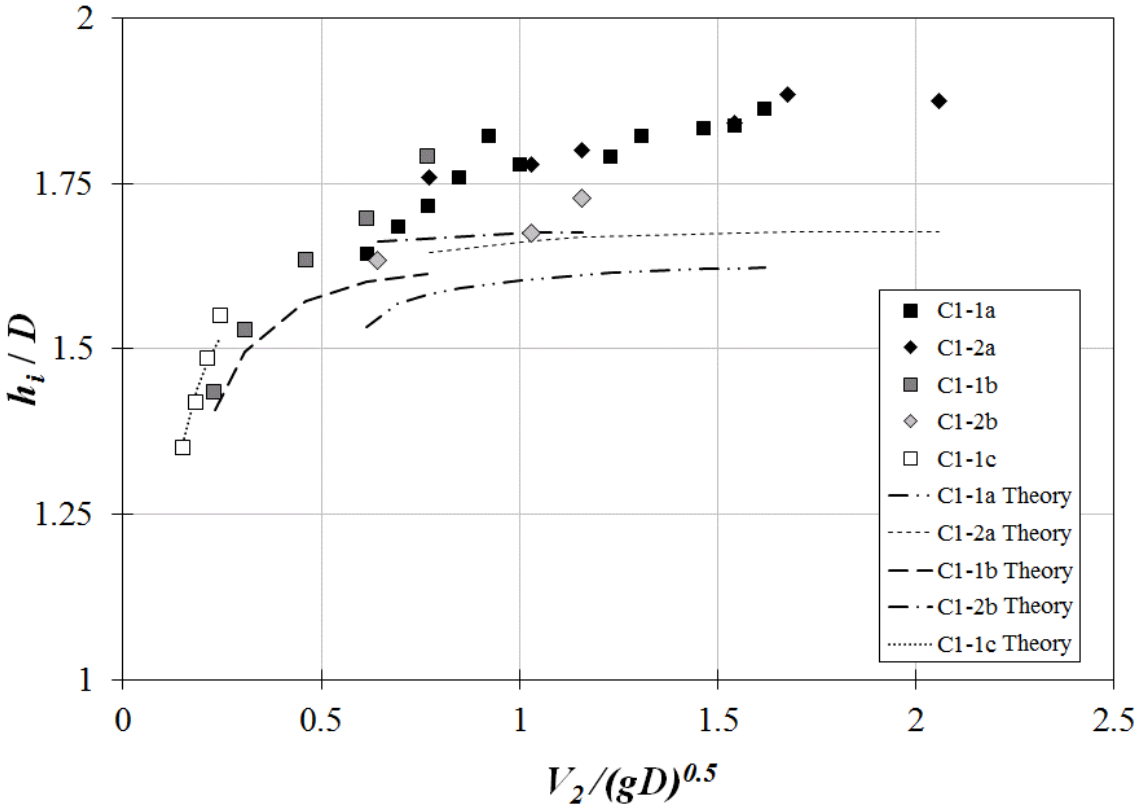

Fig. 6.9 The comparison of the measured and theoretical variation of h_i with $V_2/(gD)^{0.5}$

In DDM's experiments, r was defined as Q_1/Q_2. Since, inlet diameters were the same, V_1/V_2 is also equal to r.

$$D - x_2(r + 1) = \frac{1}{2}(h_{01} + h_{02}) + 0.03(x_2 r F_{01}^{-0.8} + x_2 F_{02}^{-0.8}) \quad (6.11)$$

By calculating x_2, y_2 and therefore h_i/D can be calculated. The comparison of the theoretical method and measurements of h_i/D has been shown in Fig. 6.9. Both the experimental and theoretical data are compared versus $V_2/(gD)^{0.5}$ as described before for 180 degree. It was found

that for r=3 this theoretical method matches the experimental data. Moreover, for other ratios the maximum difference was 12.5 %.

6.4. Discussion

In the experimental analysis, the maximum value of the water elevation for discharges larger than the discharge required to have full-pipe inlet has been represented. In case both full and partially-full inlets are consider in the regression analysis, Eq. 6.3 changes to Eq. 6.11 with R^2 =0.92.

$$\frac{H_s}{d_i} = 2.1Q_i^* - 0.46 \tag{6.12}$$

Moreover, in Fig. 6.4, the fact that H_s exceeded the inlet jet velocity, can be explained as the following. Total equivalent pressure P, is responsible for a water rise of H_s' in the absence of air entrainment to the jet. However, due to the air entrainment to the jet, H_s was observed and measured as presented in Eq. (6.13) and rewritten in Eq. (6.14), where ρ_w is the water density and ρ_m is the mixer density. Since $\rho_w > \rho_m$, H_s exceeded the inlet velocity head.

$$P = H_s \rho_m g = H_s' \rho_w g \tag{6.13}$$

$$\frac{H_s}{H_s'} = \frac{\rho_w}{\rho_m}$$

$$H_s = \frac{\rho_w}{\rho_m} H_s' = \frac{\rho_w}{\rho_m} \frac{V_i^2}{2g} \tag{6.14}$$

Besides, the fact that in Fig 6.5, H_s/d_i has a linear relation with Q_i* as shown in Eq. 3, it can be explained with a parameter that seems like Froude Number as Eq. (6.15)

$$\frac{H_s}{d_i} = 2.5 \frac{Q_i}{\sqrt{g d_i^5}} - 1.06$$

$$\frac{H_s}{d_i} = 2.5\frac{\pi V_i d_i^{\,2}}{4\sqrt{g d_i^{\,5}}} - 1.06$$

6.5. Conclusions

Experimental study of the maximum water elevation inside a pipe after impinging of the jet from the inlet on the opposite wall has been studied. Four different inlet diameters were used such that the diameter ratio of shaft to inlet D/d_i varied between 2.2 to 6. Dimensionless graphs showed that the water depth above the jet impingement depends on d_i and dimensionless discharge $Q_i^* = Q/(gdi^5)^{0.5}$ where Q is the discharge. It has been also found that the maximum water elevation not only depends on Q_i^*, but also depends on D/d_i. Then, the elevation of the impingement point and freeboard can be determined. Although full and partially-full inlets were considered in this study, maximum impingement height for partially inlets are also formulated. The results of two inlets setups with different discharge ratios are compared with one-inlet results.. At the end, a practical formula for the elevation of the impact point between two incoming jets from the inlets has been presented.

6.6. Notation

The following symbols are used in this chapter:

D = Diameter of the upper pipe

d_i = Diameter of the inlet pipe

d_o = Diameter of the outlet pipe

F_0 = $Q/(gh_0^5)^{0.5}$

g = Acceleration due to gravity

h = Mean water depth in the upper pipe

h_0 = Head ($d_i+V_i^2/2g$)

h_i = Impact point between the incoming jet from the inlets

H_s = The water height above the jet impingement point on the opposite wall

H' = Required Freeboard (elevation of the water elevation above the crone of the inlet)

I_s = The elevation of the jet impingement point on the opposite wall

J_1 = Total height of the rolling water curtain

Q = Discharge

Q_i* = Dimensionless discharge based on the inlet diameter

Q_{ic} = Incipient chocking initiation

L = Height of the upper pipe

r = Q_1/Q_2, Discharge ratio for two inlets

S = Inlet elevation

t = Vertical thickness of the inlet jets

V_i = Inlet velocity

x = X-axis

y = Y-axis

ρ = Density of water

Subscript

1 = Inlet with larger discharge in two inlet series

2 = Inlet with smaller discharge in two inlet series

i = Inlet in general term

References

Banisoltan, S., Rajaratnam, N., & Zhu, D. Z. (2015). "Experimental study of hydraulics of drill-drop manholes". *Journal of Hydraulic Engineering*, 04015021.

Camino, G. A., Rajaratnam, N., & Zhu, D. Z. (2014). Choking conditions inside plunging flow dropshafts. *Canadian Journal of Civil Engineering*, *41*(7), 624-632.

Hager, W. H. (2010). "Wastewater hydraulics: Theory and practice." S*pringer Science & Business Media*, Springer-Verlag Berlin Heidelberg.

Chapter 7) General Conclusions and Recommendations for Further Research

7.1. General Conclusions

The results of this study can be used in the design and operation of hydraulic structures consisting of vertical drains whether being affected by the incoming momentum or not. Examples of such structures are stormwater, sanitary manholes or urban water supply facilities. The most significant contributions of this study are summarized in the following.

- In the case in which the flow is significantly impacted by the momentum of inlet jet , the traditional flow regimes do not occur. Instead, three new flow regimes were observed. Two of these regimes were steady and referred to as the deflected jet (DJ) and the stable pool (SP) flow regimes. In the third regime, the water depth was oscillated between maximum and a minimum values. This flow regime was called the filling and emptying (FE) flow regime.
- It was found that in these new flow regimes, the control section is at the throat or is at the top end of the vertical pipe. Free vortex theory and the principle of maximum discharge were used to predict the head discharge relationship in these flow regimes.
- In the case where the throat does not completely form in the vertical outlet pipe with a diameter of d_o, it is possible to assume that in a length between $0.2d_o$ to $1d_o$, a throat-like section will form which controls the flow. Experimental observations have confirmed this assumption.
- Water depth variation with time showed that the outlet discharge can be represented with an orifice formula and a coefficient of discharge equal to 0.65.
- The oscillating water depth can be normalized with the Strouhal Number.

- The inlet diameter becomes important only in case of one inlet series located at a lower elevation. If the inlets are located at a higher elevation, number of inlets does not affect the flow regimes. If two inlets are located at a lower elevation, the discharge ratio becomes important.
- If a radial water supply method is used, there is this possibility that not only the oscillating water variation occurs, but also the changes from the weir flow regime to the orifice flow regime could cause a considerable head rise in a setup that has been designed for small heads within the weir flow regime.
- This study recommends operation at the SP flow regime for setups with small diameter ratios between the tank and the outlet diameter. This ensures a steady flow regime that is desirable in other type of drop structures such as vortex drops as mentioned by Ackers and Crump (1960). The SP flow regime does not depend on the inlet size or location. This can provide a safe operation within a practically feasible size of the upper tank as commonly used in urban facilities.
- In the hydraulic design of shaft spillways in dams (as studied by Indlekofer 1978, and mentioned by Vischer and Hager, 1998), it is recommended that the ratio of head h to shaft crest diameter d_o is limited to $0.1<h/d_o<0.25$. This prevents the risk of switching of the flow regime. However, this ratio is not applicable in stormwater manholes. Instead, designing a vertical drain in the SP regime will ensure safe operation with h/d_o as large as up to 1.5.
- This study showed the operation of full pipe flow regimes with dominant momentum from the inlets as well as negligible incoming momentum. If the flow is dominated by the incoming momentum, the energy loss coefficient can be as large as 3.0 and then

decreases with an increase of the dimensionless discharge. On the other hand, in case of a radial flow, the entrance loss coefficient was about 0.1 for the largest diameter of the tank size (T1) and then by decreasing the tank size it increased to 0.15 in T3.

- In this study, for the first time, the oscillatory water depths were recorded for a number of discharges. Moreover, it was found that the oscillatory water depths can be represented with the throat control or the weir control formulations. The free vortex theory and the Rankine vortex theory were used for this purpose.
- It was found that in the Borda full flow (Rahm 1953, Binnie 1938), the control section is at the end of the outlet pipe. A critical air core size to the vertical outlet diameter equal to 0.67 was determined based on the experimental results of the current study as well as Rahm's (1953) experiments and measurements in the Harspranget dam.
- It was found that the transition of the control section from the top end of the vertical pipe to the bottom end of it, was not possible in large discharges. In fact, a weir control section with a formulation based on the free vortex theory could represent the head discharge curve.
- The weir flow regime in the vertical drain with a radial water supply was found to have a discharge coefficient that varied linearly with h/d_o. It was found that unlike shaft spillways wherein the discharge coefficient decreases with h/d_o, the coefficient of discharge increased with h/d_o.
- This study also reevaluated the findings of previous studies (Kalinske, 1941) in which the variation of discharge with head has been reported to follow a second-order power law. It has been shown that a weir flow regime exists with a linear relation between the coefficient of discharge and h/d_o.

7.2. Future Research Studies

Changing from weir flow to orifice flow regime

The critical condition changing the weir flow regime to the orifice flow regime should be studied in detail. For this purpose, it is suggested that the water surface variation be recorded with a wave gauge and at the same time, pressure be recorded at the top of the vertical pipe just below of the tank bottom at several points. Velocity should also be recorded using an acoustic Doppler velocimeter (ADV). In such an experimental arrangement, all of these instruments are controlled by a central software that can simultaneously record measurements for any specific time, pressure, velocity and water depths. With this setup, it would be possible to understand more fully the hydraulics of the flow behavior.

Velocity variation in change of weir flow regime to the orifice flow regime or the FE process

With the setup described in the previous research suggestion, it would be possible to investigate the variation of tangential, vertical and radial velocities in changes of weir flow regime to orifice flow regimes and the FE process.

Effect of tailwater on oscillating water depths; e.g. in morning glory spillways

Bradley (1956) has reported water oscillations in several morning glory spillways in the world. In case of the Owyhee dam, if the head to crest diameter ratio was 1/60, a 15 m spray of water above the shaft was observed. It was found that the tailwater elevation had an effect on the occurrence of this phenomena. Therefore, the effect of tailwater on the oscillatory water depths and chocking condition should be studied.

Air entrainment

Although there are some formulations for predicting the air entrainment in overflow pipes, e.g. Viparelli (1961) and Hack (1977), their methods require determination of several parameters that, from an engineering point of view, are not always available. For example, the Froude number at the point of inception or maximum average of the air concentration are such parameters. Since Kalinske (1941) measured air entrainments in both drain and overflow pipes, it may be possible to develop more convenient formulations for air entrainment.

Other research recommendations

- Numerical simulation of the drill drop manholes with different inlet sizes and arrangements
- Numerical simulation of water depth oscillation in vertical drain with the radial water supply
- Effect of viscosity on the switch of the weir flow regime to the orifice flow regime

References

Ackers, P., & Crump, E. S. (1960). "The vortex drop". *In ICE Proceedings* (Vol. 16, No. 4, pp. 433-442). Thomas Telford.

Binnie, A. M. (1938). "The use of a vertical pipe as an overflow for a large tank." *Proceedings of the Royal Society of London. Series A, Mathematical and Physical Sciences*, 219-237.

Bradley, J. N. (1956). Morning-glory shaft spillways: a symposium: prototype behavior. *Transactions of the American Society of Civil Engineers*, *121*(1), 312-333.

Hack, H. P. (1977) "Air entrainment in dropshafts with annular flow by turbulent diffusion." *17th IAHR Congress*, Baden-Baden, Germany, August; Vol. 1.

Kalinske, A. A. (1941). "Hydraulics of vertical drain and overflow pipes." *Papers abstracts of theses and research reports, and reference list of staff publications,* J. W. Howe, ed., Iowa Institute of Hydraulic Research, Iowa City, IA.

Rahm, L. (1953). “Flow of water discharged through a vertical overflow pipe” in “Flow problems with respect to intakes and tunnels of Swedish hydro-electric power plants.” *Trans. Roy. Inst. Tech.*, Stockholm, No. 71. 71-117.

Indlekofer, H. (1978), “The computation of crest profiles of cup-shaped dam spillways.” *Bautechnik*, 55 (11), 368-371 [in German]

Viparelli, M. (1961). “Air and water currents in vertical shafts.” *La Huille Blanche*, *6*(857-869).

Vischer, D. L., Hager, W. H (1998). “Dam hydraulics.” Wiley, Chichester.

References

Ackers, P., & Crump, E. S. (1960). "THE VORTEX DROP" *ICE Proceedings*, 16(4), 433-442, Thomas Telford.

Anderson, S. H. (1961). "Model studies of storm-sewer drop shafts." *ST. Anthony falls hydraulic laboratory*, Technical paper No. 35, Series B, University of Minnesota.

Anderson, A. G., Vadiyaraman, P. P. and Chu, C. S. (1971). "Hydraulics of long vertical conduits and associated cavitation." *ST. Anthony Falls and Hydraulic Lab*, Minnesota University, Minneapolis, MN.

Anwar, H. O. (1965a). "Coefficients of Discharge for Gravity Flow in to Vertical Pipes." *J. Hydraul. Res.*, 3(1), 1-19.

Anwar, H. O. (1965b). "Flow in a Free Vortex." *Water Power*, 17, 153-161.

Anwar, H. O. (1966). "Formation of a Weak Vortex." *J. Hydraul. Res.*, 4(1), 1-16.

Anwar, H. O. (1969). "Turbulent Flow in a Vortex." *J. Hydraul. Res.*, 7(1), 1-29.

Anwar, H.O., Weller, J.A. and Amphlett, M.B. (1978). "Similarity of Free-Vortex at Horizontal Intake." *J. Hydraul. Res.*, 16(2), 95-105.

Banisoltan, S., Rajaratnam, N., and Zhu, D. Z. (2015). "Experimental Study of Hydraulics of Drill-Drop Manholes." *Journal of Hydraulic Engineering*, 04015021.

Banisoltan, S., Rajaratnam, N., and Zhu, D. Z. (2016). "Experimental and Theoretical Investigation of Vertical Drains with Radial Inflow." *Submitted to the ASCE journal of Hydraulic Engineering*.

Bradley, J. N. (1956). Morning-glory shaft spillways: a symposium: prototype behavior. *Transactions of the American Society of Civil Engineers*, *121*(1), 312-333.

Binnie, A. M. (1938). “The Use of a Vertical Pipe as an Overflow for a Large Tank.” *Proc. Royal Society of London*. Series A, Mathematical and Physical Sciences, 168, 219-237.

Binnie, A. M., and Hookings, G. A. (1948). “Laboratory Experiments on Whirlpools.” *Proceedings of the Royal Society of London.* Series A, Mathematical and Physical Sciences, 194, 1038, 398-415.

Binnie, A. M and Wright, R. K. (1941). “Laboratory Experiments on Bellmouth Spillways.” *J of the Institution of Civil Engrs*, 15(3), 197-219.

Blaisdell, F. W. (1953) “Hydraulic fundamentals of closed conduit spillways.” *ASCE J. Hydraul. Div*., 354, 1-14.

Camino, G. A., Rajaratnam, N., & Zhu, D. Z. (2014). Choking conditions inside plunging flow dropshafts. *Canadian Journal of Civil Engineering*, *41*(7), 624-632.

Chang, E and Prosser, M. J. (1987). “Basic results of theoretical and experimental work” in Knauss , J. (Ed.) “Swirling flow problems at intakes”. Rotterdam: A.A. Balkema.

Daggett, L. L., Keulegan, G. H. (1974). “Similitude in Free-Surface Vortex Formations.” *ASCE J. Hyd. Div.*, 100(11), 1565-1581.

Ettema, R. (2000). “Hydraulic modeling: concepts and practice.” *ASCE Manuals and Reports on Engineering Practice* No.97, Reston, VA.

Hack, H. P. (1977) “Air entrainment in dropshafts with annular flow by turbulent diffusion.” *17th IAHR Congress*, Baden-Baden, Germany, August; Vol. 1.

Hager, W. H. (2010). “Wastewater hydraulics: Theory and practice.” S*pringer Science & Business Media*, Springer-Verlag Berlin Heidelberg.

Heaney, J. P., Pitt, R. & Field, R. (2000) [Introduction] In Field, R., Heaney, J. P., & Pitt, R.. "*Innovative urban wet-weather flow management systems*." CRC Press, Lancaster, Pennsylvania, pp1.

Humphreys, H. W., Sigurdsson, G., & Owen, H. J. (1970). "Model test results of circular, square, and rectangular forms of drop-inlet entrance to closed-conduit spillways." State Water Survey Division.

Indlekofer, H. (1978), "The computation of crest profiles of cup-shaped dam spillways." *Bautechnik*, 55 (11), 368-371 [in German]

Kalinske, A. A. (1941). "Hydraulics of vertical drain and overflow pipes." In Howe, J. W. (Ed.) "Investigations of the Iowa Institute of Hydraulic Research: Papers, abstracts of theses and research reports, and reference list of staff publications", Iowa institute of hydraulic research, 26, Iowa, IA.

Kandaswamy, P. K., and Rouse, H. (1957). "Characteristics of flow over terminal weirs and sills." *Journal of the Hydraulics Division*, *83*(4), 1-13.

Kennedy, J., Jain, S., and Quinones, R. (1988). "Helicoidal-Ramp Dropshaft." *J. Hydraul. Eng.*, 114(3), 315–325.

Khatsuria, R. M. (2004). "Hydraulics of spillways and energy dissipators." CRC Press.

Koutsoyiannis, D., Zarkadoulas, N., Angelakis, A. N., & Tchobanoglous, G. (2008). "Urban water management in Ancient Greece: Legacies and lessons." *Journal of water resources planning and management*, 134(1), 45-54.

Laushey, L. M. (1952). "Flow in vertical shafts." *Carnegie Institute of Technology*, Department of Civil Engineering.

Leopardi, M., (2014) "Experimental study and design aspects of morning glory spillways." *New developments in dam engineering, Proceedings of the 4th International Conference on Dam Engineering, 18-20 October, Nanjing, China* (p. 461). CRC Press.

Ma, Y., Qian, Y., and Zhu, D.Z. (2013). "Effect of air core on the shape and discharge of the outflow through a bottom outlet." *Theoretical & Applied Mechanics Letters*, 3(2), 15-022003.

McDuffie, N. G. (1977). "Vortex free downflow in vertical drains." *AIChE Journal*, *23*(1), 37-40.

Quick, M. C. (1990). "Analysis of spiral vortex and vertical slot vortex drop shafts." *J. Hydraul. Eng.*, 116(3), 309–325.

Quick, M. C. (1992). Closure to "Analysis of Spiral Vortex and Vertical Slot Vortex Drop Shafts" by Michael C. Quick (March, 1990, Vol. 166, No. 3). " *J. Hydraul. Eng.*, *118*(1), 104-107.

Rahm, L. (1953). "Flow of water discharged through a vertical overflow pipe" in "Flow problems with respect to intakes and tunnels of Swedish hydro-electric power plants." *Trans. Roy. Inst. Tech.*, Stockholm, No. 71. 71-117.

Smith, D., (personal communication in email format regarding City of Edmonton's drill drops manholes, March 25, 2013)

US Army Corps of Engineers (1990–92), "Hydraulic design of spillways." EM1110-2-1603, Department of the Army, Washington DC.

Viparelli, M. (1961). "Air and water currents in vertical shafts." *La Huille Blanche*, *6*(857-869).

Vischer, D. L. , Hager, W. H (1998). "Dam hydraulics." Wiley, Chichester.

Wagner, W. E. (1956). "Morning-glory shaft spillways: A Symposium: Determination of Pressure-Controlled Profiles." *Transactions of the American Society of Civil Engineers*, *121*(1), 345-368.

Wulff, H. E. (1968). "The qanats of Iran." *Scientific American*, *218*(4), 94-105.

Appendix 1: Pictures of some of the experiments

a) Q= 0.32 L/s (DJ)

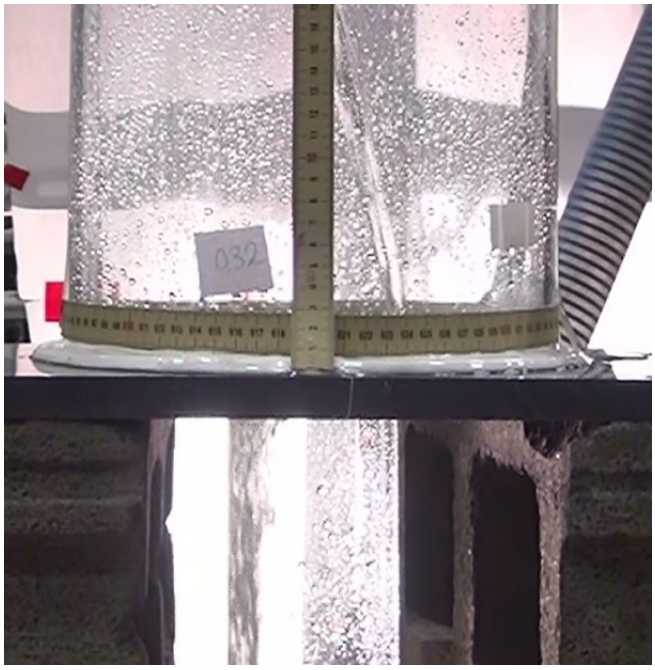

b) Q= 1 L/s (DJ)

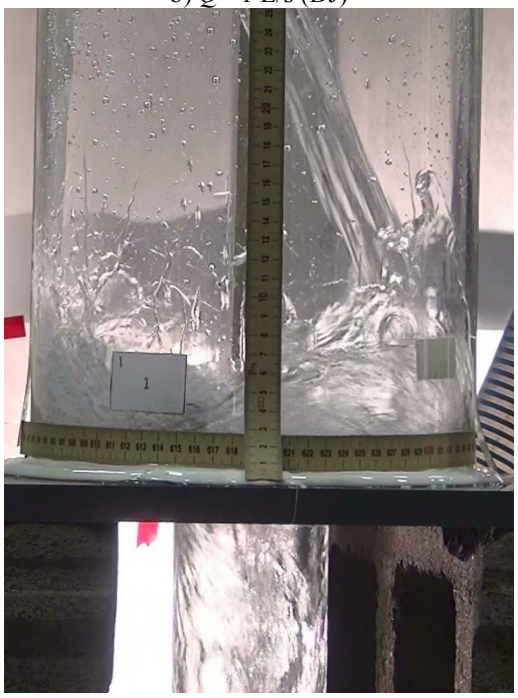

c) Q= 2.51 L/s (SP)

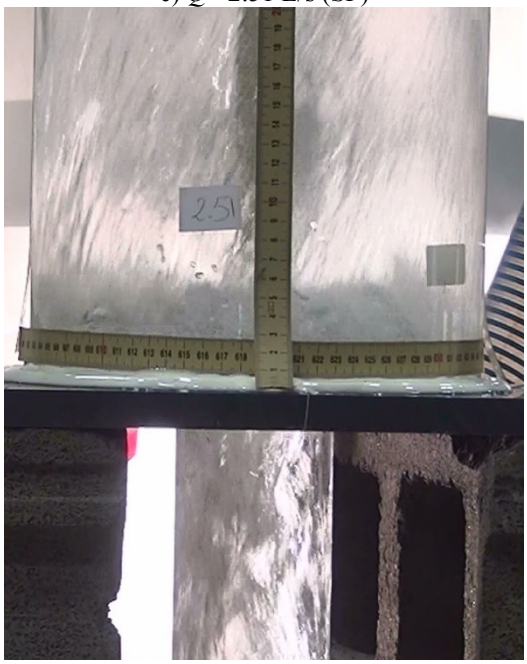

d) Q= 4 L/s (FE)

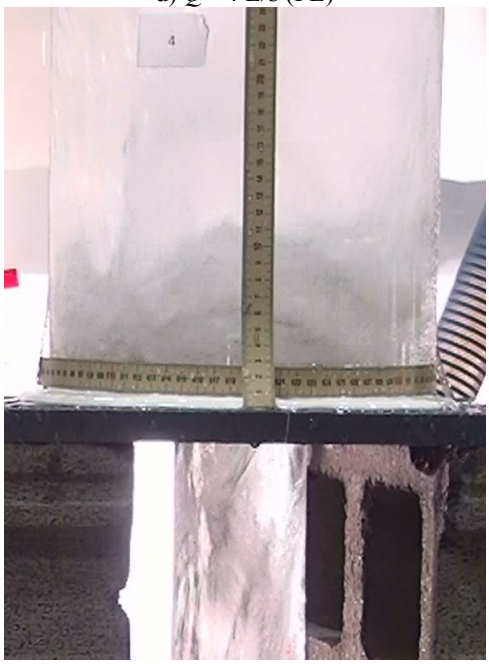

Fig A1.1 Different flow regimes in Series A1-2 (One inlet with d_i=4mm and S= 401mm, d_o=76mm)

a)Q=0.4 L/s

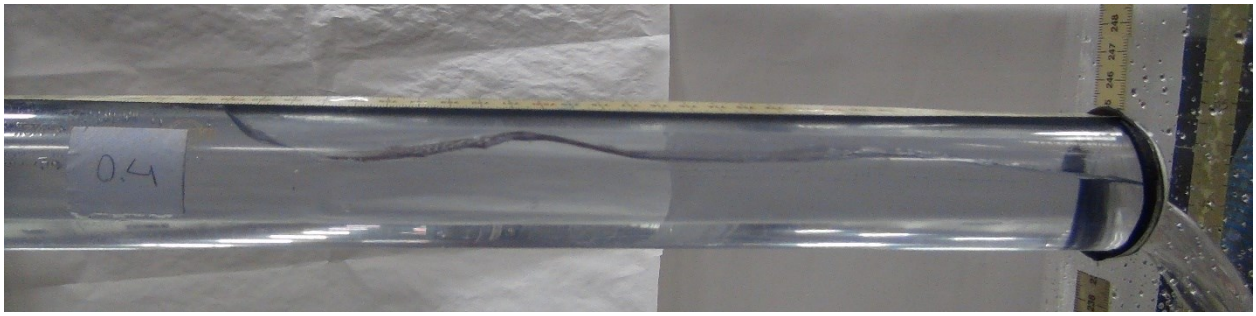

a) Q=0.5 L/s

b) Q=0.9 L/s

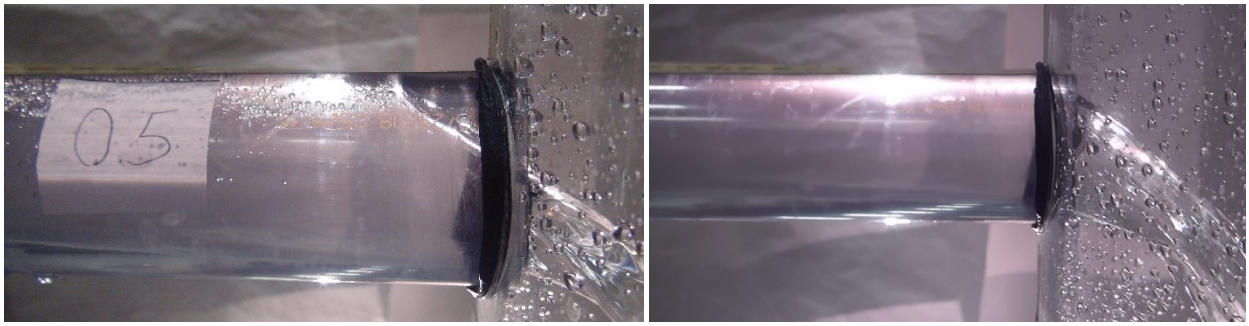

Fig A1.2 Comparing several cavity formation inside inlet in Series A1-2

a)Q=1 L/s (DJ)

b)Q=2.5 L/s (SP)

c)Q=3 L/s, Max level (FE)

d)Q=3 L/s, Min level (FE)

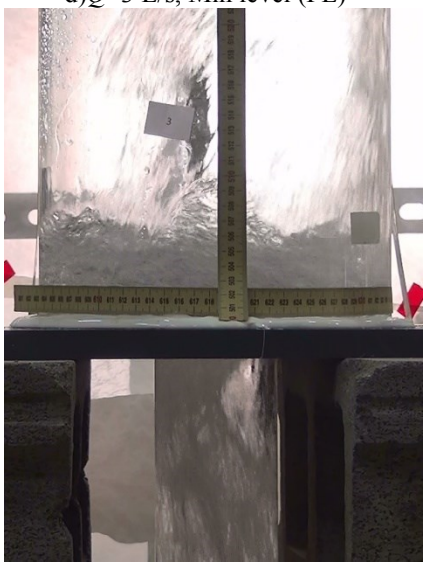

e)Q=5 L/s, Max level (FE)

f)Q=5 L/s, Min level (FE)

Fig A1.3 Different flow regimes in Series A1-3 (One Inlet with d_i=77.2 cm and S= 383mm, d_o=76 mm)

a) Q=2 L/s

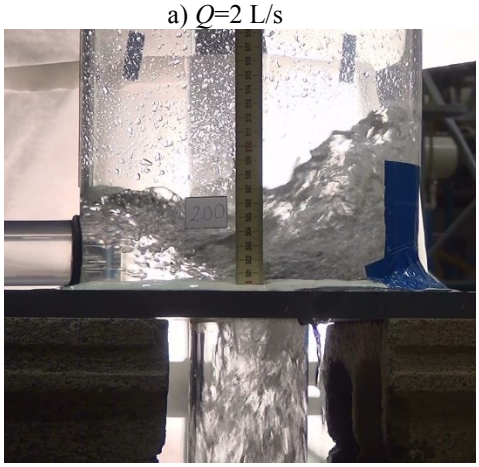

b) Q=4 L/s

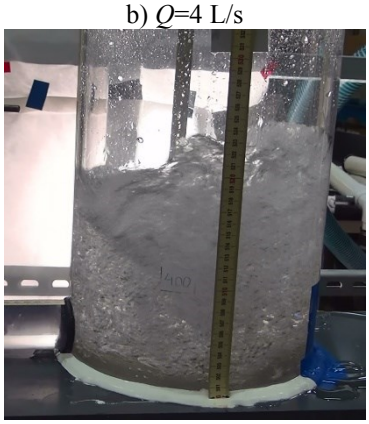

c) Q=6 L/s

d) Q=6 L/s

e) Q=9 L/s

f) Q=9 L/s

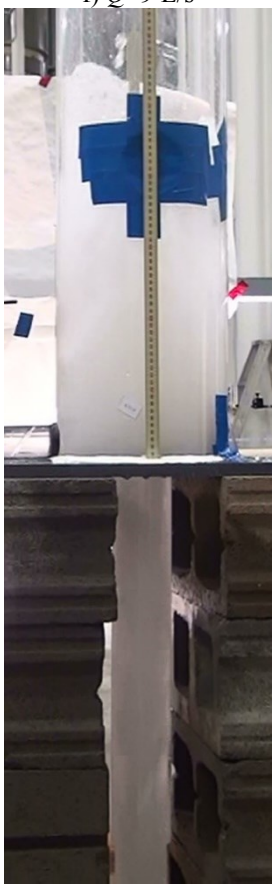

Fig A1.4 Different flow regimes in Series A2-1(One Inlet with d_i=4 mm and S= 8 mm, d_o=76 mm)

a) Q=3 L/s, Max level (FE)

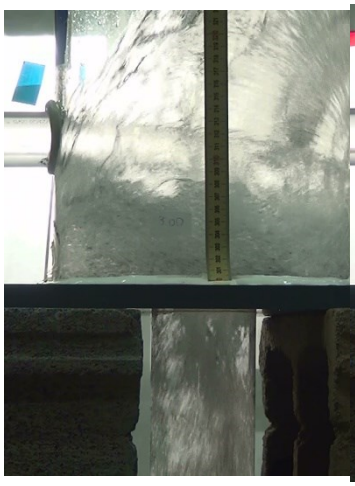

b) Q=3 L/s, Min level (FE)

c) Q=5 L/s max1 level (FE)

d) Q=5 L/s Max2 level (FE)

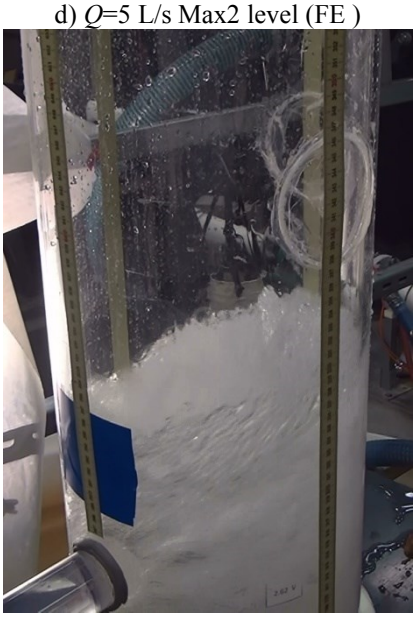

e) Q=5 L/s Min level (FE)

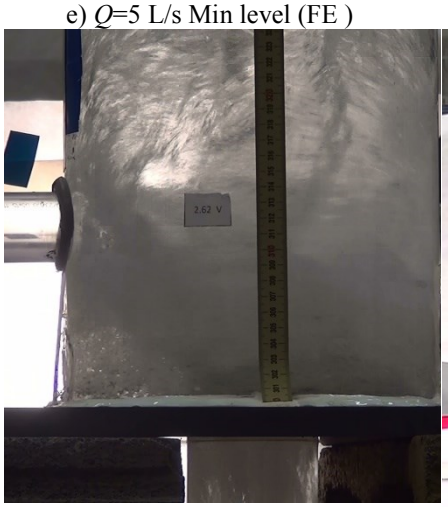

e) Q=7 L/s Max level (FE)

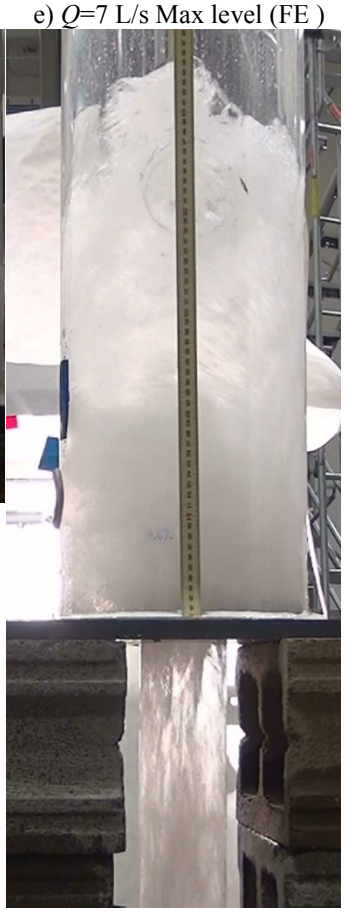

Fig A1.5 Different flow regimes in Series A2-2 (One Inlet with d_i=4 mm and S= 106 mm, d_o=76 mm)

a) Q=3 L/s, Min level (FE)

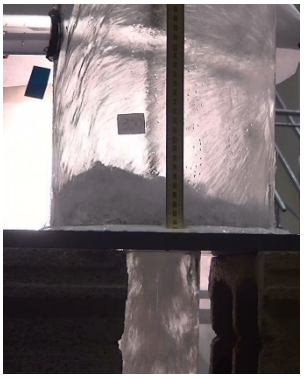

b) Q=3 L/s, Max level (FE)

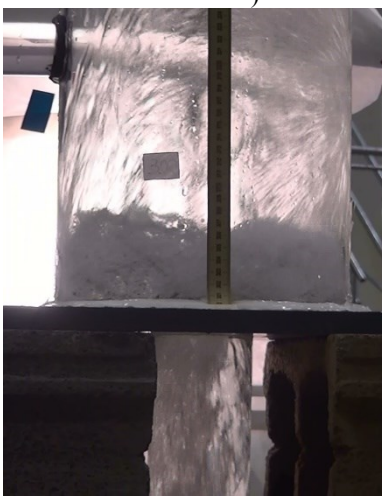

c) Q=5 L/s, Max level (FE)

d) Q=5 L/s, Min

e) Q=7.5 L/s, Max

f) Q=7.5 L/s, Min

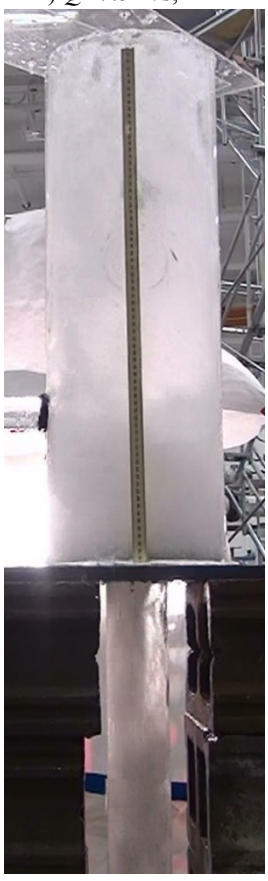

Fig A1.6 Different flow regimes in Series A2-3 (One Inlet with d_i=4 mm and S= 207 mm, d_o=76 mm)

a) Q= 1.75 L/s (DJ)

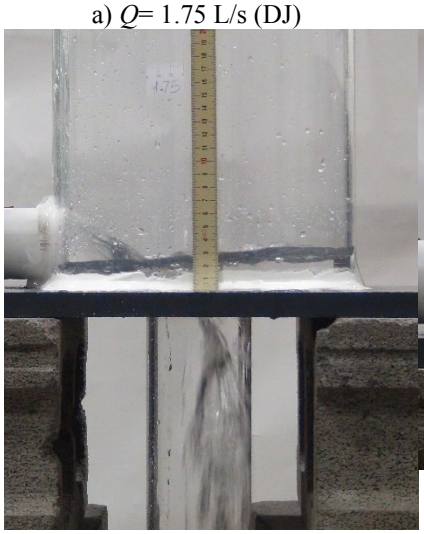

b) Q= 3.5 L/s (SP)

c) Q= 4.4 L/s Max Level (FE)

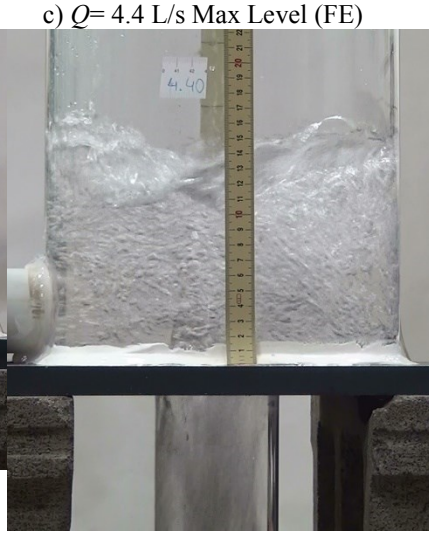

d)Q= 4.4 L/s Min Level (FE)

e)Q= 5.2 L/s Max Level (FE)

f) Q= 5.2 L/s Min Level (FE)

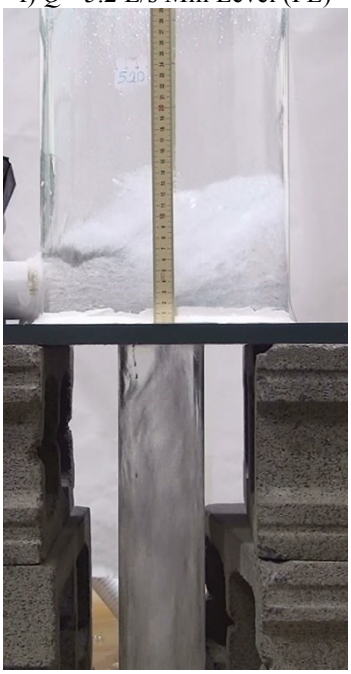

Fig A1.7 Different flow regimes in Series A4-1 (One inlet with d_i=52 mm S=12 mm, d_o=76mm)

a) Q=3.81 L/s (FE)

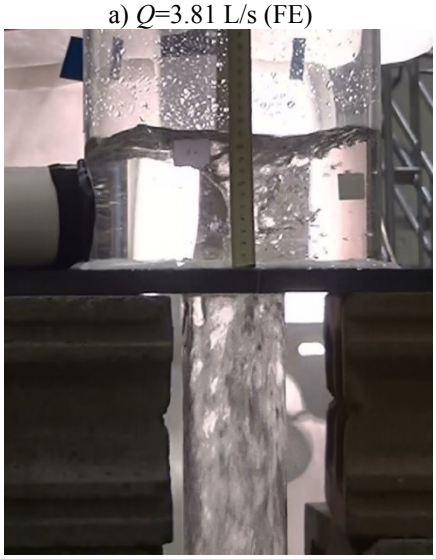

b) Q=6 L/s Max level (FE)

c) Q=6 L/s Min level (FE)

d) Q=10 L/s Max level (FE)

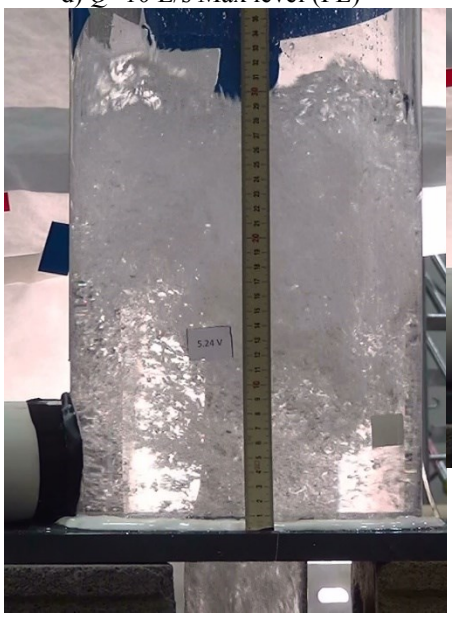

e) Q=10 L/s Min level (FE)

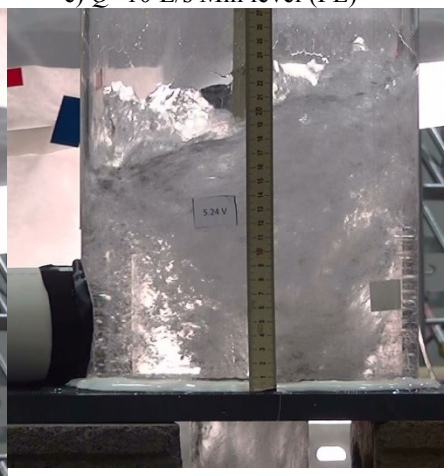

f) Q=14 L/s (FE)

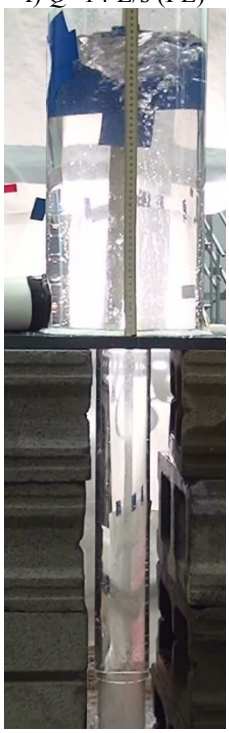

Fig A1.8 Different flow regimes in Series A4-3 (One Inlet with d_i=77 mm and S= 6 mm, d_o=76 mm)

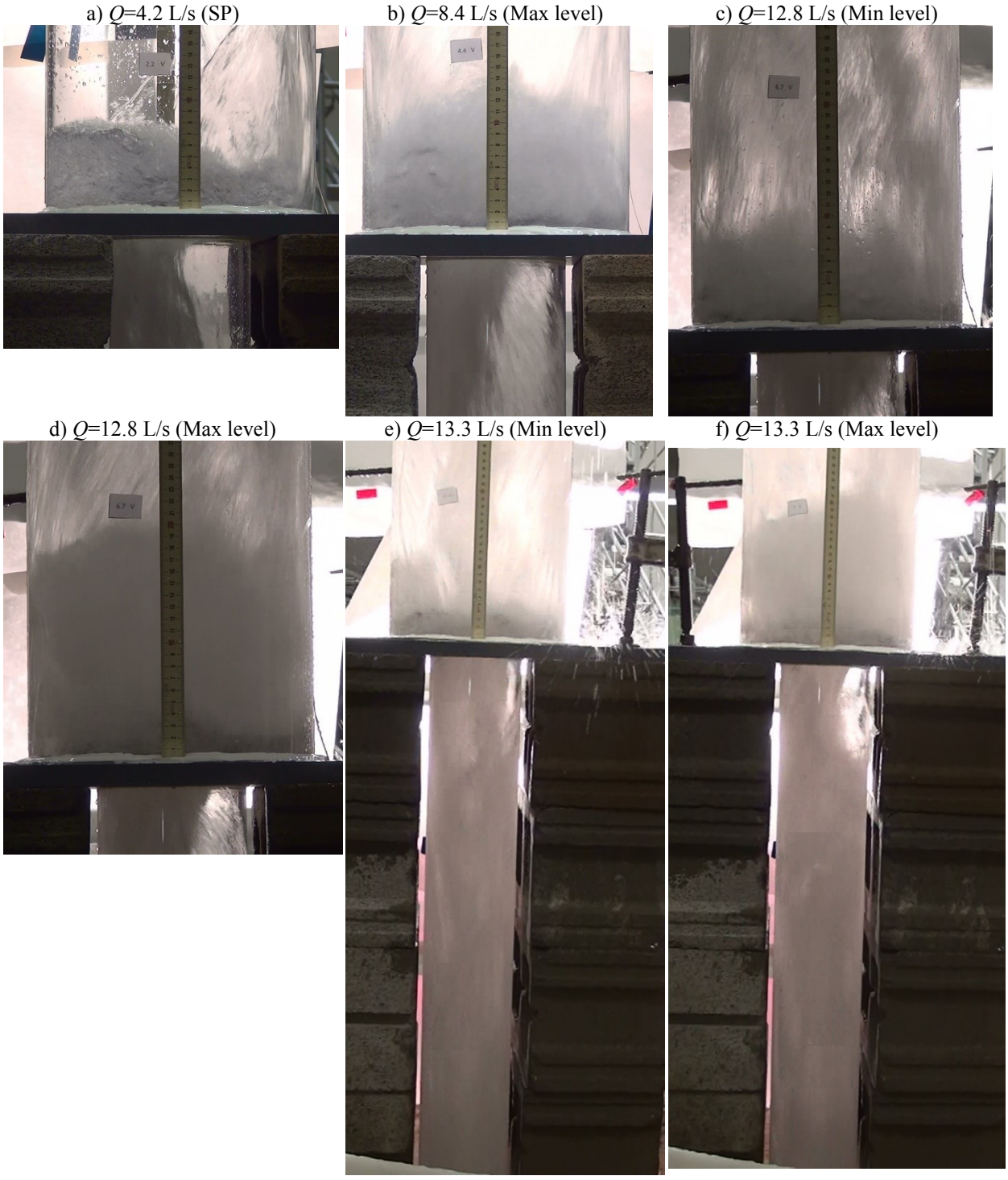

Fig A1.9 Different flow regimes in Series B1-2 (One Inlet with d_i=77 mm and S= 391 mm, d_o=121 mm)

a)Q=1 L/s (DJ) b)Q=6 L/s, Min level (FE) c)Q= 6 L/s, Max level (FE)

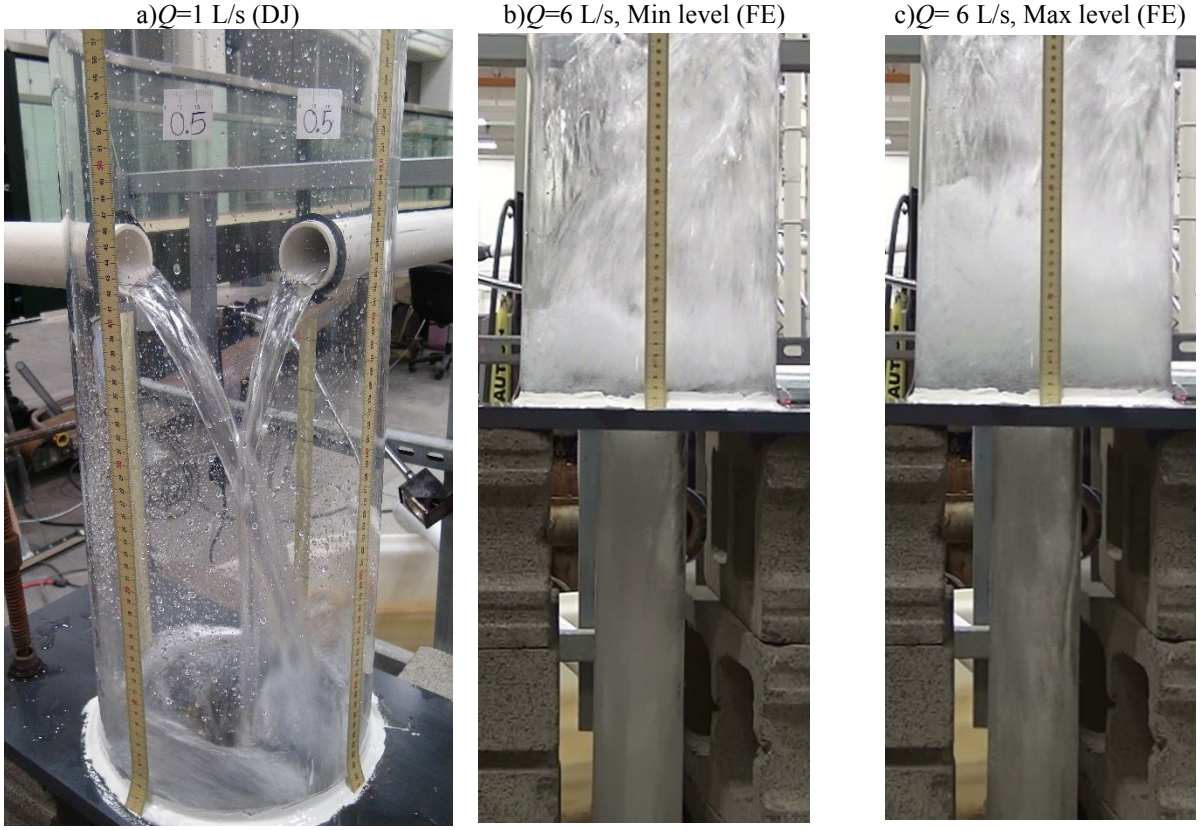

d)Q=10 L/s (SP) e)Q= 6L/s, Max Level (FE) f)Q= 6L/s, Min level (FE)

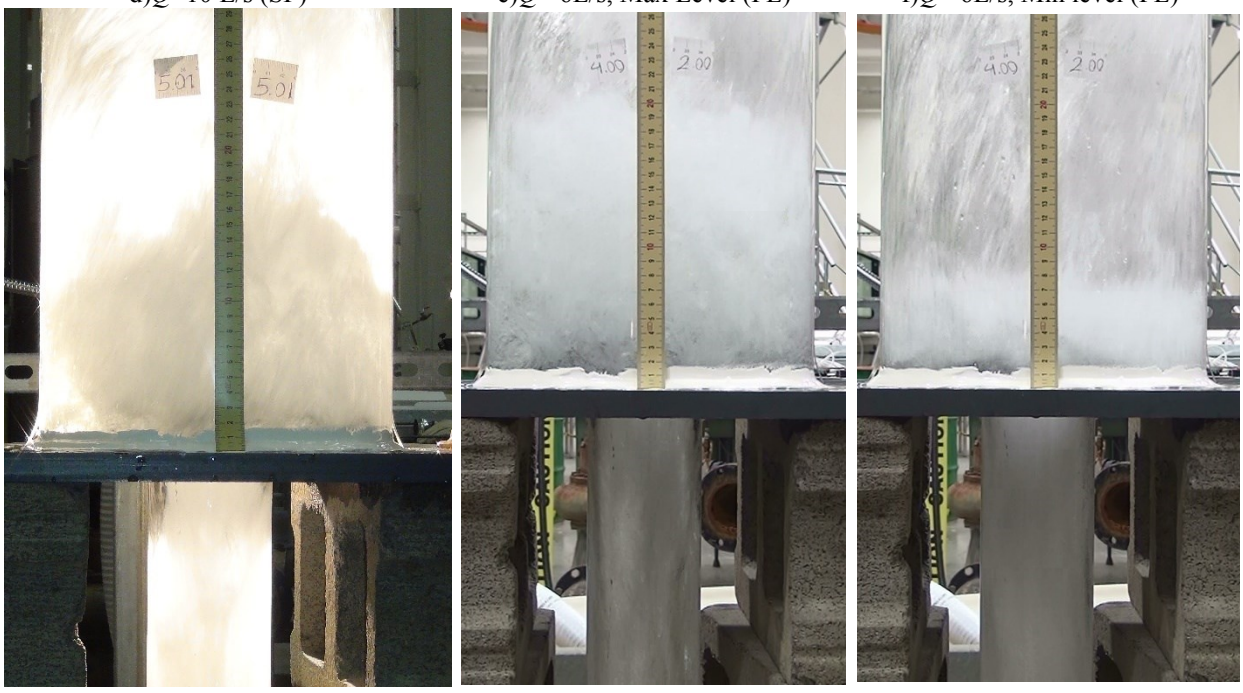

Fig A1.10 Different flow regimes in Series C1-1, Two inlets at a horizontal plane (angle: 90°): d_i=52 mm, S= 389mm and d_o=76mm

a)Q= 0.75 L/s

b)Q= 3 L/s (Max level)

c)Q= 3 L/s (Min level)

d)Q= 7.5 L/s

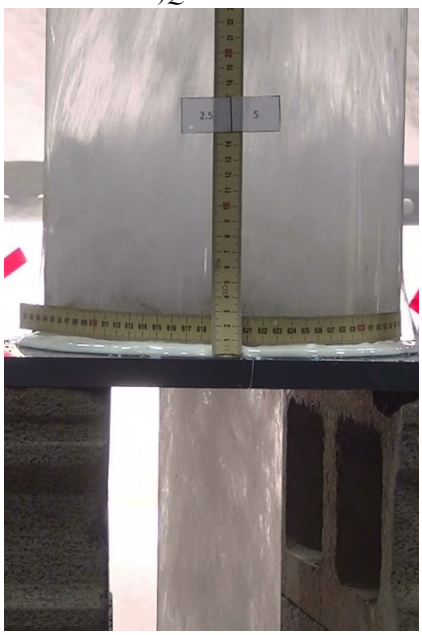

e)Q= 9 L/s

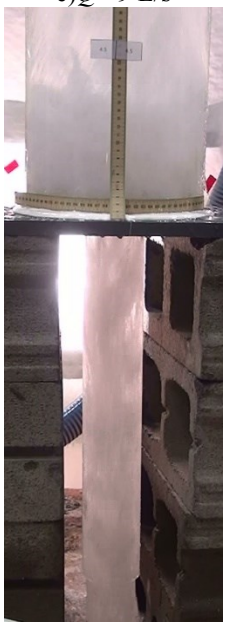

f) Q= 10 L/s

Fig A1.11 Different flow regimes in Series C1-2

Two inlets at a horizontal plane (angle: 90), d_i=40mm, S= 401 mm, d_o=76mm

a)Q= 1 L/s (DJ)

b) Q= 6 L/s, Max level (FE)

c) Q= 6 L/s, Min level (FE)

d) Q= 8. 5 L/s, Max level (FE)

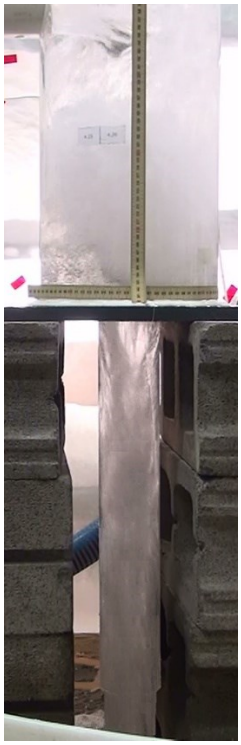

e) Q=8.5 L/s, Min level (FE)

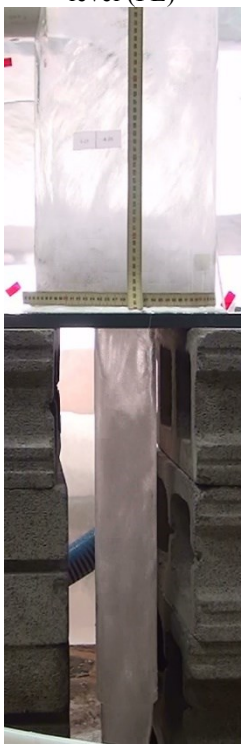

e) Q=9.5 L/s, Jet interaction

Fig A1.12 Different flow regimes in Series C1-3a, Series with two inlets at a horizontal plane (angle: 90°) with d_i=77 mm and S= 383 mm

a) Q = 2.5 L/s (SP)

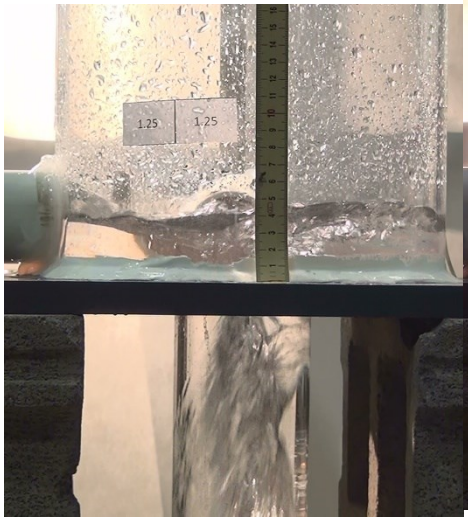

b) Q = 3.88 L/s (SP)

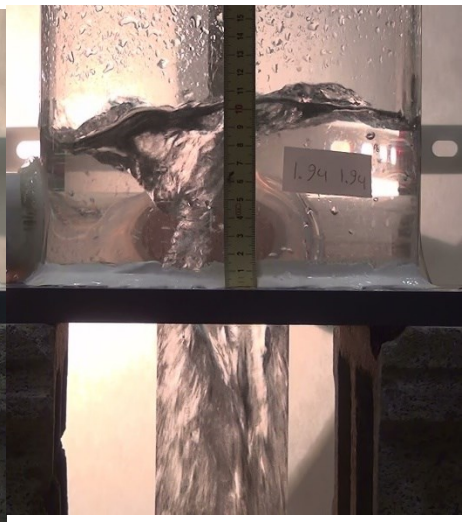

c) Q = 6 L/s**,** Max level (FE)

d) Q = 6 L/s**,** Min level (FE)

e) Q = 10 L/s**,** Max level (FE)

f) Q = 10 L/s**,** Min level (FE)

Fig A1.13 Different flow regimes in Series C2-1a (discharge ratio: 1) Two inlets at a horizontal plane (angle: 90), d_i=52 mm, S= 5 and 12 mm, d_o=76mm

a) Q = 3.75 L/s**,** Min level (FE)

b) Q = 6 L/s**,** Max level (FE)

c) Q = 6 L/s**,** Min level (FE)

d) Q = 7.5 L/s**,** Max level (FE)

e) Q = 7.5 L/s**,** Max to Min level (FE)

f) Q = 7.5 L/s**,** Min level (FE)

Fig A1.14 Different flow regimes in Series C2-1b (discharge ratio: 2) Two inlets at a horizontal plane (angle: 90), d_i=52 mm, S= 5 and 12 mm, d_o=76mm

a) Q = 2.4 L/s (SP)

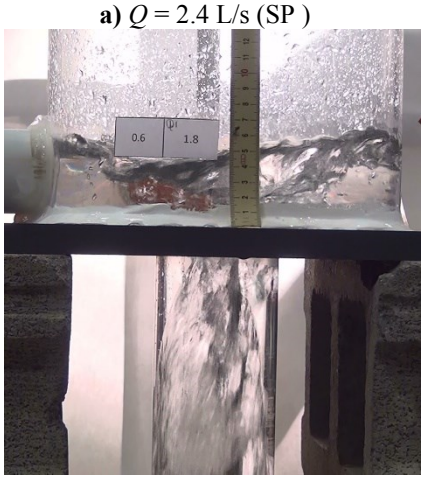

b) Q = 3.09 L/s**,** (SP)

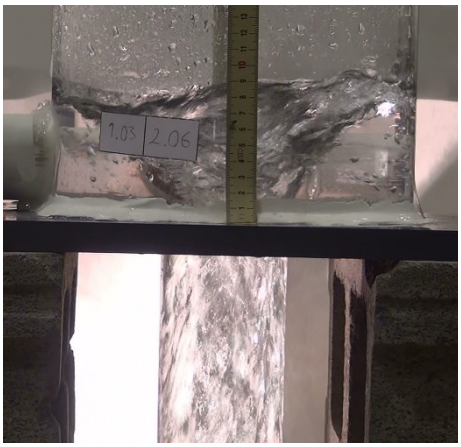

c) Q = 4.8 L/s**,** Max level (FE)

d) Q = 4.8 L/s**,** Min level (FE)

e) Q = 6.8 L/s**,** Max level (FE)

f) Q = 6.8 L/s**,** Min level

Fig A1.15 Different flow regimes in Series C2-1c (discharge ratio: 3), two inlets at a horizontal plane (angle: 90), d_i=52 mm, S= 5 and 12 mm, d_o=76mm

a)Q= 2.5 L/s

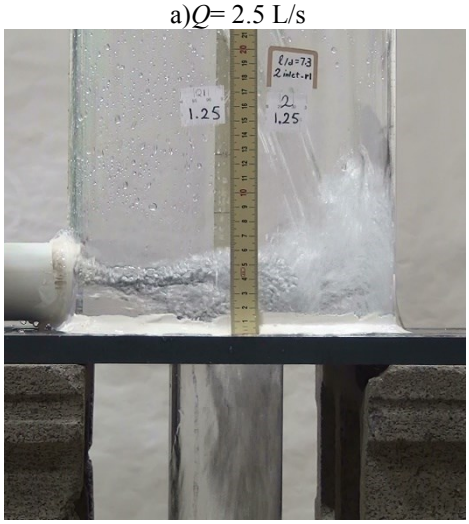

b)Q= 4 L/s

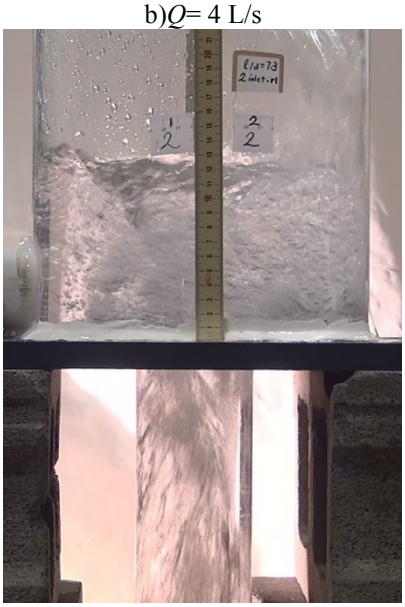

c)Q= 6 L/s Max Level (FE)

d)Q= 6 L/s Min Level (FE)

e)Q= 8 L/s Max Level (FE)

f)Q= 8 L/s Min Level (FE)

Fig A1.16 Different flow regimes in Series C2-2, (Series with two inlets at different horizontal planes with d_i=52 mm, S= 12& 389 mm, d_o=76 mm)

a) T1

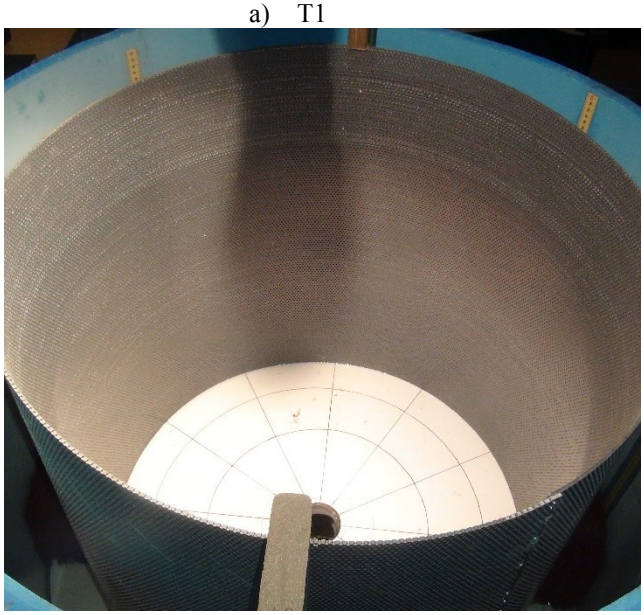

b) T2

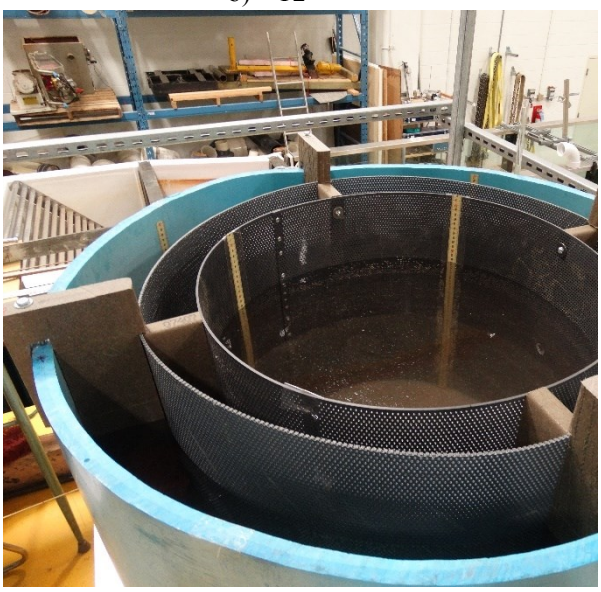

c) T3

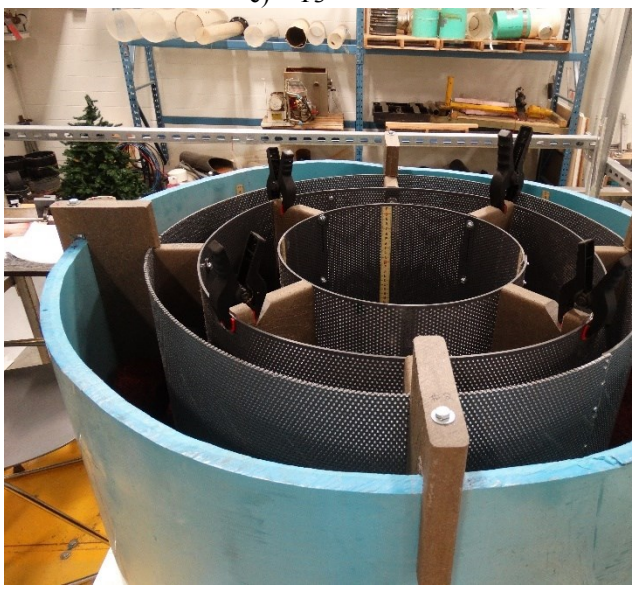

d) T4

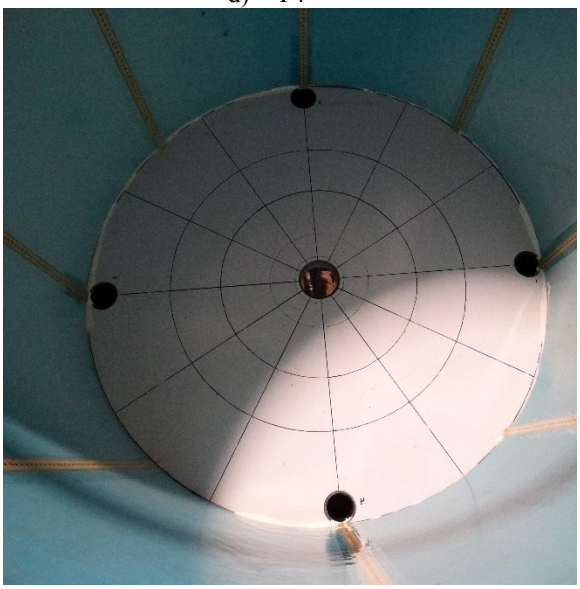

Fig A1.17 Experimental arrangement in T1 to T4 series of experiments

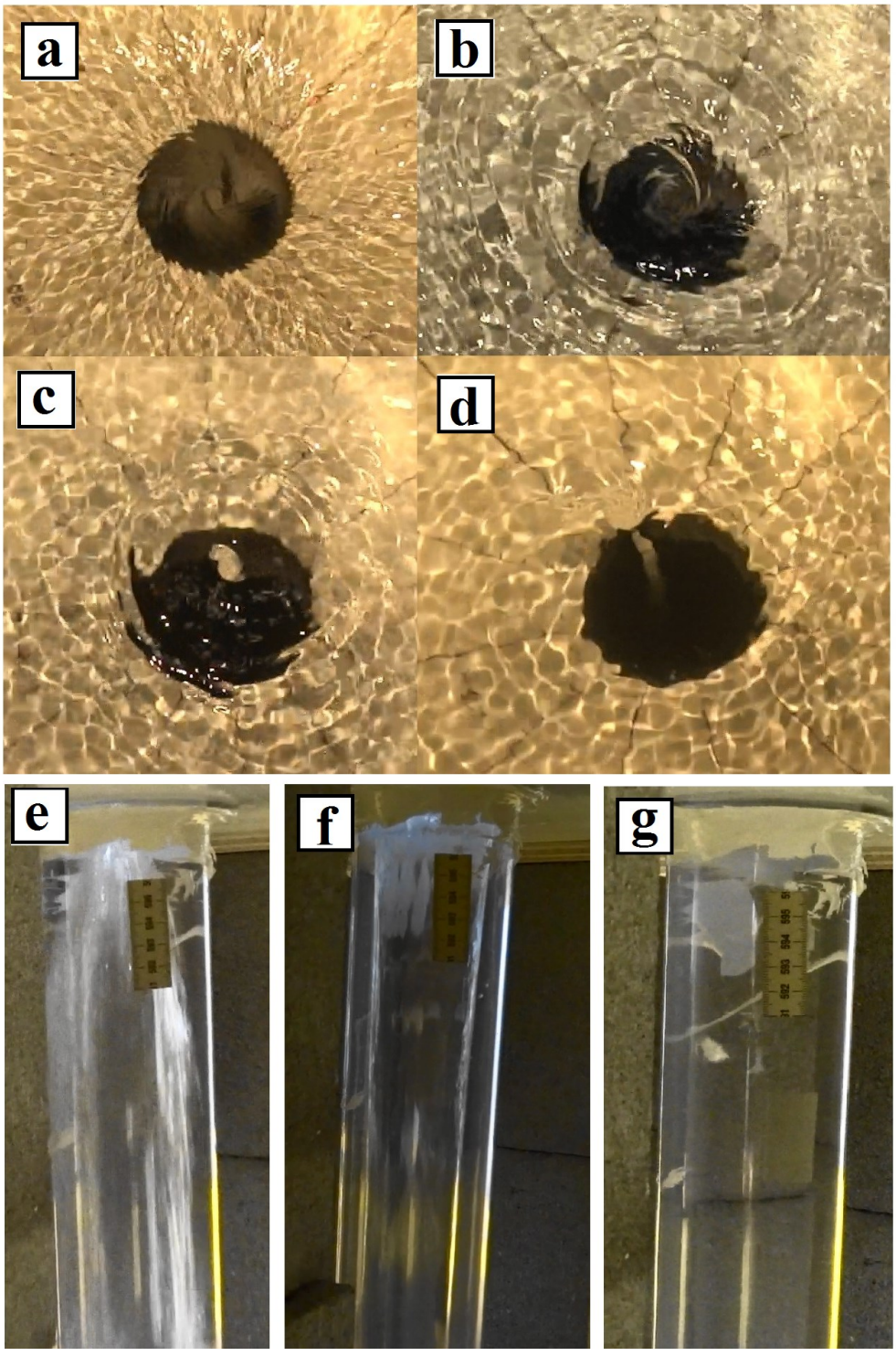

Fig A1.18 Different flow regimes in the tank in different flow regimes: a) The WF regime in T2 (Q=10.2 L/s), b) FE1 in T2 (Q=10.2 L/s), c) FE2 in T2 (Q=10.2 L/s), d) FE3-1 in T2 (Q=10.2 L/s), e) Throat air core of FE process just before it cut-off in T2 (Q=10.2 L/s), f) OF regime in T1 (Q=4.7L/s), g) FPF regime in T3 (Q=21.2L/s)

Appendix 2: Weir formulation for the FE regime

In chapter 4, it has been found that there is some difference between the proposed theory and the experimental data for D/d_o=2, In fact, it might be possible that WC will control the flow. However, since the filling occurs, the incoming discharge accumulates in the upper pipe.

It was found that the effect of velocities from the inlet could be modeled as a velocity head (V_j^2/2g) in the energy equation of WC (Eq. A2.1) in which V_j was the velocity of the jet from the inlet. In case of one inlet at the upper elevation, the incoming jet from the inlet impinged on the opposite wall and formed a rolling curtain jet of water and Eq. A2.3 could be used to represent the velocity V_j. In this equation, t_j was the thickness of the jet. The principle of maximum discharge resulted in Eqs. A2.4 to A2. 5. Therefore, Eqs. A2.4 and A2.6 could be used together to calculate the h-Q curve.

$$E = \frac{V_r^{\,2}}{2g} + \frac{V_\theta^{\,2}}{2g} + \frac{P}{\rho g} + h + \frac{V_j^{\,2}}{2g} \tag{A2.1}$$

$$E = \frac{2C^2}{gd_o^2} + \frac{Q^2}{2g(\pi d_o y_1)^2} + y_l + \frac{V_j^{\,2}}{2g} \tag{A2.2}$$

$$V_j = \frac{Q}{\pi D t_j} \tag{A2.3}$$

$$\frac{\partial E}{\partial y_l} = 0 \Rightarrow Q^2 = \pi^2 g d_o^{\,2} y_l^{\,3}$$

$$Q = \pi d_o \sqrt{g}\, y_l^{\,3/2} \tag{A2.4}$$

$$E = \frac{2C^2}{gd_o^2} + \frac{\pi^2 g d_o^{\,2} y_l^{\,3}}{2g(\pi d_o y_1)^2} + y_1 + \frac{\pi^2 g d_o^{\,2} y_l^{\,3}}{\pi^2 D^2 t_j^{\,2} \times 2g} \tag{A2.5}$$

$$E = \frac{2C^2}{gd_o^2} + \frac{3}{2} y_1 + \frac{d_o^{\,2} y_l^{\,3}}{2D^2 t_j^{\,2}} \Rightarrow h = \frac{2C^2}{gd_o^{\,2}} + \frac{3}{2} y_1 + \frac{d_o^{\,2} y_l^{\,3}}{2D^2 t_j^{\,2}} \tag{A2.6}$$

There are two assumptions in this derivation: i) a constant thickness for the annular jet and ii) same velocity between the annular jet and the approaching flow to the control section. Both Eqs. A2.4 and A2.6 can be used to determine the h-Q curve. This theoretical method is called the weir control jet (WC-JT) flow in this study. It was found that assuming t_j=8 mm, this theoretical method can represent the upper branch of the FE regime in the D_r=2 experiment as shown in Fig. A2.1 with a 10% deviation.

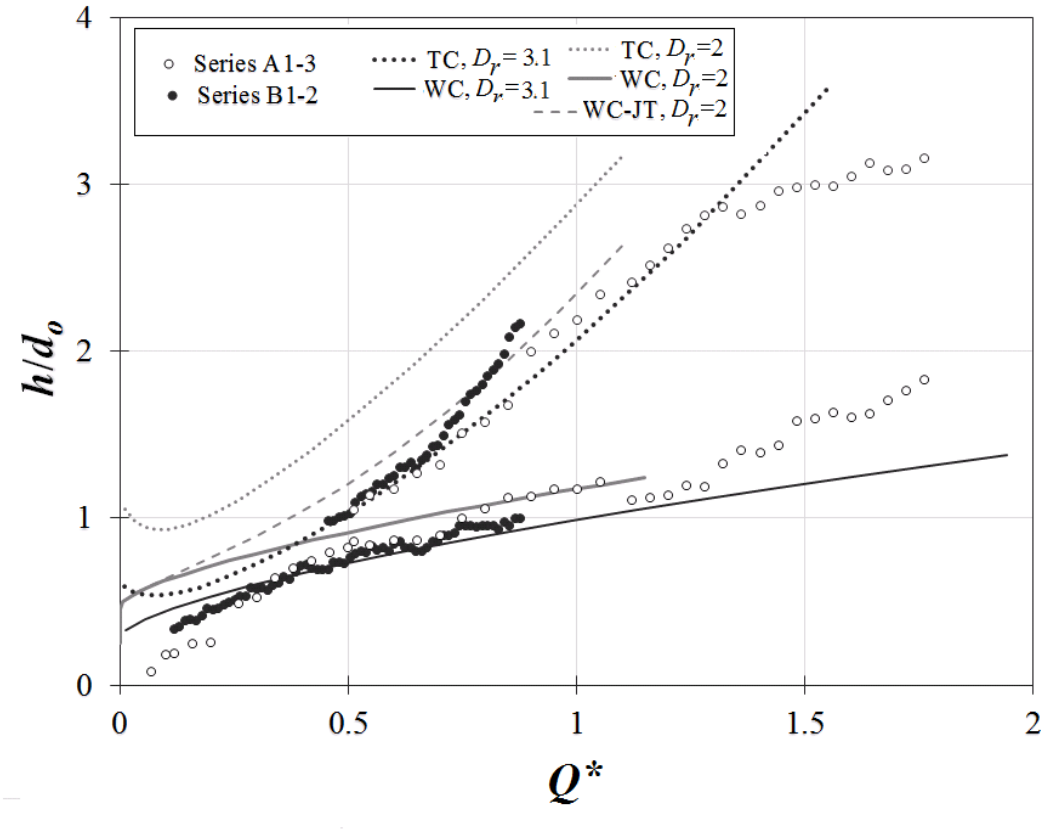

Fig A2.1 Comparison of experimental values of h/d_o versus Q^* for series A1-3 and B1-2 (experimental data of chapter 2) with theoretical results of throat control (TC), weir control (WC) as presented in chapter 4 and weir jet control section affected by jet (WC-JT)

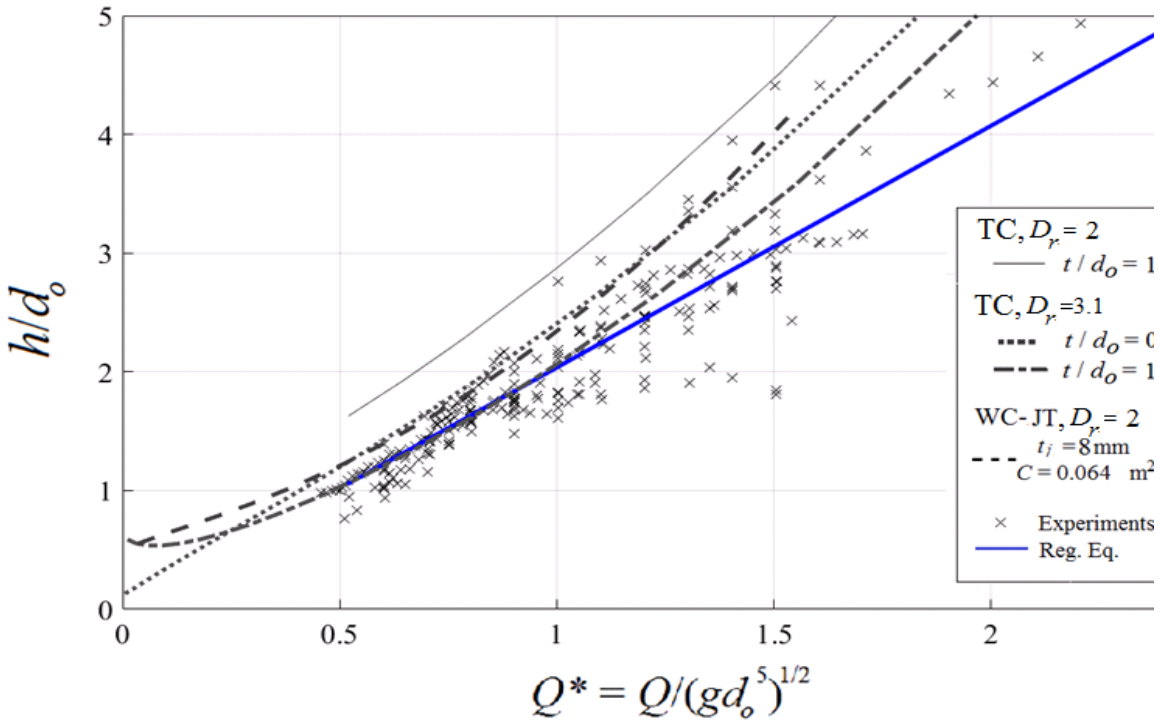

Fig A2.2 Comparison of experimental values of the h/d_o-Q^* curves for the FE regime in DDM (experimental data of chapter 2) with the theoretical results of (TC, WC) for different values of t/d_o as presented in chapter 4 and (WC-JT)